



**Titre:** Novel Reversible “Sticky” Particles Grafted With Gelling  
Polysaccharides to Control the Stability of Pickering Emulsions

**Auteur:** Faezeh Sabri  
Author:

**Date:** 2019

**Type:** Mémoire ou thèse / Dissertation or Thesis

**Référence:** Sabri, F. (2019). Novel Reversible “Sticky” Particles Grafted With Gelling  
Polysaccharides to Control the Stability of Pickering Emulsions [Thèse de doctorat,  
Citation: Polytechnique Montréal]. PolyPublie. <https://publications.polymtl.ca/4008/>

 **Document en libre accès dans PolyPublie**  
Open Access document in PolyPublie

**URL de PolyPublie:** <https://publications.polymtl.ca/4008/>  
PolyPublie URL:

**Directeurs de recherche:** Nick Virgilio, Louis Fradette, & Jason Robert Tavares  
Advisors:

**Programme:** Génie chimique  
Program:

**POLYTECHNIQUE MONTRÉAL**

affiliée à l'Université de Montréal

**Novel Reversible “Sticky” Particles Grafted With Gelling Polysaccharides to  
Control the Stability of Pickering Emulsions**

**FAEZEH SABRI**

Département de génie chimique

Thèse présentée en vue de l'obtention du diplôme de *Philosophiæ Doctor*

Génie chimique

Juillet 2019

© Faezeh Sabri, 2019.

# **POLYTECHNIQUE MONTRÉAL**

affiliée à l'Université de Montréal

Cette thèse intitulée :

## **Novel Reversible “Sticky” Particles Grafted With Gelling Polysaccharides to Control the Stability of Pickering Emulsions**

présentée par **Faezeh SABRI**

en vue de l'obtention du diplôme de *philosophiae Doctor*

a été dûment acceptée par le jury d'examen constitué de :

**Olivier HENRY**, président

**Nick VIRGILIO**, membre et directeur de recherche

**Jason Robert TAVARES**, membre et codirecteur de recherche

**Louis FRADETTE**, membre et codirecteur de recherche

**Jean-Philippe HARVEY**, membre

**Noémie-Manuelle DORVAL COURCHESNE**, membre externe

## DEDICATION

*To my beloved parents*

*&*

*Farhad*

“Nothing in life is to be feared, it is only to be understood. Now is the time to understand more, so that we may fear less”.

Marie Curie

## ACKNOWLEDGEMENTS

First, and foremost I would like to express my gratitude and appreciation to my main director **Prof. Nick Virgilio** for his endless support, guidance, and encouragement throughout my PhD study at Polytechnique Montreal. I am much indebted for his invaluable and constant support during the toughest days of my study. He always kept motivating me to work persistently and hard. His energy and creativity will always be an inspiration for me. I am very grateful to him for his patience and constructive guidance which helped me a lot during my study. My command of words (in any language) is not expressive enough to say “THANKS” to him, but I try!

I also wish to extend my gratitude to my co-supervisors **Prof. Jason R. Tavares** and **Prof. Louis Fradette** for their expert and exceptional advices and valuable contributions throughout my PhD. They have been very helpful and genius in providing clear insight into my research, as well. I appreciate their continuous and great supports for my research work during my PhD study.

I would to acknowledge the financial support of Imperial Oil through a University Research Award grant, Total (Industrial Research Chair), the National Sciences and Engineering Research Council (Discovery Grant), CREPEC (Projets Structurants), Polytechnique Montreal (UPIR undergraduate research grants) and the Canada Foundation for Innovation (John R. Evans Leaders Fund) throughout the course of this study.

I would like to immensely thank Mrs. Claire Cerclé, who put a lot of time and effort in FTIR characterizations for my samples and helped me to interpret my results. Also, a big appreciation goes to Mr. Matthieu Gauthier for helping me through training for the rheological experiments and Dr. Josianne Lefebvre who spent so much time and passion to help me to interpret the XPS spectra. In addition, I would like to acknowledge the kindest technicians in chemical engineering department at Polytechnique Montreal who always provided my requests at their earliest with a big smile on their face: Gino Robin, Martine Lamarche and Sylvain Simard Fleury.

I would also like to express my gratitude to friends and colleagues for their supports and help during my PhD study especially: my intern-students Kevin Berthomier and Antoine Marion, my colleagues especially Dr. Amir Saffar, Dr. Chang-Sheng Wang, Dr. Ebrahim Jalali, Dr. Gilles Lenfant, Dr. Benoit Liberelle, and Dr. Bing Wan, URPEI and PICVD group members in particular Dr. Donya Farhanian, Dr. David Brassard, Dr. David Vidal, Dr. Emir Tsabet, Dr. Evelyne Kasparek

and Dr. Hamed Nasri for their research insights and willingness to help throughout the duration of this research work.

Special thanks to all my friends at Polytechnique Montreal for their supports and help: Dr Philippe Leclerc, Dr. Samira Lotfi, Dr. Jaber Darabi, Dr. Nooshin Saadakhah, Dr. Christine Beaulieu, Dr. Charlotte Van Engeland, Dr. Shiva Kordjazi and Mr. Navid Elahipanah. Also, I would like to say thanks to Dr. Jonathan Bouffard for giving me the opportunity to work with him during last months of my PhD.

I would like to extend my gratitude to Mr. Wendell Raphael and Dr. Olivier Drevelle for their unforgettable favors and for all the memorable moments I had with them during my PhD study. Thank you for your support, encouragements and the times we enjoyed together inside and outside the lab! Also, I owe gratitude to Dr. Olivier Drevelle for kindly translating the abstract of this thesis to French.

Finally, special recognition goes out to my beloved family, especially Farshad and Farzad for their endless support, encouragement and love even if we were far in distance. To my very dear cousin, Dr. Ali Sabri, who always got my back during hard times with his support and encourage. To Dr. Negar Zamir-Rowshan, my sister in law who provided enormous encouragement and support during the last year of my PhD. To my very loving brother, Dr. Farhad Sabri for his selfless love, care and dedicated efforts which contributed a lot for completion of my PhD. His perseverance, hard work, wisdom, sense of discipline and above all, his love and endless support, has made him a great source of inspiration for me, since childhood until now, and I should say it will last for ever; a very big thank goes to him for everything.

Last but not least, my deepest gratitude goes to my beloved parents, who have been always supportive of me with their unconditional love and supports. I give my very special thanks to my parents for the overwhelming support they always provided and for scarifies they made throughout my life; for giving me the inspiration to work hard and never give up, and for always being there for me when I needed them. I would like to thank you “maman”, and “baba” for all you are and all you have done for me unconditionally.

## RÉSUMÉ

Les émulsions de Pickering sont stabilisées par l'adsorption de particules solides à l'interface de deux liquides non miscibles, et ceci sans l'utilisation de surfactants. Ce type d'émulsion peut être retrouvé dans les industries alimentaire, cosmétique, pharmaceutique, dans le traitement des eaux usées ainsi que dans l'exploitation pétrolière. Ainsi, le grand nombre de publications scientifiques concernant les émulsions de Pickering s'attarde tout particulièrement à l'étude du mécanisme de stabilisation ainsi qu'aux effets de la chimie de surface des particules, leur concentration ainsi que leur taille.

Cependant, il existe un besoin pour des procédés permettant de briser et de séparer les constituants des émulsions de Pickering, en particulier en utilisant une approche simple, pratique et éco-responsable. Plusieurs procédés industriels utilisant des émulsions de Pickering doivent passer par des étapes de séparation et/ou de déstabilisation. La résistance de ce type d'émulsion à la déstabilisation demeure un challenge restant à être surmonté. Dans la revue de littérature, plusieurs techniques de déstabilisation, notamment mécaniques, électriques et chimiques, sont présentées. Cependant, d'autres approches doivent être développées, en particulier pour les systèmes possédant une viscosité très élevée. Enfin, l'effet de la viscosité elle-même dans ces systèmes reste à être étudié et compris.

La première partie de cette thèse montre que la modification de surface de microparticules de silice, à l'aide d'un polysaccharide naturel, l'alginate de sodium (SA), favorise un phénomène réversible d'agrégation/désagrégation en solution aqueuse via une simple modification du pH. Tout d'abord une fonctionnalisation des particules de silice de 300 nm avec un aminosilane a été effectuée, suivie par une deuxième fonctionnalisation avec SA sensible au pH. Les particules non modifiées et modifiées ont ensuite été caractérisées avec des mesures du potentiel zêta, par spectrométrie photo-électronique X (XPS), et par spectroscopie infrarouge à transformée de Fourier (FTIR), afin de confirmer les modifications de surface. Une augmentation des propriétés d'agrégation, pour les particules modifiées avec SA à bas pH (3.0), a été observée par rapport aux particules de silice non modifiées – des agrégats 10 fois plus grand sont obtenus avec des particules modifiées. L'agrégation est également un phénomène réversible, puisqu'une augmentation du pH à 7.0 permet ainsi de briser les agrégats et de redisperser les particules. De plus, à pH 3.0, les particules modifiées présentent une vitesse de sédimentation significativement supérieure par rapport aux

particules non modifiées. Ainsi, la formation de liaisons hydrogènes entre les particules modifiées voisines à bas pH permet d'augmenter l'agrégation des particules solides. Ces résultats ont été publiés dans le journal *Carbohydrate Polymers*.

Dans la deuxième partie de cette thèse, nous avons montré que la fonctionnalisation de particules de silice avec SA permet non seulement de stabiliser des émulsions de Pickering huile-dans-eau (O/W), mais également de simplifier la séparation et la collecte des constituants initiaux via une simple filtration – ne nécessitant ainsi aucun ajout d'agent chimique ou d'énergie. Avant de greffer le SA, la mouillabilité des particules a été contrôlée par l'ajout de deux silanes : le trimethoxy(propyl)silane (TMPS) et le (3-aminopropyl)trimethoxysilane (APTMS). Afin de caractériser l'évolution de la chimie de surface des particules, des mesures d'angles de contact et de potentiel zêta ont été réalisées sur les particules non-modifiées, et après chaque étape de modification de surface. Ensuite, l'augmentation des interactions entre les gouttes d'émulsion (stabilisées par les particules) a été confirmée par des expériences de rhéologie et de filtration. Cette approche montre des perspectives très intéressantes pour des procédés de séparation d'émulsions de Pickering plus propres et plus verts. Ces résultats ont été publiés dans le journal *Green Chemistry*.

Enfin, dans la troisième partie de cette thèse, nous avons obtenu des émulsions de Pickering multiples eau-dans-huile-dans-eau (W/O/W) en utilisant des huiles de silicone très visqueuses (10,000 et 30,000 cSt) en présence de particules de silice modifiées avec SA. Cette étude était initialement un prolongement de la seconde partie de cette thèse – c'est-à-dire d'étudier l'effet de la viscosité de la phase dispersée (huile) sur la séparation des constituants des émulsions de Pickering. Résultat inattendu, nous avons obtenu des émulsions de Pickering multiples en utilisant uniquement un type de particule solide dans un procédé à une seule étape. L'inversion de phase apparaît comme étant le phénomène dominant menant à la formation de ces émulsions multiples, la viscosité de l'huile ainsi que la chimie de surface des particules jouant également des rôles importants. Par exemple, utiliser des huiles de faible viscosité (1,000 et 5,000 cSt) ne permet pas d'obtenir des émulsions multiples, alors que les huiles de 10,000 et 30,000 cSt le permettent. De plus, les émulsions multiples n'ont pu être obtenues qu'avec l'utilisation de particules modifiées avec SA. Un article présentant ces résultats a été soumis au journal *Journal of Colloids and Interface Science*.



Cette recherche ouvre la voie au développement et à la modification de micro/nanoparticules solides avec des biomacromolécules naturelles (ici l'alginate de sodium) permettant la stabilisation d'émulsions de Pickering, mais également la séparation des constituants par une simple filtration sans l'utilisation d'agents chimiques ou d'énergie. De plus, ces particules modifiées présentent la particularité de former des émulsions de Pickering stables avec des huiles très visqueuses, sujet peu abordé dans la littérature. En effet, dans de nombreux procédés du génie chimique, des liquides hautement visqueux sont utilisés, ces systèmes visqueux présentant ensuite une résistance à la stabilisation ou à la déstabilisation. Ainsi, cette étude permet de donner quelques lignes directrices fondamentales afin de comprendre l'effet de la viscosité des huiles sur l'émulsification et la séparation des constituants de liquides polyphasiques. Pour conclure, cette recherche montre que des émulsions de Pickering multiples peuvent être créées par un procédé simple. Ceci ouvre la porte pour des applications futures dans les domaines pharmaceutique, cosmétique, médical ainsi que dans l'industrie alimentaire.

## ABSTRACT

Pickering emulsions are stabilized by solid particles adsorbed at the interface of two immiscible liquids, with no use of surfactants. They can be found or are considered for applications in various industries such as food, cosmetics, pharmaceuticals, waste water treatment and oil recovery. As can be deduced from the abundant scientific publications on Pickering (solid-stabilized) emulsions, the mechanisms of stabilization and the effects of particle surface chemistry, concentration, and size have been intensively studied. However, complementary investigations are still needed to design and develop processes that can break and separate the constituents of Pickering emulsions - especially via simple, practical and green approaches. For many industrial processes, Pickering emulsion systems need to go under either separation or destabilization. The resistance of these emulsions to breaking remains an open challenge – there is a need for efficient and ecofriendly processes. In the literature review, various destabilization techniques including mechanical, electrical and chemical methods, are presented; however additional approaches are still required, especially for highly viscous systems. Finally, the effect of viscosity remains to be well studied and investigated.

The first part of this thesis demonstrates that surface modification of sub-micrometer silica particles with a natural polysaccharide, sodium alginate (SA), can enhance the reversible aggregation and disaggregation of particulates in aqueous solution via pH adjustment. An aminosilane coupling agent was first used to functionalize 300 nm silica particles, followed by a second functionalization step with the pH-sensitive SA. Pristine and modified particles were characterized by zeta potential, XPS and FTIR analyses to confirm their surface chemistry modifications. Enhanced aggregation properties were observed for the SA-modified particles at pH 3.0, compared to unmodified silica, with a 10 times increase in average aggregate diameter. The aggregation phenomena was reversible: as the pH was increased to 7.0, the aggregates were broken and could be re-dispersed again. Moreover, at pH 3.0, SA-modified particles presented significantly faster sedimentation rates, compared to the unmodified particles. The formation of hydrogen bonds between neighboring SA-modified particles most likely enhanced the aggregation phenomena. These results were published in *Carbohydrate Polymers*.

In the second part of this thesis, we demonstrated that the grafting of SA onto silane-modified silica particles could promote not only the stabilization of Pickering oil-in-water emulsions, but also

significantly simplify the separation and recovery of the initial constituents via a simple filtration approach - requiring no additional chemical agent or energy input. Prior to SA grafting, the surface wettability of particles was controlled by grafting a combination of two silane agents; trimethoxy(propyl)silane (TMPS) and (3-aminopropyl)trimethoxysilane (APTMS). To confirm surface chemistry modifications, the particles were characterized with zeta potential and contact angle measurements, before and after each step of surface modification. Moreover, the enhanced particle-particle and droplet-droplet interactions when using SA-modified particles were confirmed via rheometry and filtration experiments. Clearly, this approach shows interesting perspectives for cleaner and green separation processes for Pickering emulsions. These results were published in *Green Chemistry*.

Interestingly, in the third part of this thesis, we have obtained (to our surprise) multiple Pickering water-in-oil-in-water (W/O/W) emulsions when using highly viscous silicone oils (10,000 and 30,000 cSt) with 100 nm SA-modified silica particles. This study was initially envisioned as an extension to the second part of this thesis – i.e. to investigate the effect of the dispersed phase (oil) viscosity on the separation of Pickering emulsions constituents. We unexpectedly obtained multiple Pickering emulsions - using only one type of solid particle in a single step process. Phase inversion appears to be the main phenomena driving the formation of multiple W/O/W droplets. Oil viscosity and surface chemistry in particular also play significant roles. For example, using low viscosity oils (1,000 and 5,000 cSt) did not result in the formation of multiple emulsions, compared to 10,000 and 30,000 cSt oils. Moreover, multiple emulsions were only obtained when using surface modified SA particles. It should be noted again that these multiple emulsions were obtained via a one step emulsification process with only one type of particles, which is uncommon for producing multiple emulsions. An article presenting these results has been submitted to *Journal of Colloids and Interface Science*.

This research paves the way to design and modify solid particles with a natural biomacromolecules, herein sodium alginate (SA), which allow both enhanced Pickering emulsion stabilization properties, with the possibility of subsequently separating the constituents by a simple filtration approach - requiring no chemicals nor significant energy input. Moreover, these surface modified particles present the ability to form stable Pickering emulsions using highly viscous oils, a topic insufficiently explored in the literature. In many chemical engineering processes, highly viscous

liquids are employed, and these viscous systems show resistance to either stabilization or destabilization. Thus, this study can provide some fundamental guidelines to understand the effect of oil viscosity on emulsification or the separation of constituents for industries dealing with viscosity issues. Furthermore, this research demonstrates that multiple Pickering emulsions can be generated via a one-step emulsification process using only one type of solid particles. These are interesting results with a promising potential for applications in the pharmaceutical, cosmetics, medical, and food industries.

## TABLE OF CONTENTS

DEDICATION .....	iii
ACKNOWLEDGEMENTS .....	iv
RÉSUMÉ.....	vi
ABSTRACT .....	ix
TABLE OF CONTENTS .....	xii
LIST OF TABLES .....	xvii
LIST OF FIGURES.....	xviii
LIST OF SYMBOLS AND ABBREVIATIONS.....	xxv
CHAPTER 1 INTRODUCTION .....	1
1.1 Background and problem identification.....	1
1.2 Organization of the thesis.....	4
CHAPTER 2 LITERATURE REVIEW.....	5
2.1 Solid-stabilized (Pickering) emulsions.....	5
2.2 Physicochemical properties of solid particles .....	5
2.2.1 Type of solid particles .....	5
2.2.2 Particle size, concentration and shape.....	8
2.2.3 Oil viscosity.....	11
2.3 Wettability of particles .....	12
2.3.1 Wettability control of particles via surface modification.....	14
2.3.2 Multiple Pickering emulsions.....	18
2.4 Destabilization of Pickering emulsions.....	21
2.4.1 Microscopic destabilization mechanisms.....	21
2.4.2 Methods and processes to destabilize Pickering emulsions .....	24

2.4.3	Stimuli-responsive Pickering emulsions .....	28
2.5	Summary .....	31
CHAPTER 3 RESEARCH HYPOTHESIS AND OBJECTIVES, AND COHERENCE OF ARTICLES.....		34
3.1	Research hypothesis and objectives .....	34
3.2	Presentation of the articles and coherence with the research objectives .....	35
CHAPTER 4 ARTICLE 1: SODIUM ALGINATE-GRAFTED SUBMICROMETER PARTICLES DISPLAY ENHANCED REVERSIBLE AGGREGATION/DISAGGREGATION PROPERTIES .....		36
4.1	Abstract .....	36
4.2	Introduction .....	36
4.3	Experimental section .....	38
4.3.1	Materials.....	38
4.3.2	Particle surface modification.....	39
4.3.2.1	Silane coating grafting .....	39
4.3.2.2	Sodium alginate grafting .....	39
4.3.3	Particle surface characterization.....	40
4.3.3.1	Zeta potential measurements.....	40
4.3.3.2	High-resolution X-ray photoelectron spectroscopy (XPS) analysis .....	40
4.3.3.3	Fourier transform infrared (FTIR) spectroscopy analysis .....	41
4.3.4	Characterization of Aggregation and Disaggregation Properties.....	41
4.3.4.1	Visual inspection of sedimentation kinetics.....	41
4.3.4.2	Optical microscopy observations .....	42
4.3.4.3	Measurement of sedimentation rate by UV-Vis spectroscopy .....	42

4.3.4.4	Aggregation/disaggregation reversibility evaluation .....	42
4.4	Results and Discussion.....	43
4.4.1	Zeta potential, XPS and FTIR .....	43
4.4.2	Particle aggregation behavior.....	44
4.4.3	Sedimentation Kinetics .....	46
4.4.4	Kinetic test by UV-Visible spectroscopy .....	49
4.4.5	Aggregation/disaggregation reversibility .....	50
4.5	Discussion .....	51
4.6	Conclusion.....	52
4.7	Acknowledgment .....	53
4.8	Supporting Information Article 1: Sodium alginate-grafted submicrometer particles display enhanced reversible aggregation/disaggregation properties .....	53
CHAPTER 5	ARTICLE 2: TUNING PARTICLE-PARTICLE INTERACTIONS TO CONTROL PICKERING EMULSIONS CONSTITUENTS SEPARATION .....	60
5.1	Abstract .....	60
5.2	Introduction .....	60
5.3	Experimental section .....	62
5.3.1	Materials.....	62
5.3.2	Particles Surface Modification .....	63
5.3.2.1	Silane Grafting .....	63
5.3.2.2	Sodium alginate grafting .....	63
5.3.3	Particle surface characterization.....	64
5.3.3.1	Zeta potential measurements .....	64
5.3.3.2	Contact angle measurements .....	64

5.3.3.3	Emulsions preparation and characterization .....	64
5.3.3.4	Droplet observation and diameter measurement .....	65
5.3.3.5	Rheological behavior.....	65
5.3.3.6	Confocal microscopy (CLSM) .....	66
5.3.3.7	Separation tests and particles recovery .....	66
5.4	Results .....	67
5.4.1	Zeta potential and contact angle measurements confirm sodium alginate grafting ...	67
5.4.2	Sodium alginate modified particles stabilize oil-in-water emulsions .....	68
5.4.3	Sodium Alginate-Modified Particles Improve the Separation of Pickering Emulsions Constituents.....	75
5.5	Discussion .....	78
5.6	Conclusion.....	79
5.7	Acknowledgements .....	79
5.8	Supporting Information Article 2 : Tuning particle–particle interactions to control Pickering emulsions constituents separation.....	80
CHAPTER 6	ARTICLE 3: ONE-STEP PROCESSING OF HIGHLY VISCOUS MULTIPLE PICKERING EMULSIONS.....	87
6.1	Abstract .....	87
6.2	Introduction .....	87
6.3	Experimental section .....	89
6.3.1	Materials.....	89
6.3.2	Particle Surface Modification.....	90
6.3.2.1	Silanes Surface Grafting.....	90
6.3.2.2	Sodium Alginate Grafting .....	91



6.3.3	Particle Surface Characterization .....	91
6.3.3.1	Zeta Potential Measurements .....	91
6.3.3.2	Contact Angle Measurements .....	91
6.3.4	Emulsions Preparation and Characterization .....	92
6.3.4.1	Optical Characterization of Emulsions .....	92
6.3.4.2	Confocal Laser Scanning Microscopy (CLSM) Analysis .....	92
6.4	Results .....	93
6.4.1	Zeta potential and contact angle measurements .....	93
6.4.2	Emulsion stabilization with pristine and modified silica particles.....	94
6.4.3	Effect of oil viscosity on the formation of multiple emulsions.....	95
6.4.4	Internal drop microstructure investigated by confocal microscopy .....	97
6.4.5	Effects oil and particle concentrations .....	97
6.4.6	Effects of processing variables: duration of oil addition, processing time, and sequence of mixing .....	99
6.5	Proposed mechanism for the formation of multiple Pickering emulsions .....	101
6.6	Conclusion.....	103
6.7	Acknowledgements .....	103
6.8	Supporting information Article 3: One-Step Processing of Highly Viscous Multiple Pickering Emulsions.....	104
CHAPTER 7	GENERAL DISCUSSION.....	105
CHAPTER 8	CONCLUSION AND RECOMMENDATIONS.....	110
8.1	Conclusion.....	110
8.2	Recommendations .....	111
BIBLIOGRAPHY	.....	113

## LIST OF TABLES

Table 2.1. Published studies on solid-stabilized (Pickering) emulsions including types of particles, oil phases, and resulting emulsion type.....	6
Table 2.2 Several shapes of solid particles used in the preparation of Pickering emulsions. ....	10
Table 2.3 Published studies on the effect of oil phase viscosity for the processing of solid Pickering emulsions.....	12
Table 2.4 Typical methods for tuning particle wettability in order to form Pickering emulsions. ....	15
Table 2.5 Various stimuli-responsive particles used to stabilize Pickering emulsions.....	29
Table 4.1 Synthesis conditions of surface modified particles with APTMS and SA.....	40
Table 4.2 $\zeta$ of silica particles: untreated (SP), APTMS treated (SP-A to C), and APTMS+SA treated particles (SP-(A-1), (B-2) and (C-2)), as a function of pH (3.0, 7.0 and 10.0).....	43
Table 4.3 Average aggregate diameter $D$ as a function of particle type, at pH 3.0 (N = number of analyzed aggregates). ....	46
Table 5.1 Zeta potential $\zeta$ and contact angle $\theta_{o/w}$ of silica particles: pristine (SP), silanized (SP-Sil), and grafted with sodium alginate (SP-SA), as a function of pH (3.0, 7.0 and 10.0).....	67
Table 5.2 Gravimetric analysis of collected material after filtration experiments.....	77

## LIST OF FIGURES

Figure 1.1 Emulsions are observed in Milk and Butter.....	1
Figure 1.2 Pickering emulsions stabilized by the adsorption of solid particles (Luo, Wang, Yoo, Wei, & Pentzer, 2018; Sadeghpour, Pirolto, & Glatter, 2013). ....	2
Figure 1.3 Oil droplet dispersed in water (a) and water droplet dispersed in oil and contact angle ( $\theta$ ) of a particle at the liquid-liquid interface (b).....	2
Figure 2.1 Micrograph of an O/W emulsion stabilized by starch particles: a densely packed layer and a 3-D network (Song et al., 2015). ....	9
Figure 2.2 Irregular particles at the interface between oil and water $\gamma_{so}$ , $\gamma_{sw}$ , and $\gamma_{ow}$ are the interfacial tensions (or free interfacial energies) of the solid particle/oil, solid particle/water, and oil/water interfaces, $A_{pw}$ and $A_{po}$ represent the surface area of the solid particle in contact with the oil and water phases, and $A_c$ is for the area of the oil and water interface which occupied by the cross section of solid particle, $A_p$ represents the total surface area of the solid particle . (Marilyn Rayner et al., 2014) .....	10
Figure 2.3 Position of a solid particle at the oil/water interface with a contact angle $\theta$ measured through the water phase. Left: $\theta < 90^\circ$ (hydrophilic); Center: equal to $90^\circ$ (equally hydrophilic and hydrophobic); Right: $\theta > 90^\circ$ (hydrophobic) (Tang et al., 2015). ....	13
Figure 2.4 Chemical structure of sodium alginate showing guluronate (G) and mannuronate (M) units (Schnepp et al., 2011).....	18
Figure 2.5 Preparation process of double emulsion by phase inversion (S. Kim et al., 2018). ....	19
Figure 2.6 Schematic diagram of production of emulsions and confocal image of the resulting multiple emulsions (M. Liu et al., 2016).....	20
Figure 2.7 Different instability mechanisms in solid stabilized emulsions (Y. T. Hu, Ting, Hu, & Hsieh, 2017) .....	21
Figure 2.8 Schematic representation of catastrophic phase inversion in Pickering emulsions: the continuous addition of the dispersed phase (oil) sequentially turns the emulsion from O/W (left) to W/O (right).....	22

- Figure 2.9 Ostwald ripening: small droplets are shrinking and larger droplets are swelling by mass transfer from smaller droplets to the bigger ones (Whitby & Wanless, 2016) .....23
- Figure 2.10 Changes in emulsion microstructure during destabilization (Juarez & Whitby, 2012). .....23
- Figure 2.11 Centrifugation to induce the coalescence of drops (a). Image of coalesced drops after centrifugation at 9600g after 10 min (b). Efficiency of coalescence under different centrifugal accelerations for 15 min (Pan et al., 2017)(c). .....25
- Figure 2.12 Coalescence is induced between droplets by applying an electric field (Hwang et al., 2010).....26
- Figure 2.13 Schematic illustration of pH-induced transitional phase inversion for a system using either methyl myristate or cineole as the oil phase (a), and pH-induced demulsification process for an emulsion of n-dodecane/water, decreasing pH induced the separation of two phases (b) (E. S. Read, 2004). .....27
- Figure 2.14 Visualization of the interactions between water droplets in a 0.1 wt% naphtha-diluted bitumen emulsion (A1, A2, B1, B2, C1, and C2) and in naphtha (D1 and D2) by the micropipet technique. (A1) Water droplets interactions with no EC addition; (A2) detached from each other, no change in shape and size in the emulsion droplets; (B1) water droplets interactions in the emulsion containing EC ; (B2) deformation (stretching) of flocculated water droplets in the presence of EC; (C1) water droplets interactions in the emulsion with addition of higher amount of EC; (C2) water droplets coalesced into one large droplet in the emulsion with higher amount of EC; (D1) water droplets interactions in naphtha with EC addition; and (D2) water droplets coalesced into one large droplet in naphtha with EC addition. A3, B3, C3, and D3 are schematic representations of A1, B1, C1, and D1, respectively. (Feng et al., 2010).28
- Figure 4.1 Dark field optical microscopy micrographs showing the aggregation state, as a function of pH (3.0 or 7.0), of SP (a, b), SP-A (c, d), and SP-A-1 (e, f) particles. ....45
- Figure 4.2 Pictures of the sedimentation process (height of test tube = 15.3 cm) for SP (a, b), SP-A (c, d), and SP-A-1 (e, f) particles over 60 min at pHs 3.0 and 7.0 respectively; g, h) close-ups of SP-A-1 and SP sedimented particles, showing a clear difference in particle texture..48

Figure 4.3 Normalized transmittance $T$ as a function of time for SP, SP-A-1, SP-B-2 and SP-C-2 particles at pH 3.0 and 7.0, and fitted curves for SP, SP-A-1, SP-B-2 and SP-C-2 particles at pH 3.0 over 60 min.....	50
Figure 4.4 Reversibility test for SP (■) and SP-A-1 particles (●) over 4 cycles, during which the pH jumps back and forth from 7.0 to 3.0. ....	51
Figure 4.5 Pictures of 0.5 % solution of pure SA in DI water at pH 7.0 (a) and at pH 3.0 (b), with and without urea (16 M).....	52
Figure 4.6 SEM micrographs of bare SiO <sub>2</sub> particles (a) and SA modified particles (SP-C-2) initially dispersed at pH 7.0 (b) and subsequently brought down to pH 3.0 (c), respectively.....	54
Figure 4.7 Deconvoluted XPS spectra of bare SiO <sub>2</sub> (SP) (left column), and modified with APTMS (SP-C) (right column).....	55
Figure 4.8 FTIR spectra of bare SiO <sub>2</sub> (SP), treated with APTMS(SP-C) and with SA (SP-C-2)..	57
Figure 4.9 Aggregates size distribution for SP, SP-A-1, SP-B-2 and SP-C-2 particles, at pH 3.0. The category number indicates the upper size limit of aggregates ( <i>e.g.</i> (1) corresponds to aggregate size below 1 $\mu\text{m}$ , (10) corresponds to aggregate size in-between 1 $\mu\text{m}$ and 10 $\mu\text{m}$ , etc). ....	58
Figure 4.10 Dark field optical microscopy micrographs showing the aggregation state, as a function of pH 3.0 of SP (a) and SP-A-1 (b). ....	58
Figure 4.11 Pictures of the sedimentation process (height of test tube = 15.3 cm) for SP-B (a, b), SP-C (c, d), SP-B-2(e, f) and SP-C-2(g, h) particles over 60 min at pHs 3.0 and 7.0 respectively.....	59
Figure 5.1 Oil-in-water emulsions all comprising 4% (w/v) particles at pH 3.0 (a) and 7.0 (b). pH 3.0: (A) SP particles, $\phi_o = 0.7$ ; (B) SP, $\phi_o = 0.3$ ; (C) SP-SA, $\phi_o = 0.7$ ; (D) SP-SA, $\phi_o = 0.3$ . (E) to (H) same as (A) to (D), but at pH 7.0.....	69
Figure 5.2 CLSM pictures of Pickering emulsions ( $\phi_o = 0.8$ ) with 4% SP-SA (w/v) particles at pH 3.0 (a) and 7.0 (b). ....	69

- Figure 5.3 Dark field optical microscopy micrographs showing oil droplets, as a function of oil content  $\phi_o$ , at pH 3.0 (left column) and 7.0 (right column), for SP (a to d), and SP-SA (e to h) particles .....71
- Figure 5.4 Number average diameter  $d$  of oil droplets as a function of oil volume fraction  $\phi_o$ , for both SP and SP-SA particles, at pH 3.0 and pH 7.0.....72
- Figure 5.5 Storage ( $G'$ ) and loss modulus ( $G''$ ) as a function of time ( $t$ ) at 20 °C, for concentrated emulsions ( $\phi_o = 0.8$  and 4% (w/v) particles) at pH 3.0 (a) and 7.0 (b). All tests were performed at  $\omega = 1$  rad/s,  $\gamma_0 = 1\%$  .....73
- Figure 5.6 a) Normalized height ( $h(t)/h_0$ ) as a function of time  $t$  and applied stress on molded concentrated emulsions ( $\phi_o = 0.8$ ) comprising 4% SP or SP-SA particles, at pH 3.0 and 7.0; b-c) visual aspect of the solid-like behavior of molded Pickering emulsions comprising 4% SP-SA particles, compared to a concentrated emulsion prepared with pristine SP displaying no yield stress, at pH 3.0; .....74
- Figure 5.7 Filtration of Pickering emulsions prepared at pH 3.0 with 4% particles: a-c) emulsions prepared with pristine SP particles with oil content  $\phi_o = 0.1, 0.3$  and  $0.5$ , respectively; d-f) same as (a-c), but with sodium alginate modified particles (SP-SA).....76
- Figure 5.8 a) Remaining aqueous phase after the filtration of oil droplets, b) collected oil droplets and particles, c) re-dispersion of collected material (oil + particles) in oil phase and d) stabilization of emulsion using recovered particles. ....77
- Figure 5.9 SEM micrographs of SP and SP-SA particles before and after homogenizer processing. ....80
- Figure 5.10 Pictures of concentrated oil-in-water Pickering emulsions comprising 4% SP-SA particles ( $\phi_o = 0.8$ ) when contained into the plastic molds (a), removed from plastic molds (b, c), and under compressive stress (d, e).....81
- Figure 5.11 Effect of oil volume fraction  $\phi_o$  on emulsion aspect, with 4% (w/v) particles: a) and b), emulsions prepared with unmodified silica particles (SP) at pHs 3.0 and 7.0, respectively; c) and d), emulsions prepared with sodium alginate-modified particles (SP-SA), at pHs 3.0 and

7.0; e) emulsion composed of SP particles (4% w/v) at $\phi_o = 0.8$ , compared to f) emulsion composed of SP-SA particles (4% w/v) at $\phi_o = 0.8$ . .....	82
Figure 5.12 Number average diameter $d$ of oil droplets as a function of oil volume fraction $\phi_o$ , for both SP and SP-SA particles, at pH 3.0 and 7.0, as obtained by laser diffraction (Mastersizer). .....	83
Figure 5.13 Normalized height ( $h(t)/h_0$ ) with the error bars as a function of time $t$ and applied stress on molded concentrated emulsions ( $\phi_o = 0.8$ ) comprising 4% SP or SP-SA particles, at pH 3.0 and 7.0. ....	83
Figure 5.14 Emulsion stability in time with 3 different oil volume fraction $\phi_o$ , and constant 4% (w/v) particles.....	84
Figure 5.15 Pictures of the particle's behaviour (height of test tube = 15.3 cm) for SP (a, b), SP-A (c, d), over 60 min at pHs 3.0 and 7.0 without oil droplets.....	85
Figure 6.1 Zeta potential $\zeta$ (a) and contact angle $\theta$ (b) of silica particles: pristine (SP), silanized (SP-Sil), and grafted with sodium alginate (SP-SA), as a function of pH (2.0 to 10.0). .....	93
Figure 6.2 Macroscopic aspect and optical microscopy pictures of Pickering emulsions prepared with 4% particles (w/v) at $\phi_o = 0.1$ : a) SP particles with 10 cSt oil; b) SP-SA particles with 10 cSt oil; c) SP particles with 10,000 cSt oil (un-emulsified oil indicated with white arrow; d) SP-SA particles with 10,000 cSt oil.....	95
Figure 6.3 Macroscopic aspect and optical microscopy pictures of Pickering emulsions prepared with 4% particles (w/v) at $\phi_o = 0.1$ : a) SP particles with 10 cSt oil; b) SP-SA particles with 10 cSt oil; c) SP particles with 10,000 cSt oil (un-emulsified oil indicated with white arrow; d) SP-SA particles with 10,000 cSt oil.....	96
Figure 6.4 CLSM pictures of Pickering emulsions ( $\phi_o = 0.1$ , 10,000 cSt) with 4% (wt/vol) SP-SA particles tagged with DTAF, showing the interfacial adsorption of particles both at the oil surface and water sub-inclusions (indicated with white arrows in the latter case). ....	97
Figure 6.5 Effect of oil fraction $\phi_o$ on the formation of multiple emulsions comprised of 4% (w/v) SP-SA particles and 10,000 cSt silicone oil, at pH = 7.0: a) $\phi_o = 0.05$ ; b) $\phi_o = 0.1$ ; c) $\phi_o = 0.2$ and d) $\phi_o = 0.3$ (d). Vials display emulsion stability after 10 months. ....	98

Figure 6.6 Effect of particle concentration on the oil droplets internal structure in emulsions prepared with SP-SA particles (w/v) with 10,000 cSt silicone oil ( $\phi_o = 0.1$ ) at pH=7.0: a) 2% particles (w/v); b) 4%; c) 6% and d) 12%. .....99

Figure 6.7 Effect of mixing sequence on Pickering emulsions appearance and microstructure, prepared with 4% (w/v) SP-SA particles and 10,000 cSt oil at pH = 7.0. In (a, b), particles are first dispersed in water, then the aqueous suspension is gradually added in oil while homogenizing: a) processing stopped when phase inversion occurs (oil-in-water emulsion is formed); b) homogenizing is prolonged 2 min after the complete addition of particle suspension ( $\phi_o = 0.2$ ). In (c, d), particles are first dispersed in the oil phase, then water is gradually added in the (oil + particle) suspension while homogenizing: c) process stopped after phase inversion occurs; d) homogenizing is prolonged 2 min after complete addition of water ( $\phi_o = 0.2$ ). .....100

Figure 6.8 Schematic illustrations of the formation of multiple emulsions by gradual oil addition, first big droplets of oil formed and due to intense mixing the water droplets were formed and migrated into those big oil droplets(a) and water gradual addition resulting in dispersion of water droplets and as water addition increased, phase inversion happened and oil droplets were dispersed (b) (It should be noted because of high viscosity of oil, big droplets were formed) .....102

Figure 6.9 Effect of the duration of oil addition on the macroscopic appearance and internal structure of oil droplets, for Pickering emulsions prepared with 4% SP-SA particles (w/v) with 10,000 cSt silicone oil ( $\phi_o = 0.1$ ): a) oil added in 1 min (+ 5 min of additional processing), b) oil added in 6 min (no additional processing time). .....104

Figure 6.10 Effect of additional processing time on the macroscopic appearance, and oil drop internal structure, in Pickering emulsions prepared with 4% SP-SA particles (w/v) with 10,000 cSt silicone oil ( $\phi_o = 0.1$ ). Oil added in 4 min + (a) 2 min or (b) 8 min of additional processing. ....104

Figure 7.1 Surface grafting of functional groups on silica/glass bead (a) and Fe<sub>3</sub>O<sub>4</sub> (b).....106



Figure 7.2 Surface grafting of boronic acid and diol functional groups on silica particles and adsorption and desorption processes between these surface modified particles (Y. Wang et al., 2015).....	107
---	-----

## LIST OF SYMBOLS AND ABBREVIATIONS

### *Abbreviations*

$\text{Al}_2\text{O}_3$	Aluminium oxide
APTMS	(3-Aminopropyl) trimethoxysilane
BET	Brunauer, Emmett and Teller, specific surface area
$\text{CaCO}_3$	Calcium carbonate
C	Carbon
$^{\circ}\text{C}$	Celsius
$\text{Ca}^{2+}$	Calcium ion
CDS	Sodium dodecyl sulfate
CLSM	Confocal Microscopy
Cm	Centimeter
CNC	Cellulose nanocrystal
CNT	Carbon Nanotube
$\text{CO}_2$	Carbon oxide
$\text{CoFe}_2\text{O}_4$	Cobalt ferrite
cos	Cosine
-COOH	Carboxylic acid
cSt	Centistokes
D	Diameter
$\text{D}_2\text{O}$	Deuterium oxide
DI	Deionized water
3-D	Three dimension
EC-Br	Bromoesterified ethyl cellulose

EDC	N'-ethylcarbodiimide hydrochloride
eV	Electron volt
Fe <sub>2</sub> O <sub>3</sub>	Iron(III) oxide
Fe <sub>3</sub> O <sub>4</sub>	Iron (II, III) oxide
FTIR	Fourier-transform infrared spectroscopy
fwhm	Full width at half maximum
G	$\alpha$ -l-guluronic
g	Gram
h	Hour
HCl	Hydrogen chloride
<sup>1</sup> H NMR	Proton nuclear magnetic resonance
kDa	Kilodalton
kV	Kilovolt
LDH	2D sheet-shaped layered double hydroxide
M	$\beta$ -d-mannuronic
MAA	Methacrylic acid
mA	Milliampere
M/G	$\beta$ -d-mannuronic ratio to $\alpha$ -l-guluronic
MHz	Highly optimized tolerance
ml	Millilitre
N	Normality, Nitrogen
NA	Not applicable
NaOH	Sodium hydroxide

NHS	N-Hydroxysuccinimide
nm	nanometer
O	Oxygen
O/W	Oil-in-water
O/W/O	Oil-in-water-in-oil
Pa	Pascal
PDMAEMA	Poly[2-(dimethylamino)ethyl methacrylate]
PDMS	Poly(dimethylsiloxane)
PEG	Poly(ethylene glycol)
PEI	Poly(ethylene imine)
PINIPAM	Poly(N-isopropylacrylamide)
PIPSMA	Poly[(3-triisopropoxyloxy)silyl]propyl methacrylate]
pka	Index to express the acidity of weak acids
pH	Acidity scale
PMETAC	Poly (2-(methacryloyloxy)ethyltrimethylammonium chloride)
PMMA	block-methyl methacrylate
r	Solid particle radius
rpm	Speed of rotation of a machine expressed in revolutions per minute
SA	Sodium Alginate
SEM	Scanning electron microscope
Si	Silicone
SP	Silica Particle
SP-A	Silica Particle modified with APTMS (0.01 molecule nm <sup>-2</sup> )
SP-B	Silica Particle modified with APTMS (0.1 molecule nm <sup>-2</sup> )

SP-C	Silica Particle modified with APTMS (1 molecule nm <sup>-2</sup> )
SP-A-1	SP-A particles modified with sodium alginate (0.1/20% w/v))
SP-B-2	SP-B particles modified with sodium alginate (0.1/20% w/v))
SP-C-2	SP-C particles modified with sodium alginate (1/20% w/v))
SP-SA	particles modified with sodium alginate
SP-Sil	silane-modified silica particles
TMPS	trimethoxy(propyl)silane
UV-Vis	Ultraviolet–visible spectroscopy
v/v%	Volume concentration for percent volume
W	Watt
W/O	Water-in-oil
W/O/W	Water-in-oil-in-water
%w/v	Percent weight/volume

*Greek letters*

$\theta$	Contact angle
$\pi$	Pi
$\mu m$	Micrometer
$\Delta E$	Gibbs free energy
$\gamma_{o/w}$	Interfacial tension, oil/water interfaces
$\gamma_{s/o}$	Interfacial tension, solid particle/oil
$\gamma_{s/w}$	Interfacial tension, solid particle/water
$\phi_o$	Volume fraction of oil phase
$\zeta$	Zeta potential

## CHAPTER 1 INTRODUCTION

### 1.1 Background and problem identification

A system of stabilized droplets of one liquid dispersed in another immiscible liquid is called an emulsion. In conventional emulsions, surfactants or polymers act as stabilizers for the dispersed droplets. Common examples of this type of emulsion are observed in milk (oil-in-water) or butter (water-in-oil), as shown in **Figure 1.1**. In contrast, solid-stabilized (Pickering) emulsions (**Figure 1.2**) are composed of droplets stabilized by solid particles (**Figure 1.3**) and dispersed in a second immiscible liquid. The adsorption of particles occurs because their free energy is minimized when they are at the interface. Particle position at the interface is characterized by the formation of a characteristic contact angle  $\theta$  (the thermodynamic criteria for equilibrium). The solid particles adsorb at the oil/water interface when they are wetted by the two liquid phases, or in other words when  $0 < \theta < 180^\circ$ .  $\theta$  is measured by convention through the water phase as shown in **Figure 1.3**. Then, when the interface is sufficiently covered, droplet coalescence slows down, or is inhibited – in fact, Pickering emulsions are known to be exceptionally stable over periods of months to years.

**Oil-in-Water Emulsion**



**Water-in-Oil Emulsion**



**Figure 1.1** Emulsions are observed in Milk and Butter.

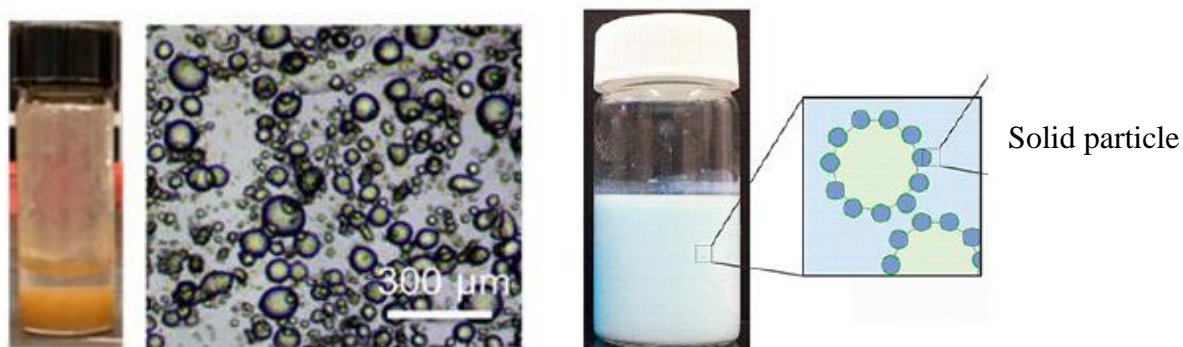


**Figure 1.2** Pickering emulsions stabilized by the adsorption of solid particles (Luo, Wang, Yoo, Wei, & Pentzer, 2018; Sadeghpour, Pirolt, & Glatter, 2013).

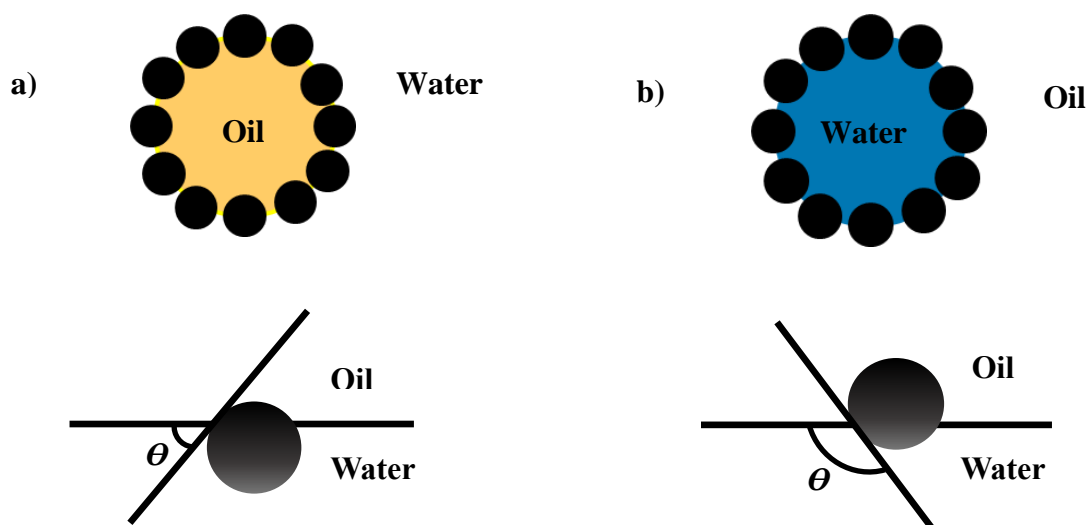


**Figure 2.3** Oil droplet dispersed in water (a) and water droplet dispersed in oil and contact angle ( $\theta$ ) of a particle at the liquid-liquid interface (b).

Generally, hydrophilic particles (contact angle  $\theta < 90^\circ$ ) tend to form oil-in-water emulsions, while hydrophobic particles (contact angle  $\theta > 90^\circ$ ) tend to generate water-in-oil emulsions (B. P. Binks, Isa, & Tyowua, 2013). Solid-stabilized emulsions offer significant potential advantages over conventional (surfactant-stabilized) emulsions, such as surfactant-free character and long-term stability while stored or transported. They have been a subject of great interest in chemistry (Y. Yang et al., 2017), physics, biology, and engineering in the last 15 years. Hence, they have been

considered in a wide range of industrial and technological processes such as drug delivery and pharmaceuticals, polymerization processing, enzyme-catalyzed reactions, micro-reactors, food systems, oil recovery and hazardous materials handling (S. Wang, He, & Zou, 2010). For example, the recovery of bitumen from oil sands can be hindered due to the creation of emulsions by the presence of natural surfactants combined with fine solids (clay) in oil sands (Whitby, Fornasiero, & Ralston, 2009). As an example, these emulsions are promising alternatives for skin care products and cosmetics since they can reduce skin irritation (Zoppe, Venditti, & Rojas, 2012). Salad dressing, cream puffs, and ice cream are examples of food that can present a solid-stabilized emulsion microstructure.

Numerous theoretical and experimental studies have been conducted over the years in order to improve the understanding of the stabilization mechanisms of Pickering emulsions. **However, investigations related to approaches that can promote the destabilization and separation of Pickering emulsions constituents have not been as widely studied so far.** In some industrial applications, Pickering emulsions are undesirable and there is a strong and important need to separate their constituents, both solid and liquids (Dyab, 2012). For example, one of the major issues in the petroleum industry is the breakdown of undesirable water-in-oil emulsions formed during different stages of the oil recovery process. **Therefore, developing green and ecofriendly methods to separate these constituents would be highly valuable.** In complement, only a limited number of studies have looked at the effect of viscosity on the processing (both stabilization and destabilization) of these multiphase fluids – an important factor to consider in many chemical engineering processes. This research provides a potential application pathway, for example, for the separation of oil and water in tar sands by minimizing the chemical residues and wastes with an easier and eco-friendly separation process.

**The main objective of this project is thus to elaborate a proof of concept to show that solid particles used to stabilize some benchmark Pickering emulsions can be functionalized by environmentally-friendly bio-macromolecules such as sodium alginate in order to destabilize on-demand, separate and reuse the fluids and solid particles initially forming the Pickering emulsions**



## 1.2 Organization of the thesis

This thesis contains two articles that have been published and one article that has been submitted to scientific journals, and consists of the following chapters:

*Chapter 2* provides a literature review on Pickering emulsions.

*Chapter 3* describes the objectives and the coherence of this work and related articles.

*Chapters 4, 5 and 6* present the articles describing the main achievements obtained in this work.

*Chapter 7* presents a general discussion about the main results.

*Chapter 8* states the conclusions and recommendations for future work.

## CHAPTER 2 LITERATURE REVIEW

### 2.1 Solid-stabilized (Pickering) emulsions

Liquid droplets stabilized by solid particles were reported for the first time in 1903 by Ramsden. However, the first systematic study on solid-stabilized liquid droplets in a second immiscible liquid was conducted by Pickering in 1907 (S. U. Pickering, 1907). Solid-stabilized emulsions studies became more sophisticated over the years and, in the past decade, became focused on a microscopic level of understanding (D. W. Liu & He, 2011). Most of the recent studies have been published on **surface chemistry, size, and structure of particles** (Kruglyakov, Nushtayeva, & Vilkova, 2004). The effectiveness of solid particles to act as surfactant-free emulsifiers in Pickering emulsion systems depend on various factors such as wettability, particle concentration, and particle size, which are discussed below.

### 2.2 Physicochemical properties of solid particles

#### 2.2.1 Type of solid particles

The most significant difference between a Pickering emulsion and a classical emulsion is the type of interfacial stabilizer between the two liquid phases. In the case of Pickering emulsions, solid particles serve as the stabilizing agent, whereas in classical emulsions molecular surfactants are used. Thus, the stability, type of emulsion – oil-in-water (O/W) or water-in-oil (W/O) –, and morphology of Pickering emulsions are strongly dependent on particle properties. In order to obtain a stable Pickering emulsion, it is important to use the right kind of nano/micro-particles at the interface between the two liquids depending on the application. Several types of particles and oil phases have been employed to prepare Pickering emulsions, as listed and summarized in **Table 2.1**.

**Table 2.1. Published studies on solid-stabilized (Pickering) emulsions including types of particles, oil phases, and resulting emulsion type.**

Particles	Type of oil phase	Type of emulsion
Silica (20 nm)	Toluene or dodecane	O/W (K. Liu, Jiang, Cui, & Binks, 2017; Zhu et al., 2017; Zhu, Jiang, Liu, Cui, & Binks, 2015)
Silica (13-53± 2 nm)	Exxsol D60: a mixture of dearomatized hydrocarbons with chain lengths of 10–12 carbons containing n-alkanes, iso-alkanes, cyclics and a small fraction of aromatics (< 2%).	O/W (Bjorkegren, Nordstierna, Torncrona, & Palmqvist, 2017)
Silica nanoparticles (15 nm) and pure cationic surfactant	Dodecane	O/W (Rodrigues, 2007)
Amorphous fumed hydrophilic silica powder (5-30 nm), highly negatively charged Ludox HS-30 silica sol (15 nm), highly positively charged colloidal zirconia sol (5–10 nm)	Various adipate oils: dodecane, diethyl adipate, dibutyl adipate, dimethyl adipate, bis(2-ethylhexyl) adipate and dipropyl adipate	O/W (B. P. Binks & Yin, 2016)
Colloidal hydrophilic silica (Snowtex 20)	Di-isopropyl adipate	O/W (Fuma & Kawaguchi, 2015)
Silica (5-30 nm)	Poly(dimethylsiloxane) (PDMS)	O/W and W/O (B. P. Binks & Lumsdon, 2000)

Aerosil 200 silica powder (12 nm)	Toluene	O/W (B. P. Binks & Lumsdon, 1999)
Silica (2-100 nm)	Paraffin oil	O/W (Sadeghpour et al., 2013)
Silica Janus nanosheets (30-50 nm)	Toluene	O/W (F. Liang et al., 2011)
Fe <sub>3</sub> O <sub>4</sub> (30 nm)	PDMS and dodecane	O/W (J. Zhou et al., 2011)
Fe <sub>3</sub> O <sub>4</sub> (NA)	Dodecane and butyl butyrate	O/W (J. Zhou, Wang, Qiao, Binks, & Sun, 2012)
Fe <sub>3</sub> O <sub>4</sub> (402 nm)	Corn oil	W/O/W (Lin, Zhang, Li, & Deng, 2016)
Montmorillonite and/or Laponite clay platelets (30 nm with thickness of 1 nm)	Mixtures of a lipid of monoglyceride type (monolinolein) with different kinds of oils (glycerol trioleate, R- (+)-limonene, and styrene)	O/W (Guillot, Bergaya, de Azevedo, Warmont, & Tranchant, 2009)
Clay Laponite XLG (40 nm)	Polydimethylsiloxane (PDMS)	O/W (Reger, Sekine, & Hoffmann, 2012)
Disc-like Laponite clay	Paraffin wax	O/W (C. Li et al., 2009)
Carbon Nanotubes	Cyclohexane	O/W (W. Chen, Liu, Liu, Bang, & Kim, 2011)
2D sheet-shaped layered double hydroxide (LDH) coupled carbon nanotube (CNT) nanohybrid (LDH-CNT)	Toluene	W/O (Shan et al., 2015)
Poly(N-isopropylacrylamide) microgels (250 - 760 nm)	Hexadecane and dodecane	O/W (Destribats et al., 2014)

Poly(N-isopropylacrylamide) microgels (PNIPAM)	Octanol	O/W (Ngai, Behrens, & Auweter, 2005)
Pure PNIPAM microgels ( $792 \pm 60$ nm) and PNIPAM-carrying particles ( $817 \pm 40$ nm)	heptane, hexadecane, trichloroethylene, 1-undecanol and toluene	O/W (Kawaguchi, 2008)
Poly(N-isopropylamide)-co-(methacrylic acid) (PNIPAM-co-MAA)	hexane	O/W (Li, Ming, Wang, & Ngai, 2009)
Poly(N-isopropylacrylamide) (PNIPAM)	Octanol	O/W (To Ngai, 2006)

---

### 2.2.2 Particle size, concentration and shape

Pickering emulsion stability can be influenced by a number of factors, including particle wettability and concentration, size and shape, and viscosities of the liquid phases. To obtain a stable Pickering emulsion, the solid particles need to be adsorbed at the interface and act as emulsifiers. Hence, we expect that if the particle concentration is increased, the stability of the Pickering emulsions will also increase; alternatively, this may increase the volume of emulsified phase in the system or decrease the emulsion droplet size (B. P. I. Binks, L., Tyowua, A. T., 2013). For many solid-stabilized emulsion systems, a complete coverage of the droplets by the particles is needed to achieve stability and to form a strong barrier against droplet coalescence. A higher particle concentration can also contribute to the formation of a 3-D network of particles surrounding the droplets as shown in **Figure 2.1**. This image illustrates the microstructure of a Pickering emulsion stabilized by starch particles at the oil-water interface, in the form of a densely packed layer (Song et al., 2015).

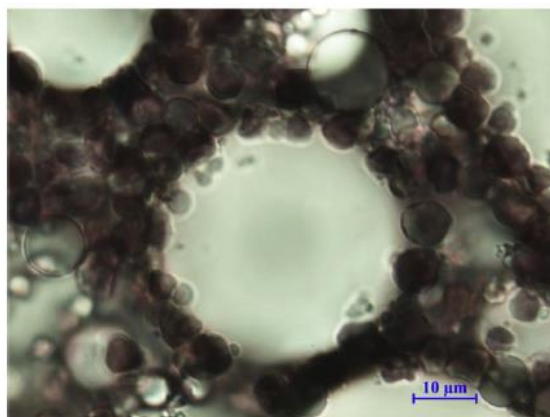


**Figure 2.1** Micrograph of an O/W emulsion stabilized by starch particles: a densely packed layer and a 3-D network (Song et al., 2015).

In addition, as the concentration of particles increases, the droplet size needs to decrease in order to accommodate more particles at the interface (Bernard P. Binks, 2002). Binks and Whitby reported that, as the particle concentration of mono-disperse silica particles increased by a factor 10, the average diameter of silicone oil droplets in water decreased by a factor of 8 (B. P. Binks & Whitby, 2004). Another factor which affects the stability of emulsions is particle shape. In most of the theoretical studies on Pickering emulsions, spherical particles have been used to simplify analysis as well as calculations. But, practically, the solid particles used for the preparation of solid-stabilized emulsions are not necessarily spherical, as illustrated in **Figure 2.2**. The morphology and surface roughness are factors that can play an important role on the capacity of emulsification. Therefore, other shapes of solid particles rather than spherical have been also investigated (**Table 2.2**). Surface roughness of non spherical particles can also influence their wetting behaviour by two liquids phases via the packing density and the free energy of detachment. Different size of particles has been used in the literature review for the production of Pickering emulsions ranging from nanometres to micrometres. It has been reported that the droplet size of Pickering emulsions decreases as the particle size decreases - however, only if the other properties of particles such as wettability, shape and concentration remain identical (M. Rayner, Timgren, Sjo, & Dejmek, 2012). Binks and Lumsdon (B. P. Binks & Lumsdon, 2001) experimentally investigated the effect of particle size on emulsion stability and indicated that larger particles form less stable emulsions compared to smaller particles. Quantitatively, the desorption energy depends on the square of the particle radius as shown in equation 2.2; therefore, less energy is required to move the particles

from the liquid interface. **Table 2.2** summarizes different shapes of solid particles used for the preparation of Pickering emulsions.

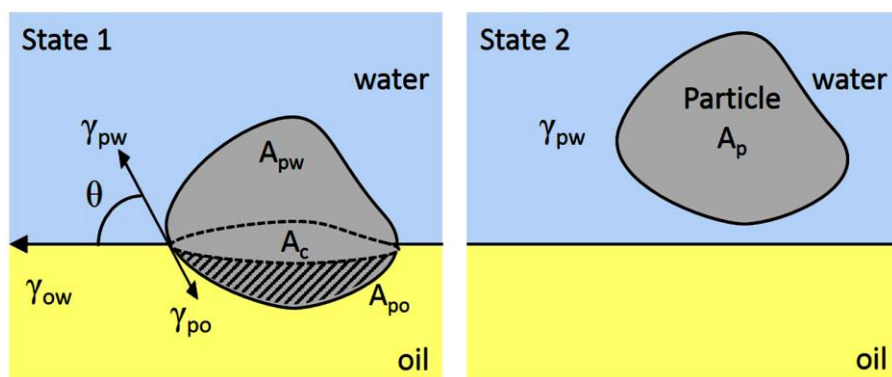


**Figure 2.2** Irregular particles at the interface between oil and water  $\gamma_{so}$ ,  $\gamma_{sw}$ , and  $\gamma_{ow}$  are the interfacial tensions (or free interfacial energies) of the solid particle/oil, solid particle/water, and oil/water interfaces,  $A_{pw}$  and  $A_{po}$  represent the surface area of the solid particle in contact with the oil and water phases, and  $A_c$  is for the area of the oil and water interface which is occupied by the cross section of the solid particle.  $A_p$  represents the total surface area of the solid particle .

(Marilyn Rayner et al., 2014)

**Table 2.2** Several shapes of solid particles used in the preparation of Pickering emulsions.

Particle type and concentration	Particle size	Particle shape	Type of emulsion
monodisperse polystyrene latex particles) (0.25-2% wt%)	0.029-2.70 $\mu\text{m}^3$	spherical	W/O (B. P. Binks & Lumsdon, 2001)
corn, tapioca, sweet potato, and waxy corn starch nanoparticles (1%)	100 -220 nm	spherical and ellipsoidal	O/W (Ge et al., 2017)
kaolinite clay particles treated with asphaltenes,			

hydrophilic and hydrophobic colloidal silica, hydrophobic polystyrene latex microspheres, as well as fumed silica dry powders treated with silanization	12 nm, 14 nm	nanospheres	W/O (Yan, Gray, & Masliyah, 2001)
Hematite ( $\alpha$ -Fe <sub>2</sub> O <sub>3</sub> ) polystyrene (1-10% (wt%))	Aspect ratio of 1.0-6.7 Aspect ratio of 1.0-3.7	spindle-like ellipsoidal and spherical	W/O, O/W (Madivala, Vandebril, Fransaer, & Vermant, 2009)
Soda lime glass (2-16 wt%)	53-63 $\mu$ m	microspheres	O/W (Wan & Fradette, 2017)

### 2.2.3 Oil viscosity

The oil phase viscosity is another key factor that can affect the stabilization of Pickering emulsions as well as their destabilization. Previous studies demonstrated that oil viscosity can affect the contact force and adsorption time of solid particles during the production of Pickering emulsions. Increasing the viscosity of the dispersed oil phase results in the formation of bigger droplets, whereas droplet size remained almost constant with lower viscosity oils. When oil viscosity decreases, more interfacial area can be generated, resulting in more particle interfacial adsorption and coverage. In addition, as the oil viscosity increases, the volume of emulsified oil reduces. This shows that the stabilization of these systems is greatly affected by viscosity. The required time of mixing to form an emulsion was also introduced as a critical key-parameter to stabilize highly viscous oil-in-water emulsions, especially with particles above 1  $\mu$ m in size. For a given mixing time, highly viscous oil-in-water emulsions form less emulsified volume, thereby suggesting that viscosity acts as a barrier to the emulsification process (Fournier, Fradette, & Tanguy, 2009). **Table 2.3** presents recent studies on the effect of oil viscosity on the emulsification of Pickering emulsions.



**Table 2.3 Published studies on the effect of oil phase viscosity for the processing of solid Pickering emulsions**

Particle	Oil type and Viscosity	Type of emulsion
Glass and polystyrene microspheres (2.35 and 65 $\mu\text{m}$ )	Silicone oils (29.1, 12.13, 8.124 and 4.85 cSt)	O/W (Tsabet & Fradette, 2016)
Bare and modified glass beads (22.4 $\mu\text{m}$ )	Silicone oils (20, 50, 100, 200, 500, 1000 and 5000 cSt)	O/W (Tsabet & Fradette, 2015a, 2015c)
Glass beads (3.49-27.6 $\mu\text{m}$ )	Silicone oils (20, 50, 100, 200, 500, 1000 and 5000 cst)	O/W (Tsabet & Fradette, 2015b)

## 2.3 Wettability of particles

Colloidal particles can be interfacially active, like surfactant molecules (B. P. Binks & Rocher, 2009), and can spontaneously adsorb and accumulate at the interface between two immiscible liquids. However, it is important to mention that their surface activity is not necessarily due to an amphiphilic nature. These solid particles can have a homogeneous surface chemical composition and still display interfacial activity, which minimizes the system's free energy (B. P. Binks et al., 2013).

The wettability is a key factor which determines the type, as well as the stability, of Pickering emulsions. Particle wettability defines how strongly the particles are adsorbed at the interface, determines their position (**Figure 2.3**), and can be quantified by the measurement of the contact angle  $\theta$  (see **Figure 1.3**). The contact angle is measured through the water phase, and is given by Young's equation:

$$\cos \theta = \frac{\gamma_{so} - \gamma_{sw}}{\gamma_{ow}} \quad \text{Equation 2-1}$$

where  $\gamma_{so}$ ,  $\gamma_{sw}$ , and  $\gamma_{ow}$  are the interfacial tensions (or free interfacial energies) of the solid particle/oil, solid particle/water, and oil/water interfaces, respectively. Hydrophilic particles present a contact angle inferior to  $90^\circ$ , and the majority of the particle's surface is wetted by the aqueous phase. Hydrophobic particles display a contact angle greater than  $90^\circ$ , and they are mostly wetted by the oil phase. Particles that are wetted nearly equally by both phases display a contact angle nearly equal to  $90^\circ$  (Tang, Quinlan, & Tam, 2015). In this case, the oil/water interface is almost planar, as **Figure 2.3** shows. Complete wetting of the particle in either the oil or water phase leads to particle instability at the interface.

The minimum free energy which is required to remove a single particle from the interface, into either the oil or water phase, can be calculated with a variation of Young's equation:

$$\Delta E = \pi r^2 \gamma_{ow} (1 \pm \cos \theta)^2 \quad \text{Equation 2-2}$$

where  $\gamma_{ow}$  is the interfacial tension between the oil and water phases, and  $\theta$  is the measured equilibrium contact angle through the water phase. For particle removal from the interface towards the water phase, the sign of  $\cos \theta$  is negative; for the removal from the interface to the oil phase, the sign is positive. For example, the amount of energy required to remove a  $65 \mu\text{m}$  polyethylene microsphere from a silicone oil/water interface ( $\gamma_{o/w} = 42 \pm 2 \text{ mJ/m}^2$ ,  $\theta_w = 94 \pm 2^\circ$ ) is  $4.6 \mu\text{N}$  (theoretically) - experimentally measured as  $4.7 \mu\text{N}$  (Tsabet & Fradette, 2016).

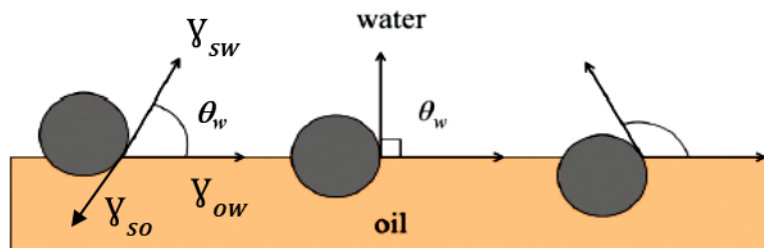


**Figure 2.3** Position of a solid particle at the oil/water interface with a contact angle  $\theta$  measured through the water phase. Left:  $\theta < 90^\circ$  (hydrophilic); Center: equal to  $90^\circ$  (equally hydrophilic and hydrophobic); Right:  $\theta > 90^\circ$  (hydrophobic) (Tang et al., 2015).

For a single solid particle located at the interface between oil and water, the three interfacial tensions ( $\gamma$ ) are related to the contact angle  $\theta_{o/w}$  (measured in the water phase) and can be calculated by the Young equation:

$$\gamma_{ow} - \gamma_{sw} = \gamma_{ow} \cos \theta_{ow} \quad \text{Equation 2-3}$$

Therefore, based on the interactions between the solid and two liquid phases, this equation can calculate the extent to which a particle will penetrate at the interface between two liquids.

### 2.3.1 Wettability control of particles via surface modification

Solid particle can be adsorbed at the interface between two phases irreversibly (Thompson et al., 2015), even if exposed to temperatures above 70°C (Dion, Raphael, Tong, & Tavares, 2014). One of the key factors that can determine the formation and stability of Pickering emulsions is particle wettability. Modifying the surface chemistry of particles allows tuning of particle wettability. A recent example is the preparation of Janus particles, which are biphasic colloids with two sides of distinct chemistry and wettability. These Janus particles can be used for the stabilization of multiphasic fluid mixtures such as emulsions because of their amphiphilicity (Tu & Lee, 2014b).

It is often necessary to tailor the wettability of solid particles via either surface chemistry or surface roughness to make them partially hydrophilic or hydrophobic in order to stabilize Pickering emulsions. There are two main approaches to adjust and control particle wettability: (1) physical adsorption or (2) chemical grafting of various surfactants, small molecules and polymers. The physical adsorption of small molecules, surfactants or supramolecular complexation between particles, is achieved via electrostatic interactions, hydrogen bonding and/or Van der Waals forces. Chemical grafting approaches are the most common and effective techniques to tune the surface properties of particles. **Table 2.4** summarizes the physical and chemical approaches to tune the wettability of solid particles, in order to form Pickering emulsions.

**Table 2.4 Typical methods for tuning particle wettability in order to form Pickering emulsions.**

Physical adsorption			
Type of solid particle	Surface modifier	Type of emulsion	Application
Silica	Oleic acid	O/W (Sadeghpour et al., 2013)	Body-care
	Palmitic acid	W/O (Santini, Guzmán, Ferrari, & Liggieri, 2014)	N/A
	Dialkyl adipate	O/W (B. P. Binks & Yin, 2016)	Health and body care
	PEI	O/W, W/O, and W/O/W (Williams, Armes, Verstraete, & Smets, 2014)	Encapsulation and retention of fragrances
	cetyltrimethylammonium bromide (CTAB) and sodium dodecyl sulfate (CDS) Cationic surfactants	O/W (Zhu et al., 2015)	Switchable cycles
	8-hydroquinoline	O/W, W/O (Haase, Grigoriev, Moehwald, Tiersch, & Shchukin, 2010)	Encapsulated corrosion inhibitor for coatings
CaCO <sub>3</sub>	Fatty acids	O/W, W/O (Cui, Cui, Zhu, & Binks, 2012)	N/A

$\text{Al}_2\text{O}_3$	Octyl gallate	W/O (Sturzenegger, Gonzenbach, Koltzenburg, & Gauckler, 2012)	Various fields of application
Cellulose nanocrystal (CNC)	Cationic alkyl ammonium surfactants dodecyldimethylammonium bromide (DMAB) and cetyltrimethyl-ammonium bromide (CTAB)	O/W, W/O (Z. Hu, Ballinger, Pelton, & Cranston, 2015)	Emulsion formulation applications
<b>Chemical modification</b>			
Type of solid particle	Surface modifier	Type of emulsion	
Silica	Organosilanes	O/W (H. Yang, Zhou, & Zhang, 2013)	Separation and recycling of solid catalysts
	$\mu$ -PEG-b-PS-b-PIPSMA	O/W, W/O and O/W/O (M. Liu et al., 2016)	Controlled encapsulation and Release of actives
	cationic poly (2- (methacryloyloxy)ethyltrimethylammonium chloride) (PMETAC)	O/W (Tan, Gautrot, & Huck, 2011)	Feature for biological systems
	N,N-dimethylacetamide	O/W, W/O (C. Liang, Liu, & Xu, 2014)	Triggering phase separation.
$\text{Fe}_3\text{O}_4$	Silane coupling agents	O/W (J. Zhou et al., 2012)	N/A
Gold nanoparticle	thiol-terminated PEG chains and short alkane-thiol molecules	O/W (Larson- Smith & Pozzo, 2012)	Nanomedicine & renewable energy

---

Cellulose nanocrystal (CNC)	poly(N-3-(dimethylamino)propyl methacrylamide) (PDMA PMAm) and poly(N,N-(diethylamino)ethyl methacrylate) (PDEAEMA)	O/W (Glasing, Bouchard, Jessop, Champagne, & Cunningham, 2017)	Industrial separation processes, stimuli-responsive Pickering emulsifier, cationic vectors for gene delivery
-----------------------------	---	--	--

---

Great efforts have been devoted to tailor the wettability of solid particles by using various molecules and chemicals which are mostly surfactants or polymers, as listed in **Table 2.4**. Some of these surface modifiers are derived from artificial synthetic chemicals, with many disadvantages such as complex synthetic process, difficult recycling and product separation, as well as toxic waste production (Kupczak, Bratasz, Krysiak-Czerwenka, & Kozłowski, 2018). In addition, emulsions stabilized with surfactants (conventional emulsions) have additional costs and environmental impacts compared to Pickering emulsions (Y. Zhang et al., 2019). Therefore, bio-based surface modifiers are promising alternatives.

Sodium alginate (SA -  $\text{NaC}_6\text{H}_7\text{O}_6$ ) can be considered as a “green” surface modifier because it is bio-based coming from cell walls of brown algae and biodegradable. It is a linear polysaccharide isolated from marine brown algae and is comprised of 1,4- $\beta$ -D-mannuronic (M) and  $\alpha$ -L-guluronic (G) acids. SA forms a gel via its G units that can be crosslinked (George & Abraham, 2006) by the addition of divalent and multivalent cations such as  $\text{Ca}^{2+}$  (K. Y. Lee & Mooney, 2012), or under acidic conditions (George & Abraham, 2006), depending on its pKa. The pH sensitivity of SA is a result of the numerous free carboxyl groups along its backbone, as **Figure 2.4** illustrates (Schnepp, Hall, Hollamby, & Mann, 2011). SA has been extensively investigated by the food and pharmaceutical industries, environmental engineering, regenerative medicine, and chemical engineering (K. Y. Lee & Mooney, 2012; Pallandre, Decker, & McClements, 2007; Szekalska, Pucilowska, Szymanska, Ciosek, & Winnicka, 2016; Thakur et al., 2018).

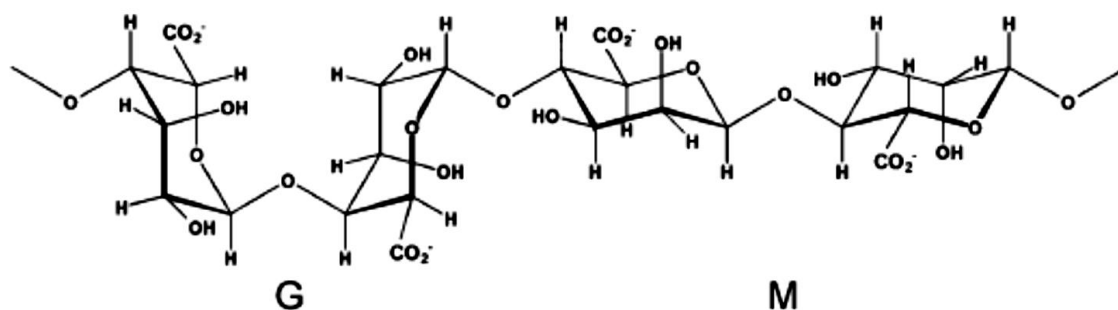


**Figure 2.4** Chemical structure of sodium alginate showing guluronate (G) and mannuronate (M) units (Schnepf et al., 2011).

SA has been used by Chen et al. (K. Chen et al., 2017) as a surface modifier for silica nanoparticles, in order to trigger the delivery of an encapsulated compound via a pH variation. SA-surface modified particles exhibited satisfactory emulsification ability via the formation of a three-dimensional network of grafted SA chains. In addition, sodium alginate surface-grafted microparticles were developed by Yang et al. (X. Yang et al., 2019) as both stabilizers for W/O Pickering emulsions, and enzyme anchors to enhance interfacial bio-catalysis. In this system, the highly hydrophilic property of SA-modified microparticles was tuned by adjusting the length of the hydrophobic carbon chain of the grafted silane coupling agent. Sodium alginate molecules were modified with degradable diacetone acrylamide to improve its hydrophobicity (W. Zhang, Sun, Fan, Li, & He, 2017). Then, SA was crosslinked by  $\text{Ca}^{+2}$  to form solid particles having the appropriate hydrophobicity and size. Finally, the pH-responsive performance of these modified SA particles was compared to the un-modified SA at different pHs. SA modified particles presented a better and acceptable pH-responsive as compared to un-modified SA for the release of curcumin as the drug model. However, there is a significant gap in the literature review to assess the use of these surface-SA modified particles for the ease separation and recovery of the emulsion's constituents by a simple filtration approach. In the present work, we used two types of silane agents simultaneously to graft SA which could control the wettability of our SA-surface “sticky particles” as described in the mechanism (**Scheme 5.1**) in chapter 5.

### 2.3.2 Multiple Pickering emulsions

In complement, double emulsions, the simplest form of multiple emulsions, have also been intensively investigated from a fundamental perspective, as well as for various potential industrial

applications. A one-step strategy for the formation of oil-in-water-in-oil (O/W/O) double emulsions using oil-soluble polymers and hydrophobic silica nanoparticles was reported by Kim et al. (S. Kim, Kim, & Choi, 2018). Poly(methyl methacrylate), polylactide, and polyvinyl acetate polymers could stabilize the O/W emulsion, while hydrophobic silica particles could form the W/O emulsions by adsorbing those polymers on their surface. The number of sub-inclusions was controlled via a phase inversion mechanism. The formation of multiple droplets in their approach was controlled by adjusting two parameters: the concentration of hydrophobic silica particles and the volume fraction of the internal phase (**Figure 2.5**).

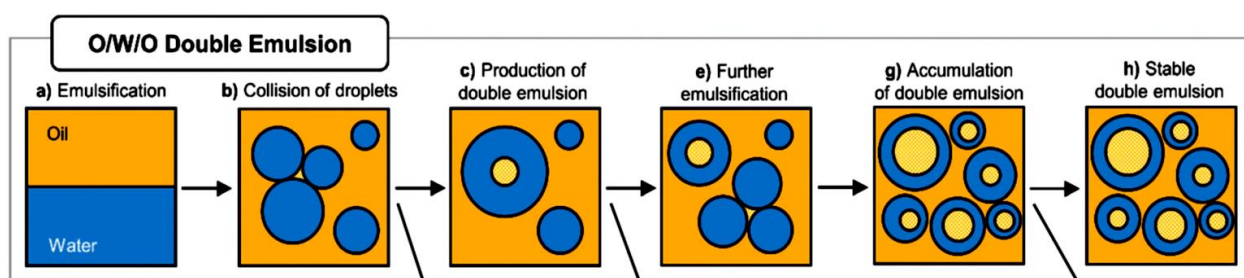


**Figure 2.5** Preparation process of double emulsion by phase inversion (S. Kim et al., 2018).

In a study by Williams et al. (Williams, Armes, et al., 2014), poly(ethylene imine) (PEI) was used to modify the surface properties of fumed silica particles in order to produce water-in-oil-in-water (W/O/W) emulsions via phase inversion. The multiple emulsions were prepared in two steps, by using two batches of hydrophilic and hydrophobic PEI/silica hybrid particles, and by varying the oil volume fraction between 5 and 42%. In another study by Liu et al. (M. Liu et al., 2016), the surface of silica nanoparticles was modified by grafting ABC miktoarm star terpolymers consisting of poly(ethylene glycol), polystyrene, and poly[(3-triisopropoxy)silyl]propyl methacrylate] ( $\mu$ -PEG-*b*-PS-*b*-PIPSMA). These designed mixed brush-coated hairy nanoparticles permitted the stabilization of oil-in-water-in-oil O/W/O multiple emulsions in a single-step process, as indicated in **Figure 2.6**.



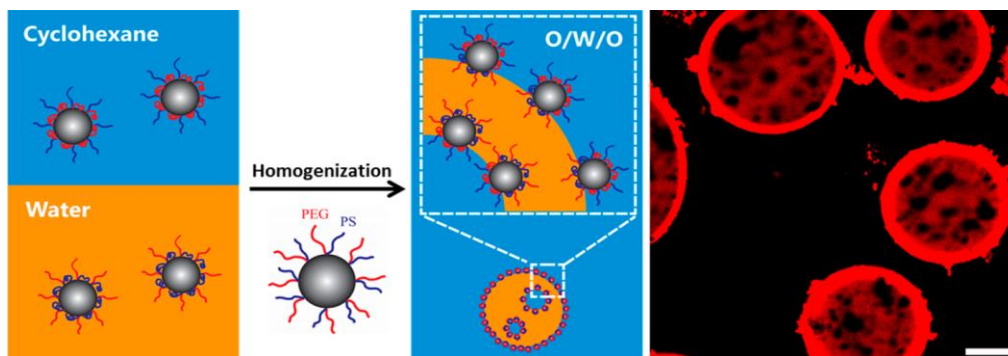


**Figure 2.6** Schematic diagram of production of emulsions and confocal image of the resulting multiple emulsions (M. Liu et al., 2016).

In another investigation by Thompson et al. (Thompson et al., 2015), a combination of hydrophilic and hydrophobic diblock copolymer worms were used to prepare both O/W/O and W/O/W Pickering double emulsions. Their approach involved two steps of processing and rational design principles based on the ability to tune the mean droplet diameter by the systematic variation of the shear rate during homogenization. In addition, they were able to obtain triple and even quadruple emulsions using highly anisotropic Pickering emulsifiers ( $G_{37}$ - $H_{60}$ - $B_{30}$  triblock and  $L_{16}$ - $B_{37}$  diblock copolymer worms).

A combination of two types of nanocelluloses (C12-modified and native) were used by Cunha et al. (Cunha, Mougel, Cathala, Berglund, & Capron, 2014) to form surfactant-free oil-in-water-in-oil (O/W/O) double emulsions. The chemical modification of cellulose involved the partial esterification of the hydroxyl groups on the surface with a fatty acid chloride, namely lauroyl chloride (C12). Those double emulsions showed different globule size, and larger droplets encapsulated hundreds to thousands of small inner droplets. By selecting specific combinations of nanocelluloses, they were able to control the average size of the globules. The concentration and surface accessibility of the modified cellulose nanoparticles, as well as the length of the nanoparticles, were crucial parameters in their system to stabilize these double emulsions. These emulsions displayed acceptable stability over a month, with limited coalescence in the first hours because of low coverage of the outer interface. Multiple emulsion's preparation typically needs a complex procedure via two steps and using two different and complementary interfacial stabilizers. The literature review highlights that mostly surfactants have been used for the preparation of multiple emulsions.

## 2.4 Destabilization of Pickering emulsions

### 2.4.1 Microscopic destabilization mechanisms

There are a number of phenomena that can cause the destabilization of Pickering emulsions, as indicated in **Figure 2.7**. The first mechanism is **coalescence**, where larger droplets are formed by the merging of smaller neighboring droplets. However, Pickering emulsions with droplets fully covered by solid particles are resistant to coalescence. Solid particle layers at the interface of droplets create mechanical barriers and inhibit droplets merging together. Partially coated droplets are also resistant to coalescence, since solid particles can move to the area of droplet-droplet contact (Fredrick, Walstra, & Dewettinck, 2010), and there is a threshold coverage where resistance to coalescence drops (Whitby & Wanless, 2016). **Flocculation** is a second type of destabilization that is usually reversible, and which tends to increase the creaming rate as the apparent drop density is smaller than that of the continuous phase, otherwise, the drop is regimenting. During the flocculation process, emulsion droplets come together and form aggregates.

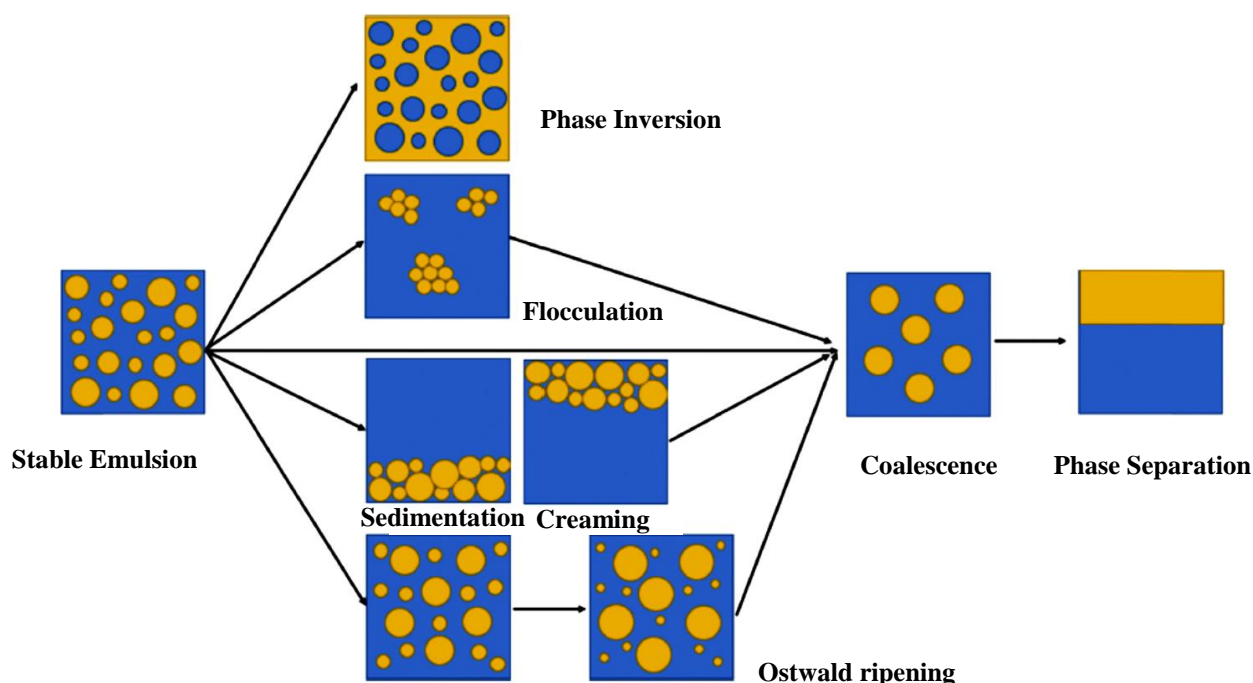


**Figure 2.7** Different instability mechanisms in solid stabilized emulsions (Y. T. Hu, Ting, Hu, & Hsieh, 2017)

It should also be noted that extensive flocculation can lead to the formation of emulsions with a gel-like structure by adjusting the surfactant/particle ratio (B. P. Binks & Rodrigues, 2007). Due to gravity, **creaming and sedimentation** processes take place in emulsions; a concentration gradient is created because of density differences between the two immiscible liquids (Fredrick et al., 2010). For instance, oil droplets in an oil-in-water emulsion can be subjected to creaming if the oil has a lower density compared to the water phase. Destabilization can occur via a fourth mechanism, called **Ostwald ripening**, during which the emulsion droplets change size over time without any direct contact. Ostwald ripening takes place when the Laplace pressure in smaller droplets, which is larger compared to large droplets, leads to mass transfer from the smaller droplets to the larger ones, via the continuous phase – small droplets decrease in size, and larger ones grow. Experimentally, it is presented (Cervantes Martinez et al., 2008) that resistance to Ostwald ripening in a particle-stabilized foam is when  $E > \gamma_{aw}/2$ . Finally, a last destabilization process in emulsion systems can occur via **phase inversion**. During this process, the dispersed phase becomes the continuous phase, and vice versa, as demonstrated in **Figure 2.8**. An increase in the dispersed phase volume fraction can induce a catastrophic phase inversion in Pickering emulsions, while transitional phase inversion can be triggered by the variation of the solid particle wettability (B. P. Binks & Olusanya, 2017). Coalescence can play a key role in phase inversion (Whitby & Wanless, 2016) via the incorporation of continuous phase drops into the dispersed phase.

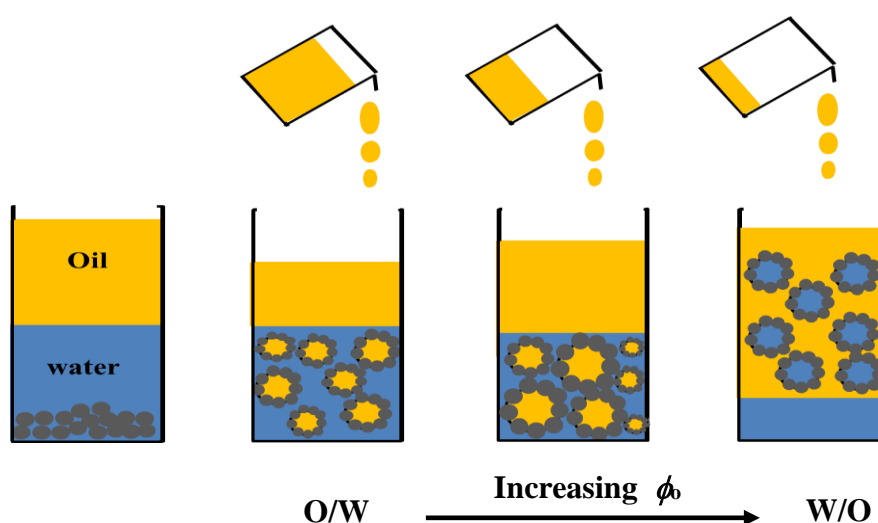


**Figure 2.8** Schematic representation of catastrophic phase inversion in Pickering emulsions: the continuous addition of the dispersed phase (oil) sequentially turns the emulsion from O/W (left) to W/O (right).

The mass transfer between drops of different sizes, or between drops and the continuous phase can induce the destabilization in Pickering emulsions. Close contact between the liquid droplets caused molecules transfer from smaller droplets to the larger drops (Ostwald ripening) (Whitby & Wanless, 2016) as shown in **Figure 2.9**. Larger drops increased in size over time and could not resist the coalescence process because of the insufficient particle surface density.

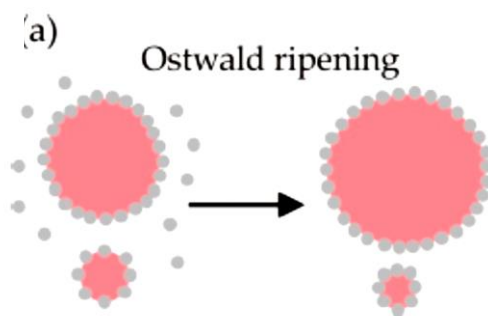


**Figure 2.9** Ostwald ripening: small droplets are shrinking and larger droplets are swelling by mass transfer from smaller droplets to the bigger ones (Whitby & Wanless, 2016)

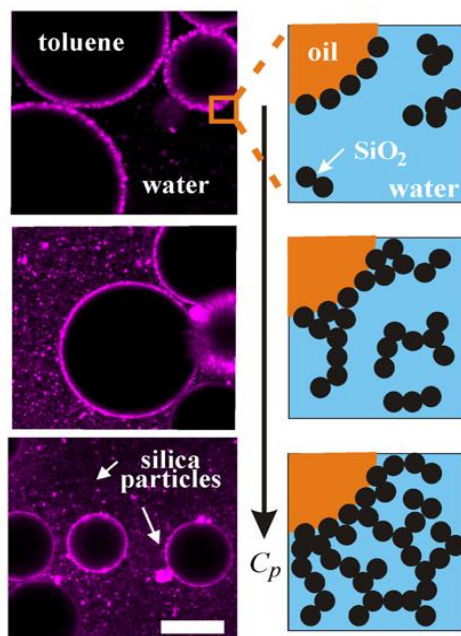


**Figure 2.10** Changes in emulsion microstructure during destabilization (Juarez & Whitby, 2012).

At the same time, the coagulation of free silica particles in the aqueous phase caused the formation of aggregates and compact clusters, leading to emulsion instability via droplets flocculation and toluene transfer through the pores (**Figure 2.10**), as described above.

## **2.4.2 Methods and processes to destabilize Pickering emulsions**

There are much fewer studies on processes to break and separate Pickering emulsions constituents. In some applications, solid stabilized emulsions are undesirable and need to be broken or destabilized in order to separate the constituents – for example for targeted drug delivery (McClements, 2012). Also, as mentioned previously, a major challenge in the petroleum industry is the formation of undesirable water-in-oil emulsions, which are formed at various stages of the oil recovery process (Fan, Simon, & Sjoblom, 2010). These undesirable stable emulsions are formed due to a physically cross-linked film of asphaltenes at crude oil-water interfaces during various stages of oil recovery.

There are three general methods to break solid stabilized emulsions: thermal (B. P. Binks, Murakami, Armes, & Fujii, 2005; Martinez-Palou et al., 2013), mechanical, electrical and chemical approaches (Dyab, 2012).

For the mechanical approach, Pan et al. (Pan, Lyu, & Tang, 2017)| used centrifugation at different speeds and durations to induce separation in fluorinated Pickering emulsions, as illustrated in **Figure 2.11**. They observed that coalescence efficiency increased with increasing centrifugal speed and for longer duration – as expected intuitively.

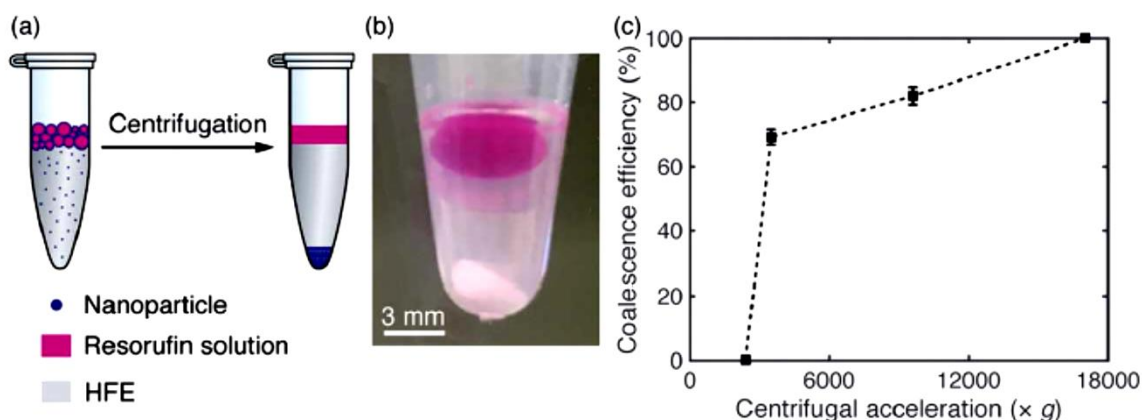


**Figure 2.11** Centrifugation to induce the coalescence of drops (a). Image of coalesced drops after centrifugation at 9600g after 10 min (b). Efficiency of coalescence under different centrifugal accelerations for 15 min (Pan et al., 2017)(c).

Fournier et al. (Fournier et al., 2009) presented that Pickering emulsions can be destroyed by shear forces during mixing. Their experiments were performed at different mixing intensities and time for the different oil viscosities. After emulsification, and a given rest period, those emulsions were subjected to the second intense agitation for a given mixing time. That second mixing caused a decrease in emulsified oil fraction in their systems inducing the destabilization process.

Hwang et al (Hwang, Singh, & Aubry, 2010) experimentally demonstrated that Pickering emulsions can be destabilized using external electric fields. The coalescence of water droplets in decane, and silicone oil droplets in corn oil, stabilized with extendospheres, was studied with the application of a uniform electric field. The primary phenomenon taking place during coalescence was the movement of particles on the droplet surface. Although there are no electrostatic forces between neutral particles in a uniform electric field, particles could move along the drop surface due to dielectrophoretic forces coming from the non-uniform electric field induced by the drop itself. Consequently, particles motion could break the particles barrier, leading to coalescence, as illustrated in **Figure 2.12**.

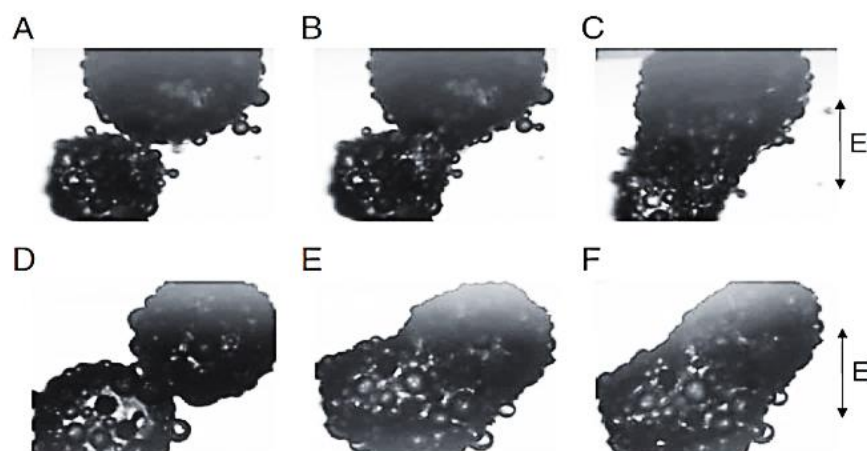


**Figure 2.12** Coalescence is induced between droplets by applying an electric field (Hwang et al., 2010).

Whitby et al. studied the addition of an anionic surfactant and/or salt on the stability of dodecane-in-water emulsions, stabilized by partially hydrophobized silica particles (Whitby et al., 2009). Their emulsions containing sodium dodecyl sulfate and sodium chloride displayed stability against coalescence but revealed creaming over time. The level and rate of creaming gradually reduced as the salt concentration in the diluted emulsion increased (Whitby et al., 2009). It was concluded that the presence of a surfactant in the emulsion may cause depletion flocculation, as well as the dramatic release of excess particles in concentrated emulsions, resulting in droplets creaming. Read et al (E. S. Read, 2004) prepared O/W and W/O emulsions using pH-sensitive polystyrene latexes. A number of parameters were varied, such as the polarity of the oil phase, the concentration of latex, surface concentration of copolymer which were poly(2-(dimethylamino)ethyl methacrylate and poly(methyl methacrylate), and pH. Non-polar oils, such as *n*-dodecane, formed O/W emulsions, while polar oils such as 1-undecanol gave W/O emulsions. These pH-responsive emulsions could go under either rapid phase inversion (**Figure 2.13a**) or demulsification (**Figure 2.13b**) via pH adjustment. In case of phase inversion, the initially formed O/W emulsions turned to W/O emulsions as illustrated in **Figure 2.13a**. While using *n*-dodecane, changing the pH from 8 to 3 induced demulsification, separation of oil phase on the top as presented in **Figure 2.13b**.



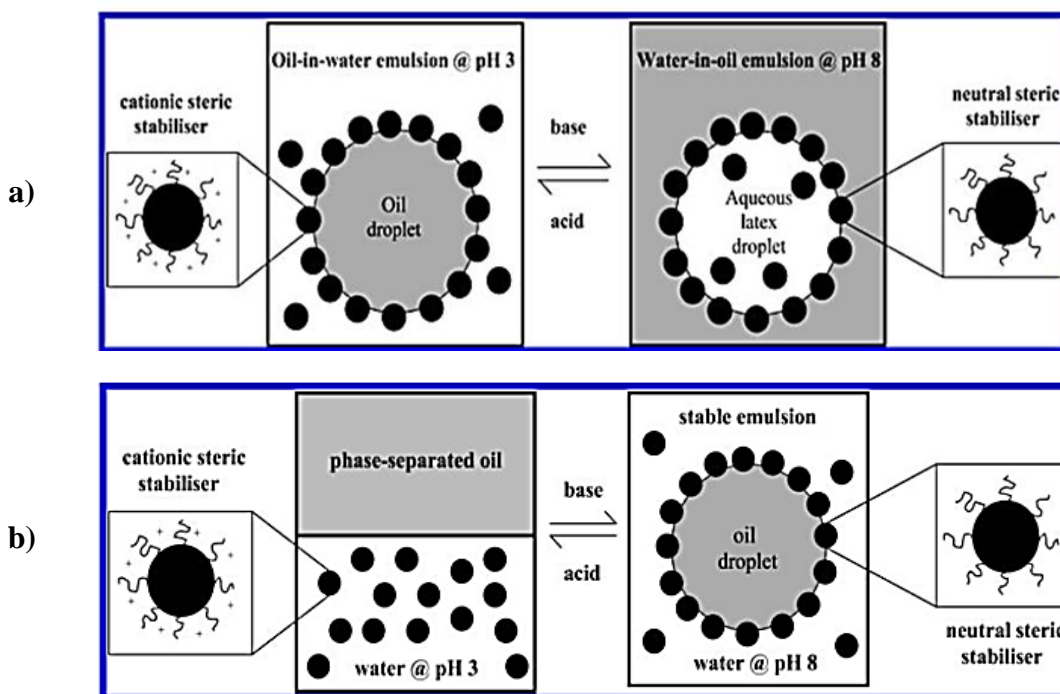


**Figure 2.13** Schematic illustration of pH-induced transitional phase inversion for a system using either methyl myristate or cineole as the oil phase (a), and pH-induced demulsification process for an emulsion of n-dodecane/water, decreasing pH induced the separation of two phases (b) (E. S. Read, 2004).

A mechanistic study on the demulsification process of water-in-diluted bitumen emulsions using ethyl cellulose as an effective, nontoxic, and biodegradable natural polymer, was performed by Feng et al (Feng et al., 2010). The addition of ethyl cellulose decreases the interfacial tension between the naphtha-diluted bitumen and water significantly. The results then showed that demulsification due to ethyl cellulose took place via both flocculation and coalescence of water droplets. Due to the competitive adsorption of ethyl cellulose at the oil-water interface, and the gradual disruption of the originally formed protective interfacial particle film from the surface-active components of bitumen, demulsification could take place in this system. **Figure 2.14** shows how water droplets flocculated in the presence (or absence) of ethyl cellulose.



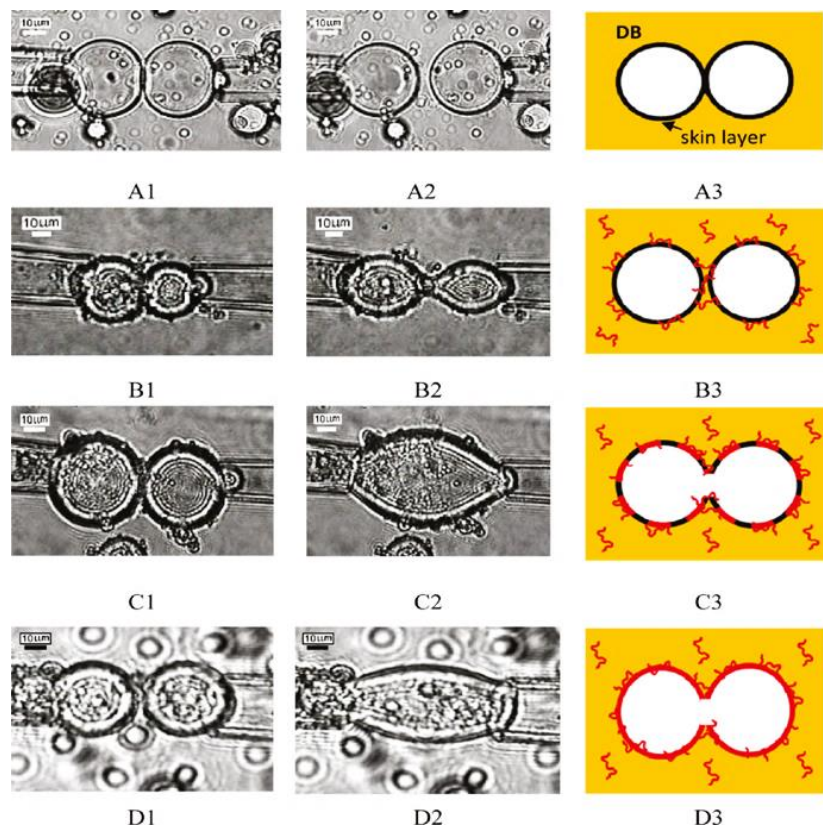


**Figure 2.14** Visualization of the interactions between water droplets in a 0.1 wt% naphtha-diluted bitumen emulsion (A1, A2, B1, B2, C1, and C2) and in naphtha (D1 and D2) by the micropipet technique. (A1) Water droplets interactions with no EC addition; (A2) detached from each other, no change in shape and size in the emulsion droplets; (B1) water droplets interactions in the emulsion containing EC ; (B2) deformation (stretching) of flocculated water droplets in the presence of EC; (C1) water droplets interactions in the emulsion with addition of higher amount of EC; (C2) water droplets coalesced into one large droplet in the emulsion with higher amount of EC; (D1) water droplets interactions in naphtha with EC addition; and (D2) water droplets coalesced into one large droplet in naphtha with EC addition. A3, B3, C3, and D3 are schematic representations of A1, B1, C1, and D1, respectively. (Feng et al., 2010)

### 2.4.3 Stimuli-responsive Pickering emulsions

Pickering emulsions with stimuli-responsive properties have received a considerable amount of interest, and their response to various external triggers such as pH, temperature, CO<sub>2</sub> concentration, light, magnetic field and ionic strength, or their combinations, have been widely studied. In many

cases, the surface properties of the solid particles undergo some sharp physical or chemical transition in response to an external trigger. When the particle surface chemistry undergoes some type of modification in response to changes in proton concentration, that can be considered as a pH-responsive particle (Dai, Ravi, & Tam, 2008). Temperature is another commonly investigated stimulus which can trigger to modulate Pickering emulsion stability. Thermo-responsive particles can stabilize, destabilize or invert the Pickering emulsions via the temperature change in system (Tang et al., 2015). CO<sub>2</sub>-responsive systems are simply sensitive to CO<sub>2</sub> gas. When the CO<sub>2</sub> is sparged into solution, the gas becomes dissolved in equilibrium with carbonic acid increasing the acidity of solution similar to pH-responsive systems. Therefore, it leads in certain chemical moieties on the surface of particles to undergo some type of ionic or conformational change, changing the wettability of the particles. Sparging another gas such as air or N<sub>2</sub> into system results in removing the CO<sub>2</sub> gas which helps to strip the dissolved CO<sub>2</sub> from the solution (Tang et al., 2015). For magnetic-responsive systems, emulsions stabilized by magnetic solid particles can be triggered for rapid and complete destabilization under applying external magnetic field. Upon the removal of external stimuli, these emulsions can be stabilized again (H. Yang et al., 2018). **Table 2.5** presents various stimuli-sensitive particles that have been used for the preparation of Pickering emulsions.

**Table 2.5 Various stimuli-responsive particles used to stabilize Pickering emulsions.**

Stimuli type	Type of particles	Type of liquids	Type of emulsions
<b>pH-responsive particles</b>	Silica nanoparticles modified by poly(styrene- <i>b</i> -2-vinylpyridine-ethylene glycol)	Toluene and water	O/W and W/O (Motornov et al., 2007)
	Silica modified with mixed organosilanes	Toluene and water	O/W and W/O (H. Yang et al., 2013)
	Graphene oxide	Toluene and water	O/W (J. Kim et al., 2010)
	Fe <sub>3</sub> O <sub>4</sub> nanoparticles modified with oleic acid	Paraffin and water	W/O and O/W (Lan et al., 2007)

<b>Thermo-responsive particles</b>	Polystyrene modified by poly[2-(dimethylamino)ethyl methacrylate-block-methyl methacrylate] (PDMAEMA-b-PMMA).	n-hexadecane and water	O/W, W/O and W/O/W (B. P. Binks et al., 2005)
	Silica nanoparticles modified by poly[2-(dimethylamino)ethyl methacrylate-block-methyl methacrylate] (PDMAEMAb-PMMA).	Xylene and water Cyclohexane and water	O/W (Saigal, Dong, Matyjaszewski, & Tilton, 2010)
	Cellulose nanocrystal (CNC) modified by poly(N-isopropylacrylamide) (PNIPAM)	Heptane and water	O/W (Zoppe et al., 2012)
	Poly(N-isopropylacrylamide) microgels	Hexadecane and water	O/W (Destribats et al., 2012)
<b>CO<sub>2</sub>-responsive</b>	Nanosilica modified with <i>N,N</i> -Dimethylacetamine dimethylacetal	Toluene and water	O/W and W/O (C. Liang et al., 2014)
	Nanosilica modified with <i>N'</i> -Dodecyl- <i>N,N</i> -dimethylacetamidine	n-octane and water	O/W (Jiang, Zhu, Cui, & Binks, 2013)
	Crosslinked polymer particles modified with poly (2-(diethylamino)ethyl methacrylate)	n-Dodecane and water	O/W (P. Liu, Lu, Wang, Li, & Zhu, 2014)

	Lignin nanoparticles modified with modified with poly(2-(diethylamino)ethyl methacrylate)	Decane and water	O/W (Qian, Zhang, Qiu, & Zhu, 2014)
<b>Magnetic-responsive</b>	Fe <sub>3</sub> O <sub>4</sub> nanoparticles	1-decanol, dodecane, polydimethylsiloxane and butyl butyrate and water	O/W and W/O (J. Zhou et al., 2011)
	Fe <sub>3</sub> O <sub>4</sub> nanoparticles functionalized with amino and bromoesterified ethyl cellulose (EC-Br)	Naphta and water	O/W (Peng, Liu, Xu, & Masliyah, 2012)
	CNC/CoFe <sub>2</sub> O <sub>4</sub>	Styrene, hexadecane and water	O/W

## 2.5 Summary

As can be deduced from the abundant scientific publications on Pickering emulsions, mostly the mechanism of stabilization, surface chemistry, particle concentration, and size have been investigated. Also, the overall understanding about solid particles at fluid-fluid interface has been progressing but complementary investigations are still needed to establish the link between interfacial and microstructural properties of solid stabilized emulsions during stabilization/destabilization processes. Since, the stability of Pickering emulsions depends mainly on the stabilizer/solid particle used, the majority of studies in literature reviews studied the physicochemical properties of solid particles and described how these factors can influence the stability of Pickering emulsions.

Choosing a right and simple surface chemistry which can promote and enhance the aggregation and disaggregation of solid particles involved in Pickering emulsions has not been well addressed. A few studies have looked at using natural polysaccharides such as sodium alginate (SA) for the surface modification of solid particles to stabilize Pickering emulsions. However, complex pathways of surface modification have been employed to prepare these surface grafted-SA particles, as described in Chapter 2. The reversible aggregation/disaggregation properties of SA-

surface modified particles as an approach to promote and facilitate the separation of Pickering emulsions constituents has not been considered so far.

For various applications, the stabilization and destabilization of Pickering emulsions is of utmost importance. There is an abundant amount of scientific publications on the development of stimuli-responsive Pickering emulsions via changes in pH, temperature, light and CO<sub>2</sub> concentration, for example. Fewer studies have been found however on the separation and recovery of Pickering emulsions constituents in Pickering emulsions. As a result, eco-friendly and energy-efficient methods to separate and recover the constituents of Pickering emulsions are still required.

Viscosity as an important factor of stabilization/destabilization process is still a matter of debate and remains to be well studied and investigated. In addition, complex techniques in the literature review have been used to prepare and design multiple Pickering emulsions via two steps of processing as well as using two types of stabilizers. Mostly, combination of solid particles and surfactants have been used in the processing of multiple Pickering emulsions, which causes environmental issues due to the presence of those synthetic and toxic surfactants. This study can provide a simple pathway for the preparation of multiple emulsions via one step of processing.

Applying SA-surface modified particles can significantly facilitate the separation of droplets in Pickering emulsions by sticking all those dispersed oil droplets together using an external stimulus such as pH, herein. For many industrial processes, Pickering emulsion systems need to go under destabilization process and the resistance of such emulsions submitted to breaking remains an open challenge as how to be overcome this issue efficiently. In literature review, various destabilization techniques such as mechanical, electrical and chemical methods have been proposed however it is still required to develop methods to break Pickering emulsions especially for highly viscous systems.

The novelty of this project is that for first time a simple filtration has been used as an approach for the separation and recovery of constituents in Pickering emulsions. This approach leads to breakthrough in different technologies and later can be developed to use in large scales for various industries. This research proposes a big step for improvements in destabilization process in terms of recycling the destabilizers as well as energy and time. In addition, the effect of viscosity during

destabilization process has not been well addressed in literature review as in many industries viscous systems are subjected to destabilize, therefore it has been studied in the current research.

In summary, this study has the potential to inspire change in a wide range of research domains such as drug delivery, food industry, waste water treatment, and assist in the development of simple and green separation process applied in crude oil recovery.

## CHAPTER 3      RESEARCH HYPOTHESIS AND OBJECTIVES, AND COHERENCE OF ARTICLES

### 3.1 Research hypothesis and objectives

As the state-of-the-art in the literature reveals, there is still a strong need, and a lack of knowledge and know-how, on the design and development of efficient and green processes for the destabilization and separation of Pickering emulsions constituents, for both low- and high-viscosity systems (even more so for the latter). Ideally, such a process should minimize the amount of generated waste, allow reuse of both particles and fluids, and avoid or minimize the use of toxic chemicals. Recent works have shown for example that soft microgel particles have the capacity to adsorb and desorb reversibly at the oil/water interface by the application of an external stimuli – i.e. a pH change as summarized in **Table 2.5** previously. Such an approach destabilizes a Pickering emulsion and allows the separation of the fluids – however, the particles remain difficult to separate since they remain dispersed in the aqueous phase. **Thus, based on these considerations, the main objective of this research project is to develop a process to destabilize, easily separate, and reuse the fluids and solid particulates initially forming a Pickering emulsion.**

Using filtration to separate the constituents of Pickering emulsions has not been investigated so far. Furthermore, sticking droplets together to form larger aggregates or flocs, without breaking the droplets, could significantly facilitate the filtration approach and minimize the amounts of wastes and toxic chemicals.

Our research hypothesis is that solid particles surface modified with SA can both form solid-stabilized emulsions, and “stick” droplets strongly together, by altering the pH - facilitating the separation, recovery and reuse of the constituents by a simple filtration approach. SA grafting will further impact the synthesis and processing properties of Pickering emulsions.

**This project comprises three specific objectives:**

1. Develop and prepare surface-modified particles grafted with a gelling natural polysaccharide, SA, that can undergo reversible gelling via intermolecular hydrogen bonding in aqueous solution by changing the pH;
2. Evaluate the potential of these “sticky” SA surface-modified particles for the separation and reuse of Pickering emulsions constituents via droplet aggregation and filtration;

3. Assess the effect of SA grafted on particle surface, on the processing and properties of Pickering emulsions, for both low and high viscosity systems;

## 3.2 Presentation of the articles and coherence with the research objectives

The main scientific findings of this work are presented in the form of three peer-reviewed journal articles in the following three chapters:

**Chapter 4** is entitled “Sodium Alginate-Grafted Submicrometer Particles Display Enhanced Reversible Aggregation/Disaggregation Properties” and has been published in *Carbohydrate Polymers*. In this work, we demonstrate that grafting SA onto the surface of silica particles significantly enhance their aggregation/disaggregation properties via the formation of interparticle hydrogen bonds, as we changed the pH between 3.0 and 7.0.

**Chapter 5** presents a second article entitled “Separating Pickering Emulsion Constituents by Tuning Particle-Particle Interactions”, published in *RSC Green Chemistry*. In this work, we further demonstrate that grafting SA macromolecules onto silane-modified sub-micrometer silica particles can stabilize and form Pickering O/W emulsions. In addition, via rheometry and filtration experiments, we demonstrate that grafting SA can enhance the separation and recovery of the initial constituents by a simple filtration approach in an environmentally-friendly way, without any toxic chemicals.

**Chapter 6** presents the results of a third article, entitled “One-Step Processing of Highly Viscous Multiple Pickering Emulsions”, submitted to *Journal of Colloids and Interface Science*. In this work, we studied the formation of multiple W/O/W Pickering emulsions using surface modified SA particles and highly viscous oils. We demonstrate that phase inversion during processing leads to the formation of those multiple emulsions, in a one-step process using only one type of solid particles.



## **CHAPTER 4      ARTICLE 1: SODIUM ALGINATE-GRAFTED SUBMICROMETER PARTICLES DISPLAY ENHANCED REVERSIBLE AGGREGATION/DISAGGREGATION PROPERTIES**

Faezeh Sabri, Kevin Berthomier, Antoine Marion, Louis Fradette, Jason R. Tavares, Nick Virgilio\*

Research Center for High Performance Polymer and Composite Systems (CREPEC), Department of Chemical Engineering, Polytechnique Montréal, Montréal, Québec, H3C 3A7, Canada

This work was published in *Carbohydrate Polymers* on August 15, 2018

<https://doi.org/10.1016/j.carbpol.2018.04.012>

### **4.1 Abstract**

In this article, we demonstrate that submicrometer particles with surface-grafted sodium alginate (SA) display enhanced and reversible aggregation/disaggregation properties in aqueous solution. 300 nm silica particles were first functionalized with an aminosilane coupling agent, followed by the grafting of pH-sensitive SA, as confirmed by zeta potential, XPS and FTIR analyses. The SA-modified particles show enhanced aggregation properties at acidic pH compared to unmodified silica, with a 10 times increase in average aggregate diameter. The process is reversible, as the aggregates can be broken and dispersed again when the pH is increased back to 7.0. As a result, the sedimentation rate of SA-modified particles at pH 3.0 is both significantly faster and complete compared to the unmodified particles. This enhanced aggregation is most likely due to the formation of intermolecular hydrogen bonds between neighboring SA-modified particles. This work illustrates how surface-grafted macromolecules of natural origins can be used to tune interparticle interactions, in order to improve separation.

### **4.2 Introduction**

The controlled aggregation and dispersion of colloids is a key step in separation processes involving complex fluids comprised of immiscible liquids and/or micro/nanoparticles (e.g. Pickering emulsions), in fields such as petrochemistry (Doshi, Repo, Heiskanen, Sirvio, &

Sillanpaa, 2017; Hosseini et al., 2016; Mohammadi, Rashidi, Mousavi-Dehghani, & Ghazanfari, 2016) and waste water treatment (Bakhteeva et al., 2016; Chai et al., 2015; Leudjo Taka, Pillay, & Yangkou Mbianda, 2017). When particle separation is required, it is often desirable to form aggregates and flocs as large as possible, in order to ease the separation process and decrease costs. Furthermore, if those particles were originally added to the process, for example as supports for much smaller catalytic nanoparticles (Ballauff & Lu, 2007), reversible aggregation/disaggregation behavior would be a desirable feature for recycling purpose. The Derjaguin–Landau–Verwey–Overbeek (DLVO) theory is a classical framework to understand and analyze the stability of colloidal suspensions (Ching-Ju Chin, 2001; Shinpei Ohki a, 1999). It models particle-particle interactions as a combination of repulsive double-layer overlap forces and attractive dispersion (van der Waals) forces (Verwey, 1947). In the energy landscape, the contribution of the electrostatic repulsion superimposes to the Van der Waals attraction and generates an energy barrier that can reduce or inhibit particle aggregation in a suspension (Rodgers, Velicky, & Dryfe, 2015). Other forces that can also enhance or inhibit aggregation include the hydrophobic effect, hydrogen bonding, steric interactions, and depletion forces (Céline Durand-Gasselín, 2011). As a result, the typical ways to control the aggregation level of micro/nanoparticles in a suspension are via pH and/or ionic strength (salt addition) adjustments (Yunfeng Yan, 2013), which control the electrical double layer properties. Grafting water-soluble polymer/polyelectrolyte chains on particle surface, which promote stabilization via steric interactions (Hemraz, Lu, Sunasee, & Boluk, 2014), and/or adding polyelectrolytes (Borkovec & Papastavrou, 2008) or water-soluble macromolecules (Bakumov & Kroke, 2008) are two other approaches. Recently, nanoparticles responding reversibly to external stimuli, such as changes in pH (K. Chen et al., 2017; Jia et al., 2016; Stular, Jerman, Naglic, Simoncic, & Tomsic, 2017; Xu et al., 2015) or temperature (Abreu et al., 2016; Qiao, Niu, Wang, & Cao, 2010), have generated an interest for chemical engineering processes, drug delivery and biomedical applications. For example, thermo- and pH-sensitive particles have been employed to stabilize (Morelli, Holdich, & Dragosavac, 2016; Tsuji & Kawaguchi, 2008) and destabilize Pickering emulsions (B. P. Binks et al., 2005), – allowing separation of the liquid constituents. They were also used as carriers for  $\approx 1\text{--}10$  nm catalytic nanoparticles, easing their separation and recovery process (Ballauff & Lu, 2007). However, separating particles from a liquid phase remains an energy intensive process. As a result, the

formation of flocs or aggregates facilitates separation and, if reversible, allows re-dispersion for multiple reuse. We hypothesize that grafting sodium alginate (SA) polymer chains onto the surface of submicrometer particles can increase interparticle interactions and enhance their aggregation properties reversibly, since SA undergoes reversible gelling at low pH due to the protonation of its carboxylate groups and the formation of intermolecular hydrogen bonding. The main objective of this work is to design, synthesize and evaluate the stabilization and aggregation properties of model submicrometer silica particles modified with SA, and to compare the results to unmodified particles in order to confirm if the aggregation/ disaggregation process is enhanced.

## 4.3 Experimental section

### 4.3.1 Materials

Sub- $\mu\text{m}$  silica particles (SP) were supplied by Nippon Shokubai Trading Co., Ltd (average diameter  $d=290 \pm 13.2$  nm by SEM, see Supporting Information **Figure 4.6**; specific surface area  $S=42 \pm 2\text{ m}^2\text{ g}^{-1}$ , measured by BET with an ASAP 2020 instrument from Micromeritics Instrument Corporation). Sodium alginate (SA) from brown algae was supplied by Sigma-Aldrich (CAS. 9005-38-3, low viscosity, molecular weight  $\approx 60$  kDa,  $\text{pK}_a=3.5$ ) (T. Harnsilawat, Pongsawatmanit, R., McClements, D.J., 2006). The M/G ratio ( $= 1.83$ ) was measured at  $80^\circ\text{C}$  with a  $10\text{ mg ml}^{-1}$  solution in  $\text{D}_2\text{O}$  for the  $^1\text{H}$  NMR using a Bruker Avance 500 instrument ( $11.7\text{ T}$ ) at a frequency of  $500\text{ MHz}$  (Rahelivao, Andriamanantoanina, Heyraud, & Rinaudo, 2013). 128 scans using 32 000 data points were acquired with a relaxation time (D1) of  $5\text{ s}$ , a  $4\text{ kHz}$  spectral window and a  $30^\circ$  impulsion. (3-Aminopropyl) trimethoxysilane (APTMS, 97%), N-(3-Dimethylaminopropyl)- N'-ethylcarbodiimide hydrochloride (EDC,  $>98\%$ ), N-Hydroxysuccinimide (NHS, 98%) and urea ( $>98\%$ ) were all purchased from Sigma-Aldrich and used without further purification. Ethanol (99.8%) was obtained from Thermo Fisher Scientific. HCl 1N and NaOH 12N solutions were of analytical grade and prepared without further purification with Milli-Q water ( $\text{DI water}$ ,  $18.2\ \Omega$ , Synergy 185 system by Fisher Scientific).

## 4.3.2 Particle surface modification

### 4.3.2.1 Silane coating grafting

In order to graft SA on silica sub- $\mu\text{m}$  particles, a silane coupling agent was first covalently grafted on its surface. In a typical batch, 10 g of SP particles were added in a hydrophobized Erlenmeyer flask containing 100 ml of a 95% v/v ethanol solution and DI water, while stirring at 600–700 rpm with a magnetic stirrer (Arkles, 2006). The pH was then adjusted to 4.5–5.5 using HCl 1N. APTMS was then added dropwise while stirring at room temperature, following three targeted surface concentrations: 0.01 (SP-A), 0.1 (SP-B) and 1 (SP-C) APTMS molecule  $\text{nm}^{-2}$  (based on particle specific surface) (K. L. Pickering, Khimi, & Ilanko, 2015). For example, to treat 10 g of particles with a desired surface APTMS density of 1 molecule  $\text{nm}^{-2}$  (SP-C), 0.131 ml of APTMS was added to the reaction medium. The reaction was then carried for 12 h. The particles were collected by centrifugation (Sorvall RC 6+, Thermo Fisher Scientific) at 8000 rpm for 15 min, and cleaned by washing twice with ethanol in order to rinse off any remaining unreacted silane. The particles were finally dried in a vacuum oven at 70 °C for 2 h.

### 4.3.2.2 Sodium alginate grafting

A fraction of the APTMS modified SPs were further modified by grafting SA using two different solution concentrations (Table 1): 0.1% (1) and 1% (2) w/v. As an example, following this terminology, SP-C-2 particles were modified with a silane coating targeting an APTMS surface density of 1 APTMS molecule  $\text{nm}^{-2}$ , followed by grafting of SA with a 1% w/v solution. In a typical experiment for the preparation of SP-((B-2) or (C-2)) particles, 0.2 g of SA was first dissolved in 20 ml of DI water (1% w/v). 0.29 g of EDC and 0.17 g of NHS (EDC/NHS molar ratio=1) were then added to the solution (EDC/-COOH molar ratio=0.5, relative to the -COOH groups of alginate) (G. Giani, S. Fedi, & R. Barbucci, 2012). Then, 2 g of APTMS modified SPs were added to the mixture and the pH was adjusted to 4.5 with HCl 1N. The reaction proceeded for 15 h at room temperature and the mixture was subsequently centrifuged at 8000 rpm to collect the modified particles, which were washed with DI water 3 times. Finally, the particles were dried in a vacuum oven at 70 °C for 10 h. The synthesis conditions of the surface modified SPs are summarized in **Table 4.1**.

**Table 4.1 Synthesis conditions of surface modified particles with APTMS and SA**

Particle ID	Targeted APTMS density (molecule·nm <sup>-2</sup> )	APTMS (ml) <sup>a</sup>	EDC <sup>b</sup> (g)	NHS <sup>b</sup> (g)	SA solution concentration/volume <sup>b</sup> ((%w/v)/ml)
SP-A	0.01	1.31×10 <sup>-3</sup>	-	-	-
SP-B	0.1	1.31 ×10 <sup>-2</sup>	-	-	-
SP-C	1	1.31×10 <sup>-1</sup>	-	-	-
SP-A-1	0.01	1.31×10 <sup>-3</sup>	0.29×10 <sup>-2</sup>	0.17×10 <sup>-2</sup>	0.1/20
SP-B-2	0.1	1.31×10 <sup>-2</sup>	0.29×10 <sup>-1</sup>	0.17×10 <sup>-1</sup>	0.1/20
SP-C-2	1	1.31×10 <sup>-1</sup>	0.29	0.17	1/20

<sup>a</sup>For the modification of 10 g of SP; <sup>b</sup>For 2 g of APTMS modified SP

### 4.3.3 Particle surface characterization

#### 4.3.3.1 Zeta potential measurements

Particle zeta potential ( $\zeta$ ) was measured with a Zetasizer Nano ZSP instrument (Malvern Instruments Ltd., Worcestershire, UK). Samples were dispersed in DI water at pH 7.0 (adjusted by adding NaOH 12N), and the measurements were performed at 25 °C.  $\zeta$  after modification with APTMS and SA, at different pHs (3.0, 7.0 and 10.0), were measured on at least three different samples by microelectrophoresis at a particle concentration of 0.001 g ml<sup>-1</sup>. Disposable zeta potential folded capillary cells (DTS1070) were used and all samples tested were freshly prepared. The instrument determined the electrophoretic mobility, and the Smoluchowski model was then applied by the software for the calculation of  $\zeta$  (Lattuada & Hatton, 2007).

#### 4.3.3.2 High-resolution X-ray photoelectron spectroscopy (XPS) analysis

Elemental analyses of unmodified and modified silica particles with APTMS were realized with a VG ESCALAB 3 MKII X-ray photoelectron spectroscope (XPS) equipped with a non-monochromatic Mg K $\alpha$  radiation source operated at 300W (15 kV, 20 mA). XPS analyses were conducted to detect electrons with a takeoff angle normal to the surface of the sample, yielding a probed depth around 10 nm. The pass energy was 100 eV for survey scans and 20 eV for high-resolution scans, at 1.00 and 0.05 eV increments, respectively. The pressure during analysis was

kept under  $5 \times 10^{-9}$  Torr ( $6.67 \times 10^{-11}$  Pa). Particles were stored under vacuum overnight prior to analysis. The results were analyzed using the Advantage XPS software package. The elemental distribution of the samples was determined on the basis of peak area comparison (C1s, O1s, etc.), normalized to their corresponding sensitivity factors, after the removal of the scattered electron background. In the case of higher resolution spectra, binding energies were referenced to the C1 s peak at 285.0 eV to adjust for possible charging effects, and the Shirley method was applied for background noise subtraction. According to the data trend for each distribution of binding energy, the baseline was manually placed. Each curve is represented by its maximum binding energy (BE) in the Supporting information (**Figure 4.7**). The species' elemental distributions are obtained via Gaussian/Lorentzian curve fitting on the original curve. The number of sub-curves and their corresponding species were obtained with full width at half maximum (fwhm)=1.6, 1.8, 2.2, and 2.4 eV for C, O, Si, and N, respectively.

#### **4.3.3.3 Fourier transform infrared (FTIR) spectroscopy analysis**

A Perkin Elmer Spectrum 65 FTIR spectrometer operating in attenuated total reflectance mode (Zn/Se crystal) in the range of  $650\text{--}4000\text{ cm}^{-1}$  was used to characterize unmodified  $\text{SiO}_2$  sub- $\mu\text{m}$  particles, as well as modified particles with APTMS and SA. For each sample, 32 scans were recorded at a resolution of  $4\text{ cm}^{-1}$ . The spectra of SP, SP-C and SP-C-2 are presented as Supporting Information (**Figure 4.8**).

### **4.3.4 Characterization of Aggregation and Disaggregation Properties**

#### **4.3.4.1 Visual inspection of sedimentation kinetics**

0.2 g of each particle type was dispersed in 10 ml of DI water using an ultrasonic homogenizer equipped with a microtip (Cole-Parmer, instrument model CP505, 500 watts) at an amplitude of 20 % for 1 min (approximately  $60\text{ J}\cdot\text{ml}^{-1}$ ). The pH was then adjusted to 3.0 with HCl 1N when required. Particle sedimentation was monitored by taking photographs every 3 min after dispersion, for a total duration of 60 min. For all particle types, three samples were tested.

#### **4.3.4.2 Optical microscopy observations**

Unmodified and surface modified particles were observed by dark field optical microscopy (Olympus BX51 by Cytoviva, Objectives = 10x and 50x Plan Fluorite, and 60x UPL Fluorite Oil, and 100x UPL Fluorite Oil camera Q imaging, Retigna 2000R fast 1394, cooled color 12 bit). For each type of particle, 0.02 g of particles was dispersed in 2.0 ml of DI water at pH 7.0 using the ultrasonic homogenizer at a 20% amplitude for 1 min ( $\approx 300 \text{ J}\cdot\text{ml}^{-1}$ ); the pH was subsequently adjusted to 3.0 with HCl 1N when required. Solutions were subsequently diluted by adding 3 droplets into 5 ml of water at the corresponding pH while stirring with a magnetic stirrer for 30 s at 600 rpm. Finally, three drops of freshly prepared samples were placed on microscope glass slides and observed at different locations and magnifications. The images were analyzed using the ImageJ software, to calculate the average size (Feret diameter) of the observed aggregates.

#### **4.3.4.3 Measurement of sedimentation rate by UV-Vis spectroscopy**

UV-Vis transmittance measurements as a function of time were performed to determine the sedimentation rate of unmodified and surface modified particles, using a UV-Vis spectrometer (Model DH-2000 from Ocean Optics, 10 ms integration time). For each particle type, one concentration was analyzed ( $0.01 \text{ g}\cdot\text{ml}^{-1}$ ) at 2 different pHs (3.0 and 7.0), by dispersing the required amount of particles in 2 ml of DI water (pH 7.0) using an ultrasonic homogenizer, as described previously; the pH was subsequently adjusted to 3.0 with HCl 1N when required. Then, 1 ml of each sample was transferred into a disposable polystyrene cuvette with a 1 cm path length for transmittance measurements at 656 nm every 3 min for a total duration of 60 min. The height of the beam path was located at 1.3 cm from the bottom of the cuvette. For each particle type, the transmittance measurements were repeated 3 times. The spectral measurements were normalized with the DI water transmittance values at pH 3.0 and 7.0 respectively.

#### **4.3.4.4 Aggregation/disaggregation reversibility evaluation**

Each sample was prepared by dispersing 0.01 g of particles (SP, SP-A or SP-A-1) in 1 ml of DI water at pH 7.0. UV-Vis transmittance at 656 nm was then measured as a function of time for 60 min, using 1 ml disposable polystyrene cuvettes. Subsequently, the sample was transferred back into a vial and the pH was adjusted to pH 3.0 with HCl 1N. The sample was again transferred into

a disposable cuvette for transmittance measurements at 656 nm for 60 min. Once the experiment was completed, the sample was transferred back again into a vial and the pH was again brought back to 7.0 with NaOH 12.0N. The particles were next re-dispersed by ultrasonication (20% amplitude for 20 sec). This whole cycle process was repeated 4 times. The spectral measurements were normalized with DI water transmittance values at pH 3.0 and 7.0 respectively.

## 4.4 Results and Discussion

### 4.4.1 Zeta potential, XPS and FTIR

The particles zeta potential  $\zeta$  was measured as a function of pH for bare silica particles (SP), modified particles with APTMS (SP-A to C), and with SA (SP-(A-1), (B-2), and (C-2)) (Table 4.2).

**Table 4.2  $\zeta$  of silica particles: untreated (SP), APTMS treated (SP-A to C), and APTMS+SA treated particles (SP-(A-1), (B-2) and (C-2)), as a function of pH (3.0, 7.0 and 10.0).**

Particle ID	$\zeta$ (mV)		
	pH = 3.0	pH = 7.0	pH = 10.0
SP	$5.7 \pm 0.8$	$-56.4 \pm 1.4$	$-57.0 \pm 1.4$
SP-A	$11.0 \pm 1.2$	$-58.4 \pm 1.1$	$-57.0 \pm 1.3$
SP-B	$49.4 \pm 4.7$	$24.7 \pm 0.7$	$-24.2 \pm 0.7$
SP-C	$52.1 \pm 1.4$	$13.3 \pm 0.3$	$8.4 \pm 0.4$
SP-A-1	$6.5 \pm 1.0$	$-50.9 \pm 1.1$	$-49.4 \pm 0.6$
SP-B-2	$3.4 \pm 0.8$	$-45.6 \pm 0.6$	$-45.1 \pm 1.6$
SP-C-2	$-0.8 \pm 0.3$	$-43.2 \pm 1.0$	$-43.8 \pm 1.4$

SP particles display a slightly positive  $\zeta$  at pH 3.0 that decreases to negative values at pHs 7.0 and 10.0. This behavior is expected due to the deprotonation of hydroxyl groups on the SP surface as the pH increases (Knoblich & Gerber, 2001). SP particles modified with APTMS (SP-A SP-B, SP-C) generally display higher positive values at pH 3.0. Increasing the initial concentration of APTMS in solution results in an increasing positive  $\zeta$ , from +11.0 mV to +52.1 mV. At pH 3.0, SP-A particles present a similar behavior as compared to unmodified SP particles. For SP-B and



SP-C,  $\zeta$  increases significantly (49.4 and 52.1 mV) due to the expected higher APTMS surface density, confirming grafting of APTMS. Grafting of APTMS was also confirmed by XPS, the spectra revealing two different components related to N-H bonds (revealed from the N1s peak using high resolution XPS), and one component related to C-N bonds. The component at a BE  $\cong$  399.8 eV corresponds to  $-\text{NH}_2$  and the component at BE  $\cong$  401.5 eV corresponds to  $-\text{NH}_3^+$  groups (see Supporting Information, **Figure 4.7**). Grafting of APTMS was independently confirmed by FTIR with the appearance of a band at  $1450\text{ cm}^{-1}$ , associated with N-H bond asymmetrical deformation vibration (**Figure 4.8**).

When the pH increases to 7.0 and 10.0,  $\zeta$  of SP-A, SP-B and SP-C all shift towards lower positive (almost neutral) or negative values. This is explained by (1) the significant deprotonation of surface bound hydroxyl groups, yielding negatively charged  $-\text{O}^-$  (Knoblich & Gerber, 2001), and (2) the gradual deprotonation of APTMS  $-\text{NH}_3^+$  groups.

At pH 3.0, SA modified particles (SP-A-1, SP-B-2 and SP-C-2) display nearly neutral  $\zeta$  values (slightly positive or negative). This behavior is due to the protonation of the SA carboxylate groups ( $\text{pK}_a = 3.5$ ) – confirming the subsequent grafting of SA with APTMS. At pH 7.0 and 10.0, similar trends of  $\zeta$  are observed for SP-A-1, SP-B-2 and SP-C-2 particles. At pH 7.0,  $\zeta$  drops to negative values ranging from -43.2 mV to -50.9 mV, while at pH 10.0 it reaches nearly -50 mV. This is expected since at pH 7.0 and 10.0, above the  $\text{pK}_a$  of SA, the  $-\text{COOH}$  groups on the surface are deprotonated and become negatively charged, like a number of other polysaccharides (*e.g.* xanthan gum) (C. S. Wang, Natale, Virgilio, & Heuzey, 2016). Grafting of SA was also confirmed by FTIR (see **Figure 4.8**). Observed bands at  $1649$  and  $1460\text{ cm}^{-1}$  were attributed to asymmetric and symmetric stretching vibrations of carboxylate  $-\text{COO}^-$ . Finally, the disappearance of the N-H band at  $1450\text{ cm}^{-1}$  is attributed to the grafting of SA and the formation of N-C=O bonds. Zeta potential measurements, XPS and FTIR analyses confirm graftings of the silane coupling agent and sodium alginate. The next section will look at the aggregation state of the particles as a function of pH and surface chemistry.

#### 4.4.2 Particle aggregation behavior

**Figure 4.1** displays the aggregation behavior of SP, SP-A, and SP-A-1 particles at pH 3.0 and 7.0, respectively. At pH 3.0, unmodified SP particles tend to form small aggregates due to their

slightly positive charge (**Figure 4.1a**), while at pH 7.0 they are almost individually dispersed (**Figure 4.1b**). These observations agree with the  $\zeta$  measurements reported in **Table 4.2**: at pH 3.0, the small positive value results in an unstable dispersion, while at pH 7.0, the significant negative value leads to a stable dispersion.

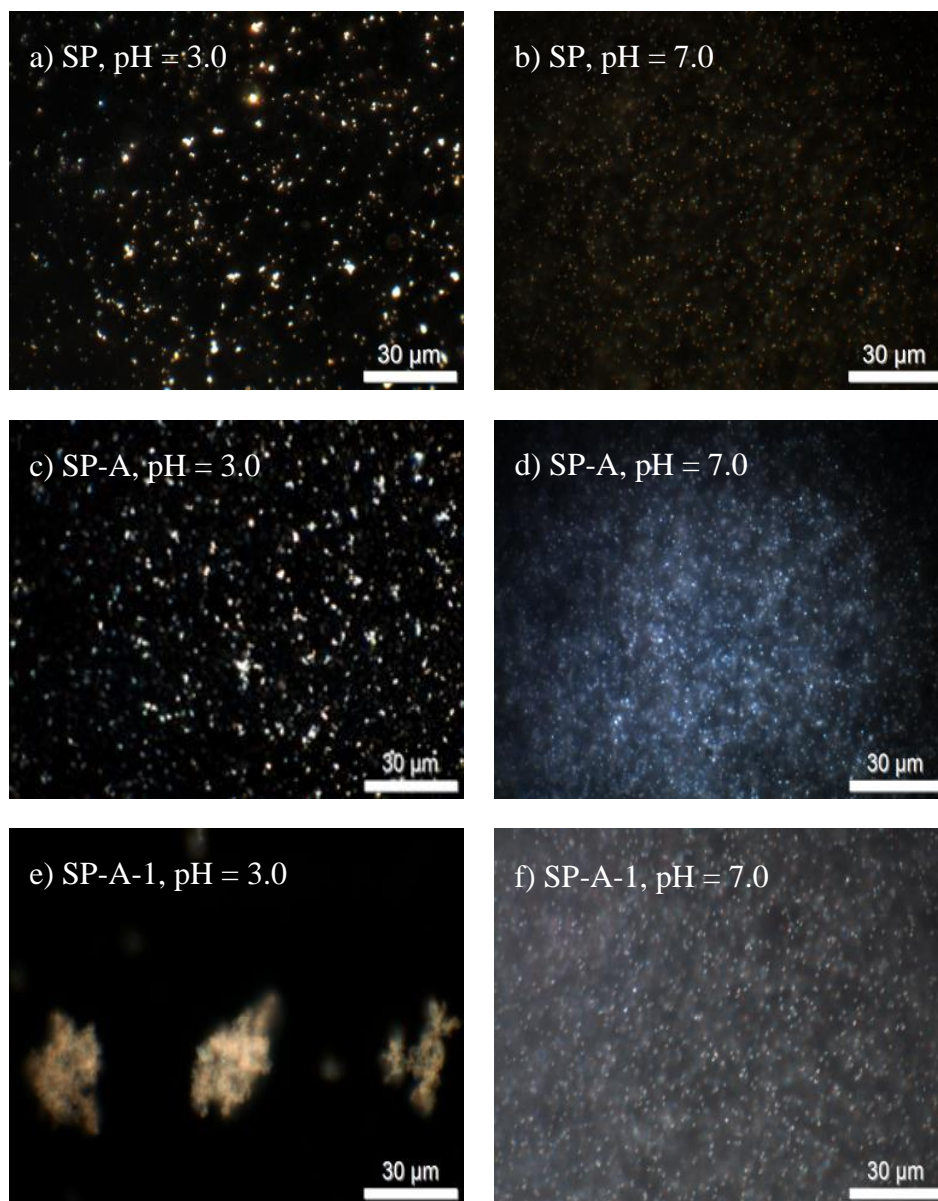


**Figure 4.1** Dark field optical microscopy micrographs showing the aggregation state, as a function of pH (3.0 or 7.0), of SP (a, b), SP-A (c, d), and SP-A-1 (e, f) particles.

Grafting APTMS at the surface of SP changes their electrostatic surface potential (**Table 4.2**) and their state of aggregation (**Figure 4.1c and d**). **Table 4.3** reports arithmetic mean diameter  $\pm$  mean absolute deviation, as a function of particle type – the size distributions are reported in **Figure 4.9**. For SP-A, at pH 3.0 (**Figure 4.1c**), the aggregates' average diameter ( $D = 1.5 \pm 0.9 \mu\text{m}$ , **Table 4.3**) is comparable to unmodified SP particles ( $D = 1.7 \pm 1.0 \mu\text{m}$ ), SP-B and SP-C particles ( $D = 0.9 \pm 0.4 \mu\text{m}$  and  $D = 0.8 \pm 0.5 \mu\text{m}$ , respectively). At pH 7.0, the presence of APTMS at the surface increases the average aggregate size (**Figure 4.1d**), as compared to unmodified SP at pH 7.0, due to the low zeta potential value.

$D$  approximately increases by an order of magnitude, at pH 3.0, when SA is subsequently grafted onto the particles' surface (**Figure 4.1e**, **Table 4.3**), as compared to unmodified particles (**Figure 4.1a**). The effect is quite striking, as lower magnification micrographs demonstrate (**Figure 4.10**). At pH 7.0 however (**Figure 4.1f**), SA grafted particles form much smaller aggregates ( $D = 1.3 \pm 0.3 \mu\text{m}$ ) due to the deprotonation of SA carboxylate groups.

**Table 4.3 Average aggregate diameter  $D$  as a function of particle type, at pH 3.0 (N = number of analyzed aggregates).**

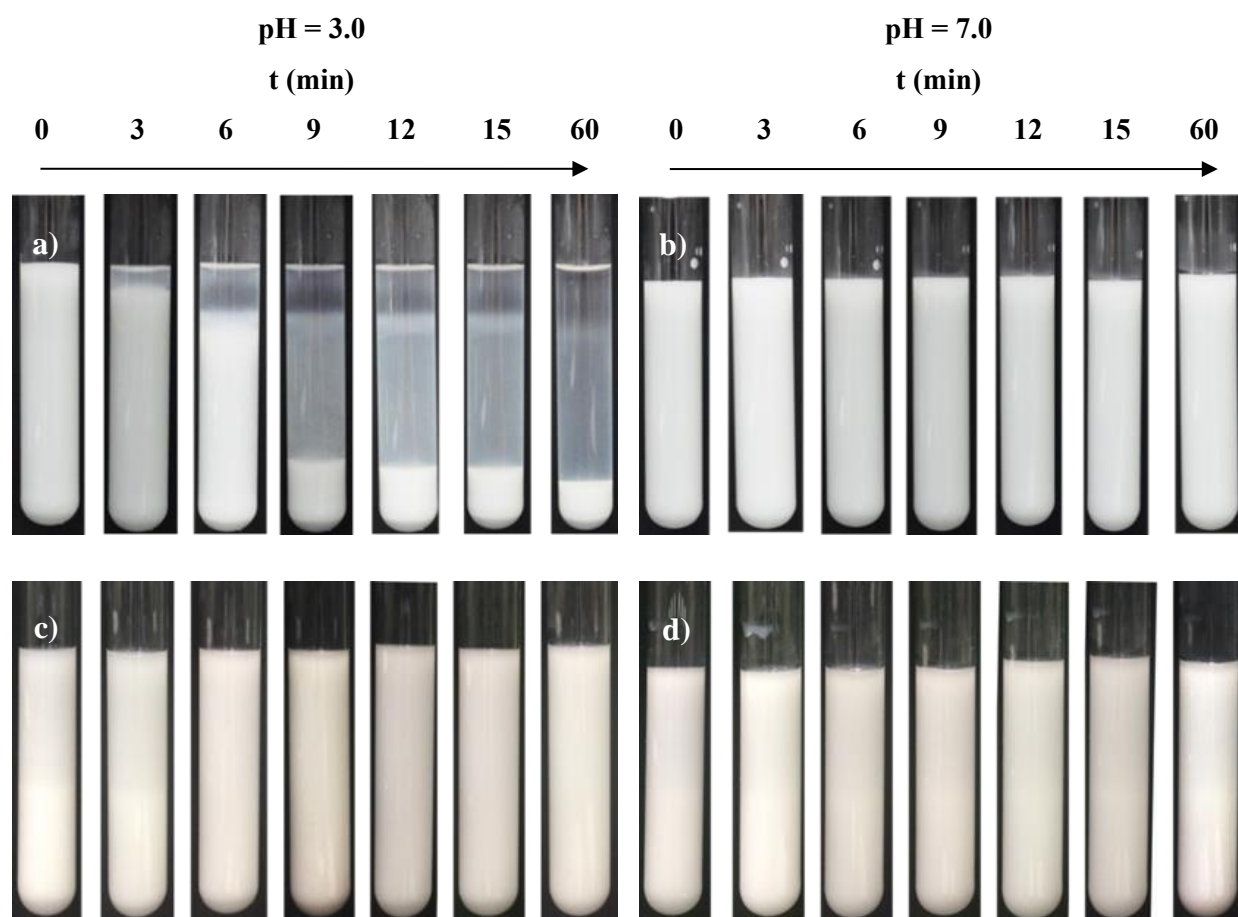
Particle type	Aggregate average diameter $D$ ( $\mu\text{m}$ )	Average number of particles per aggregate <sup>a</sup>
SP	$1.7 \pm 1.0$ (N = 659)	182
SP-A	$1.5 \pm 0.9$ (N = 917)	128
SP-B	$0.9 \pm 0.4$ (N = 3634)	28
SP-C	$0.8 \pm 0.5$ (N = 1979)	22
SP-A-1	$17 \pm 10$ (N = 231)	$18.2 \times 10^4$
SP-B-2	$12 \pm 7$ (N = 1124)	$5.8 \times 10^4$
SP-C-2	$12 \pm 8$ (N = 915)	$6.4 \times 10^4$

<sup>a</sup>average number of particles per aggregate was obtained from  $(D_{\text{aggregate}}/D_{\text{particle}})^3$

#### 4.4.3 Sedimentation Kinetics

**Figure 4.2** displays the sedimentation behavior of SP, SP-A and SP-A-1 particles dispersed in water at pHs 3.0 and 7.0, respectively. At pH 3.0, SP particles display a clear sedimentation onset after 3 min – the process is fast for the first 9 min, and then slows down since most of the particles

have then sedimented. In contrast, no sedimentation is observed at pH 7.0 even after 60 min (**Figure 4.2a and b**). This difference is consistent with the measured  $\zeta$  values. SP-A particles do not display any significant sedimentation over the whole duration of the experiment, for both pHs tested (**Figure 4.2c and d**). At pH 3.0, the positively charged protonated amino groups' repulsive forces lead to a stable dispersed state, while at pH 7.0 the remaining negatively charged deprotonated hydroxyl groups stabilize the dispersion. However, as the surface density of APTMS increases (SP-B and SP-C), sedimentation occurs at pH 7.0 (results not shown).



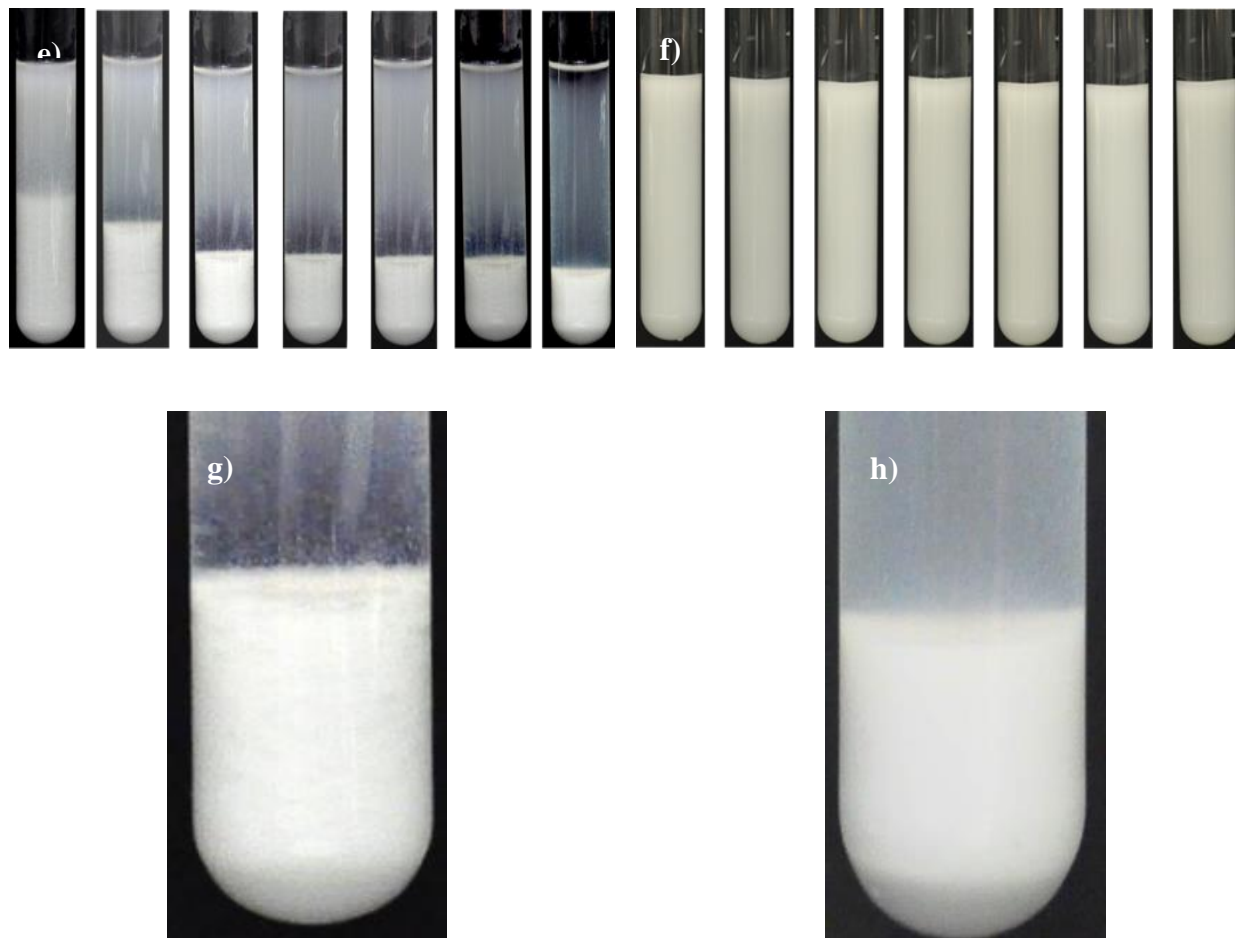


**Figure 4.2** Pictures of the sedimentation process (height of test tube = 15.3 cm) for SP (a, b), SP-A (c, d), and SP-A-1 (e, f) particles over 60 min at pHs 3.0 and 7.0 respectively; g, h) close-ups of SP-A-1 and SP sedimented particles, showing a clear difference in particle texture.

For SP-A-1 particles, shown in **Figure 4.2e-f**, sedimentation starts right away at pH 3.0 and after 3 minutes, it is already fairly advanced. After 6 min, the process significantly slows down, whereas at pH 7.0, SP-A-1 particles stay well dispersed for the whole duration of the experiment, as shown in **Figure 4.2f**. Note that a similar behavior was observed for SP-B-2 and SP-C-2 particles (results not shown). Another distinct feature is the “grainy” texture of the sedimented SP-A-1 particles (**Figure 4.2g**), as compared to unmodified SP particles (**Figure 4.2h**) – indicating the presence of large aggregates at pH 3.0, which is not the case for SP particles.

#### 4.4.4 Kinetic test by UV-Visible spectroscopy

**Figure 4.3** displays the normalized UV-Vis transmittance results  $T$  of the solutions during 60 min, right after processing, at both pHs 3.0 and 7.0. The results at pH 3.0 were fitted with power laws ( $T = A + B \exp(-t/C)$ ). SP particles sediment moderately fast at pH 3.0 (as indicated by the initial transmittance slope  $(-B/C) = 0.03$ ,  $R^2 = 0.98$ ), while no net sedimentation is detected at pH 7.0 ( $T = 0$ ). These results are consistent with the behavior expected based on zeta potential results (**Table 4.2**) and visual observations (**Figure 4.2**). After  $\approx 35$  min,  $T$  has increased up to 50 % for SP particles, and to 60 % after 60 min, with sedimentation still in progress. In contrast, sedimentation is occurring significantly faster at pH 3.0 for SA modified particles (initial slope  $(-B/C) = 0.22$  ( $R^2 = 0.98$ ), 0.22 ( $R^2 = 0.95$ ) and 0.07 ( $R^2 = 0.98$ ) for SP-A-1, SP-B-2 and SP-C-2 particles respectively). For SP-A-1,  $T$  increases up to 50 % after only  $\approx 5$  min, and reaches a plateau value of nearly 90 % after 30 min. Similar results are obtained for SP-B-2 particles, while SP-C-2 particles show a slower sedimentation process compared to SP-A-1 and SP-B-2, but still faster compared to SP. Finally, note that all solutions at pH 7.0 displayed no significant UV-Vis  $T$  increase.

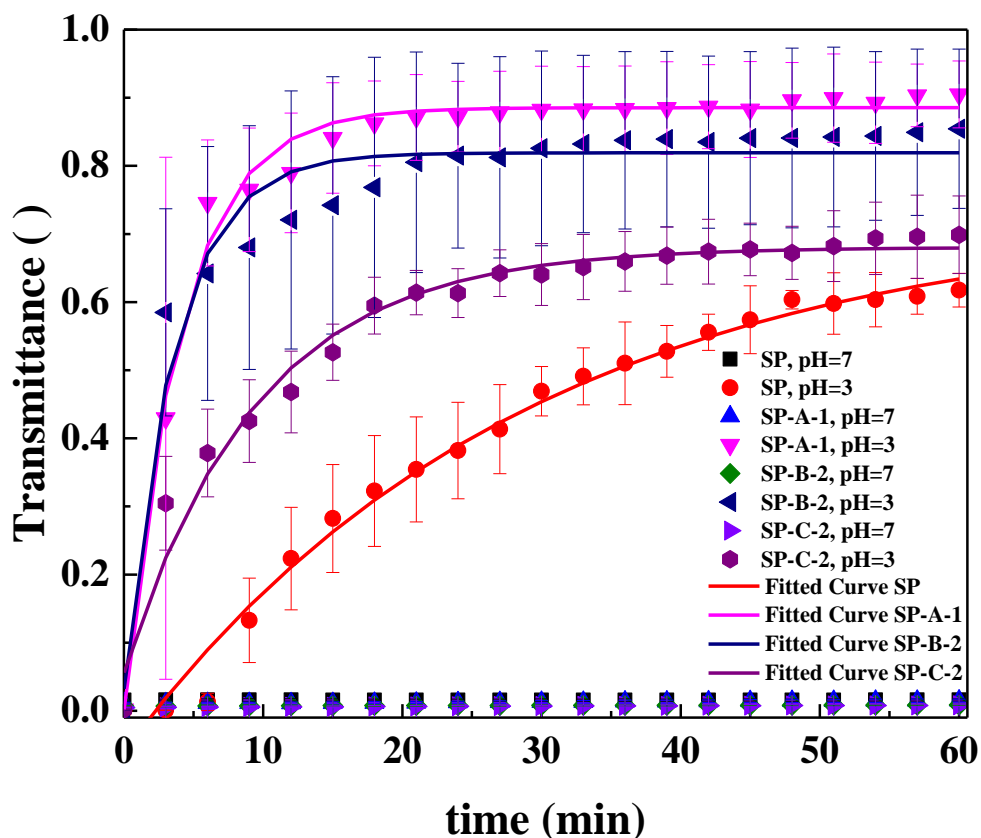


**Figure 4.3** Normalized transmittance  $T$  as a function of time for SP, SP-A-1, SP-B-2 and SP-C-2 particles at pH 3.0 and 7.0, and fitted curves for SP, SP-A-1, SP-B-2 and SP-C-2 particles at pH 3.0 over 60 min.

#### 4.4.5 Aggregation/disaggregation reversibility

**Figure 4.4** illustrates the reversible nature of the aggregation process for SP and SP-A-1 particles over 4 pH-swing cycles using UV-Vis spectroscopy, starting at pH 7.0, for 60 min. After that time, the pH is decreased to 3.0 for 60 min, and the cycle is repeated 3 other times. Both SP-A-1 and SP particles are able to aggregate and disaggregate reversibly over the course of the 4 tested cycles. At pH 3.0, SP-A-1 particles sediment rapidly within minutes and form aggregates, with UV transmittance reaching a maximum near 90% each time the pH is brought down to 3.0. When the pH is increased to 7.0 and the solution is sonicated, the dispersion remains stable ( $T \approx 0\%$ ). SP

particles also display a reversible aggregation behavior, but the maximum transmittance after 60 min never goes over 60% - in fact, it decreases as the process is repeated. Furthermore, slight aggregation is also observed at pH 7.0 as the process is repeated. It should be noted however that if the pH is just increased without any sonication, the disaggregation process is very slow.

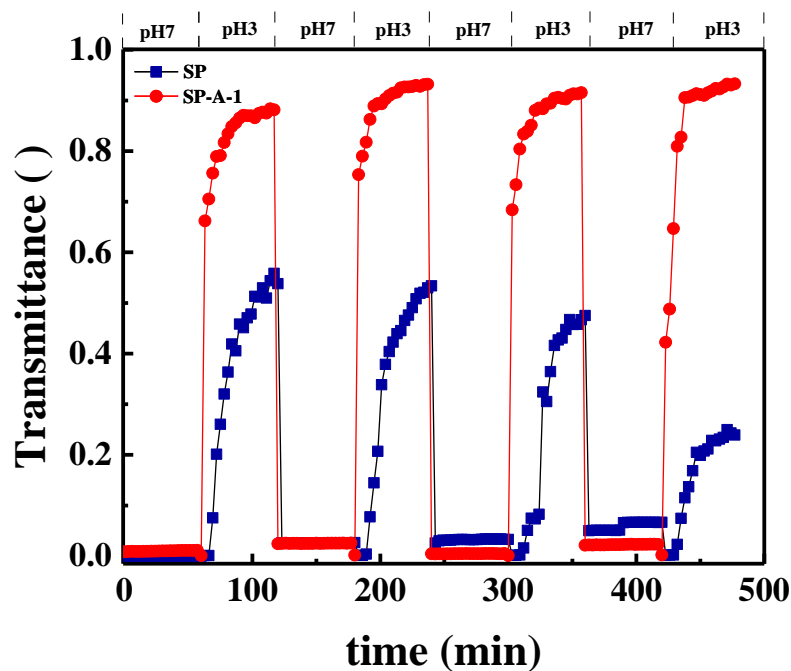


**Figure 4.4** Reversibility test for SP (■) and SP-A-1 particles (●) over 4 cycles, during which the pH jumps back and forth from 7.0 to 3.0.

## 4.5 Discussion

The  $\zeta$  measurements, along with the XPS and FTIR results, confirm that the SP particles have been modified sequentially with covalently grafted APTMS and SA. The average diameter of individual silica particles is  $d \approx 300$  nm - in contrast, the average diameter  $D$  of particle aggregates at pH 3.0, for SA modified particles, is about 10 times superior as compared to aggregates of unmodified particles. Since the volume of an aggregate  $\sim D^3$ , there is approximately  $10^3$  more particles in an aggregate of SA modified particles as compared to an aggregate comprising unmodified particles, as reported in the third column of **Table 4.3** – a significant difference. We



propose that the main mechanism leading ultimately to the reversible, enhanced aggregation properties of SA modified particles, compared to unmodified particles, originates from hydrogen bonding between neighboring particles grafted with SA. At pH 7.0, SA carboxylic acid groups are deprotonated and maintain the particles in suspension. However, once the pH is brought down to 3.0, the carboxylate groups are protonated and  $\zeta$  is in-between 0 and 10 mV, which leads to an unstable suspension and particle aggregation. This gives rise to SA intermolecular interactions via hydrogen bonding, enhancing aggregate formation.

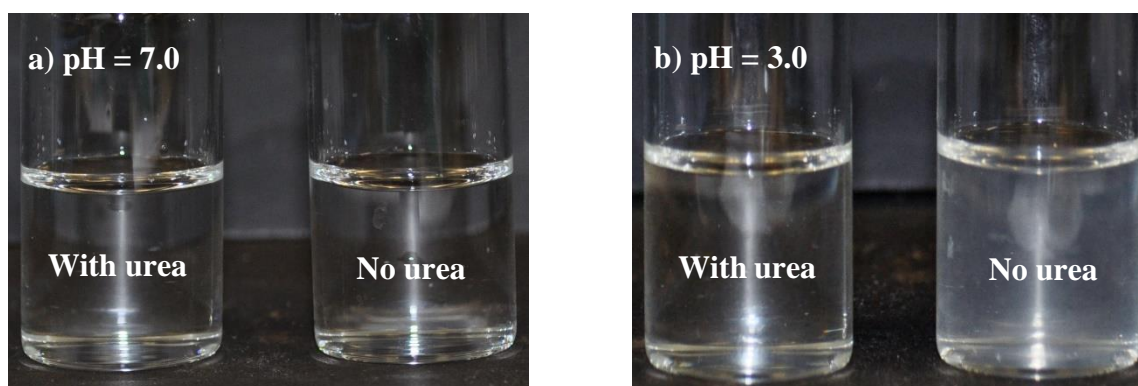


**Figure 4.5** Pictures of 0.5 % solution of pure SA in DI water at pH 7.0 (a) and at pH 3.0 (b), with and without urea (16 M).

Recently, Chen et al. (K. Chen et al., 2017) used SA-modified nanoparticles to prepare pH-sensitive Pickering emulsions. Their work demonstrated that SA significantly alters the emulsions' rheological behavior due to pH-dependent interparticle interactions. **Figure 4.5a** and **b** illustrates the effect of urea on alginate association in solution at pHs 7.0 and 3.0, respectively. Urea is a well-known hydrogen bond disruptor, which should then limit or inhibit hydrogen bonding and aggregate formation. At pH 7.0, urea has no visible effect on solution turbidity. However, when the pH is brought down to 3.0, alginate phase separate (and can ultimately form a gel when the SA concentration is high enough), a phenomena that is not observed when urea is added to the solution.

## 4.6 Conclusion

This article demonstrates that submicrometer silica particles functionalized with a pH sensitive polysaccharide, sodium alginate, display enhanced aggregation properties at low pH, and reversible aggregation/ disaggregation properties in aqueous solutions. The aggregation properties are due to

interparticle hydrogen bonding between neighboring sodium alginate modified particle. The particles surface modification was characterized by zeta potential measurements, XPS and FTIR analyses, and UV–vis was used to characterize the sedimentation kinetics. The results illustrate how stimuli sensitive surface modified particles can be used as a potential approach to facilitate the aggregation of particles, and to ease separation processes.

## **4.7 Acknowledgment**

We acknowledge the financial support of Imperial Oil through a University Research Award grant, the Total company, the National Sciences and Engineering Research Council (Discovery Grant), CREPEC (Projet Structurant), Polytechnique Montreal (UPIR undergraduate research grants) and the Canada Foundation for Innovation (John R. Evans Leaders Fund). We would like to thank Dr. Donya Farhanian and Dr. Josianne Lefebvre for performing XPS experiments, Mr. Wendell Raphael for optical microscopy observations, Dr. Benoît Liberelle, Mr. Chang-Sheng Wang, Mr. Philippe Leclerc, Dr. David Vidal and Mr. David Brassard and Ms. Claire Cerclé for fruitful discussions and technical support.

## **4.8 Supporting Information Article 1: Sodium alginate-grafted submicrometer particles display enhanced reversible aggregation/disaggregation properties**

Silica particles SEM micrographs, XPS and FTIR spectra of unmodified and modified particles; particle aggregates size distribution.

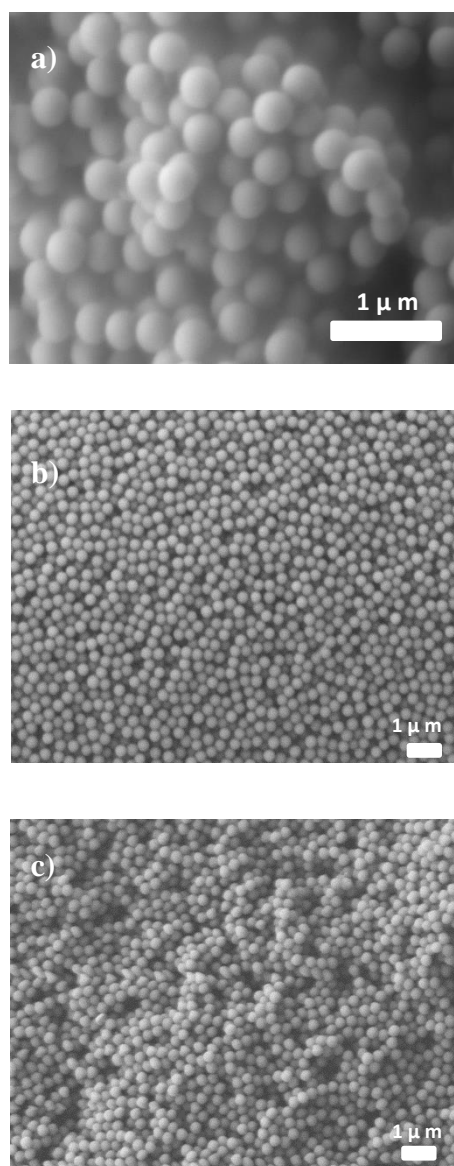


**Figure 4.6** SEM micrographs of bare SiO<sub>2</sub> particles (a) and SA modified particles (SP-C-2) initially dispersed at pH 7.0 (b) and subsequently brought down to pH 3.0 (c), respectively

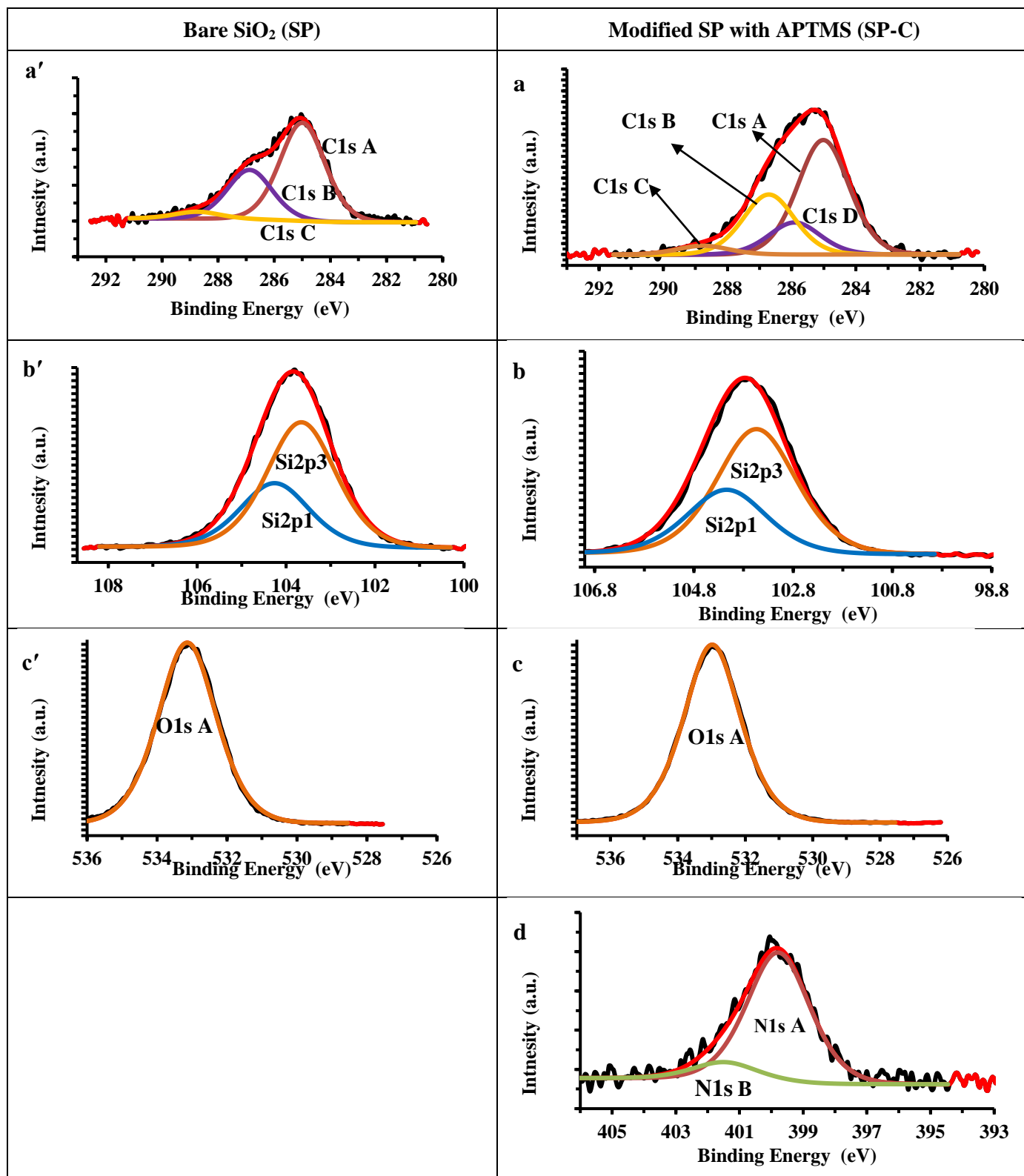


**Figure 4.7** Deconvoluted XPS spectra of bare SiO<sub>2</sub> (SP) (left column), and modified with APTMS (SP-C) (right column).

High resolution X-ray photoelectron spectroscopy (XPS) analysis provided insight into the chemical composition of the surface modified silica particles with APTMS. In order to obtain the information on the chemical bonding states and confirm the successful modification of SP with APTMS, the XPS peaks for bare SP and samples modified with APTMS (SP-C) were peak fitted (**Figure 4.7**). A summary of the high resolution spectral peak fit along with their possible structure assignment and At % is presented. Before surface modification with APTMS, the SP surface was mainly composed of silicon, oxygen and contained a small amount of carbon, most likely due to adventitious contamination due to exposure to air (~7.8%). These contaminants (**Figure 4.7 a'**) exhibited a high-resolution C1s peak with components at binding energy BE  $\cong$  285.0 (C1s A), 286.9 eV (C1s B) and 288.7 (C1s C), which were assigned to C–C and C–H bonds (such as –CH, –CH<sub>2</sub>, –CH<sub>3</sub> and C<sub>2</sub>H<sub>2</sub>, C<sub>2</sub>H<sub>5</sub>, etc.), C–O, C–O–C groups, and O–C=O groups respectively. Silicon sub-oxide, SiO<sub>2</sub> (Si<sup>4+</sup>) was assigned to the Si2p<sub>3/2</sub> and Si2p<sub>1/2</sub> peaks observed at BE of 103.7 and 104.3 eV. The oxygen peak, O1s, observed at BE  $\cong$  533.1 eV was assigned to oxygen in silicon oxide as well as oxygen in hydroxyl groups. High-resolution spectral deconvolution of Si2p and O shows that the atomic percentage of oxygen, and silicon did not match. Indeed, in terms of stoichiometry, the Si/O ratio should be 1/2, but the amount of oxygen was determined to be higher (for 24 At% Si, the corresponding atomic percentage for oxygen should be 48%. The observed higher oxygen amount (+24%) was attributed to surface hydroxyl groups (Si–OH). After surface modification with APTMS, the intensity of the C1s peak increased from 7.8% to 10%, and the Si2p peak was attenuated, which was in agreement with survey results (**Figure 4.7 b**). The C1s spectrum (**Figure 4.7 a**) showed a group of overlapping peaks with BE from 285.0 eV to 288.8 eV, attributed to four significantly different surface carbon phases (identified as A, B, C, and D). The dominant Phase A peak (C1s A, BE  $\cong$  285eV) was attributed to C–C, C–H and C–Si groups. Phase B (C1s B, BE  $\cong$  286.7eV) could correspond to C–O and phase C (C1s C, BE  $\cong$  288.8 eV) was designated as a contaminated carbon layer, in the form of O–C=O. Phase D (C1s D, BE  $\cong$  285.9 eV) contained C–N, an additional feature as compared to unmodified particles. The high resolution spectrum of the silicon Si2p peak presents a single doublet with Si2p<sub>3/2</sub> and Si2p<sub>1/2</sub> peaks at BE  $\cong$  103.5 eV and 104.1 eV respectively, attributed to silicon in SiO<sub>2</sub> and Si–O of APTMS. After modification with APTMS, two different components related to NH groups were resolved for N1S spectra in the high resolution XPS. The component at a BE  $\cong$  399.8 eV corresponds to –NH<sub>2</sub> and the component

at BE  $\cong 401.5$  eV corresponds to  $-\text{NH}_3^+$  groups. From the ratio  $-\text{NH}_2/-\text{NH}_3^+ \cong 6$ , it can be concluded that the major part of the  $-\text{NH}_2$  groups are oriented away from the  $\text{SiO}_2$  surface based on literature.(Jakša, Štefane, & Kovač, 2013)

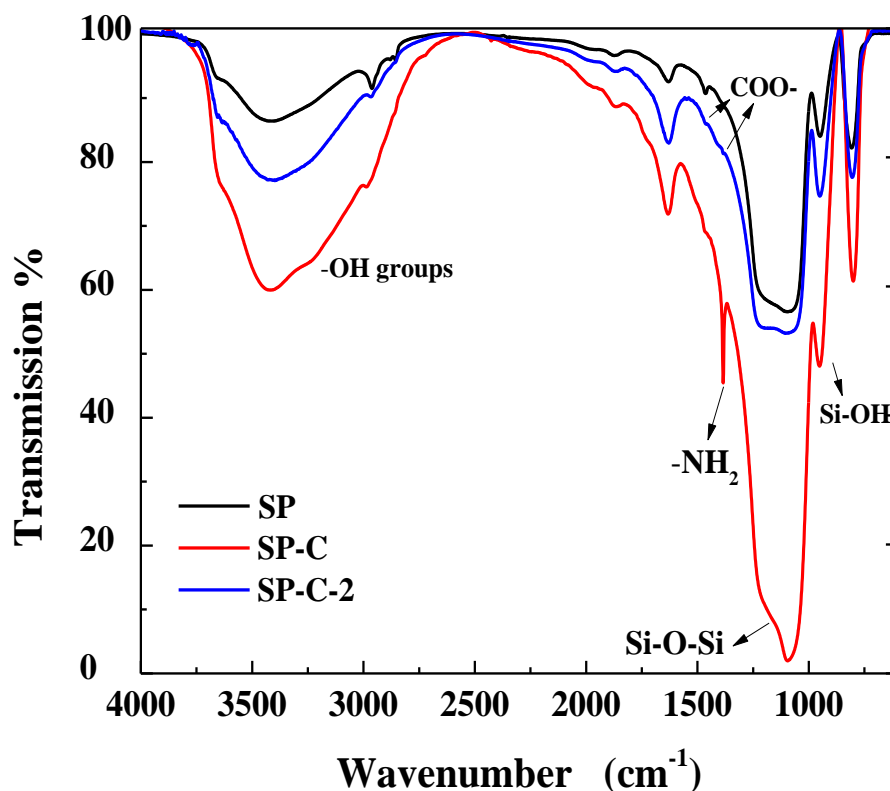


**Figure 4.8** FTIR spectra of bare SiO<sub>2</sub> (SP), treated with APTMS(SP-C) and with SA (SP-C-2).

The spectrum of bare SiO<sub>2</sub> clearly reveals the peaks due to Si-O-Si bonds (1080 cm<sup>-1</sup>) and Si-OH bonds (3500 cm<sup>-1</sup> and 960 cm<sup>-1</sup>). By contrast, SP-C particles modified with APTMS show the asymmetrical deformation vibration of the amino group at 1450 cm<sup>-1</sup>, indicating the APTMS was covalently bonded onto the SiO<sub>2</sub> particle surface as- their -NH<sub>2</sub> groups peak appeared in its spectra (Feifel & Lisdat, 2011). Further modification of SP particles with SA (SP-C-2) is revealed by FT-IR through the occurrence of carboxylate peaks at 1550 and 1490 cm<sup>-1</sup>. It can then be concluded that a sequential modification on the SiO<sub>2</sub> particle surface takes place successfully.

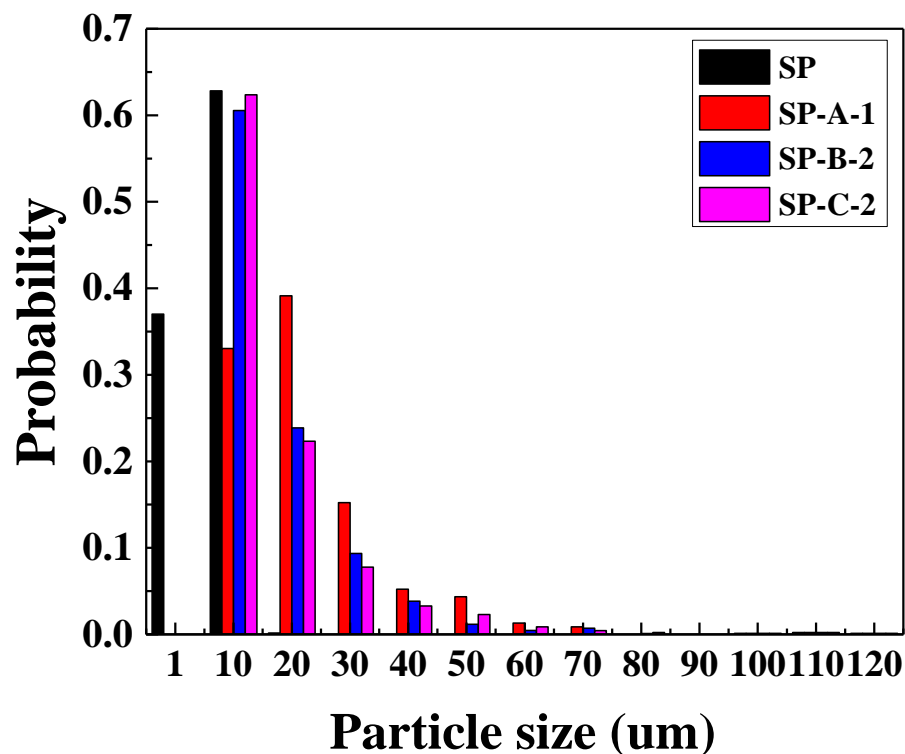


**Figure 4.9** Aggregates size distribution for SP, SP-A-1, SP-B-2 and SP-C-2 particles, at pH 3.0.

The category number indicates the upper size limit of aggregates (*e.g.* (1) corresponds to aggregate size below 1  $\mu\text{m}$ , (10) corresponds to aggregate size in-between 1  $\mu\text{m}$  and 10  $\mu\text{m}$ , etc).

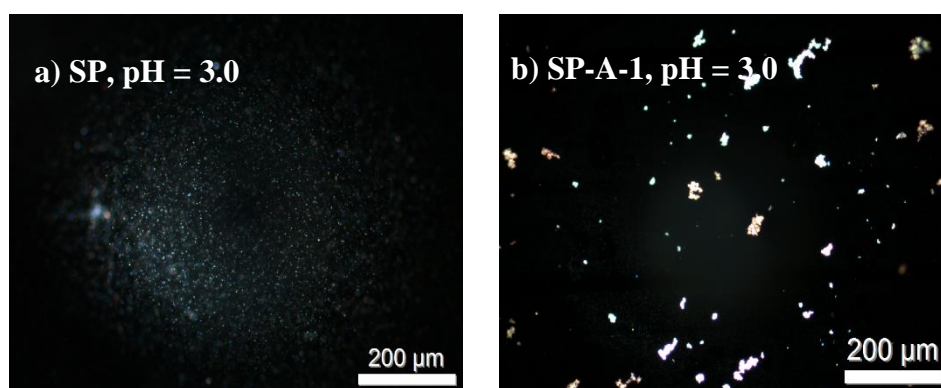


**Figure 4.10** Dark field optical microscopy micrographs showing the aggregation state, as a function of pH 3.0 of SP (a) and SP-A-1 (b).

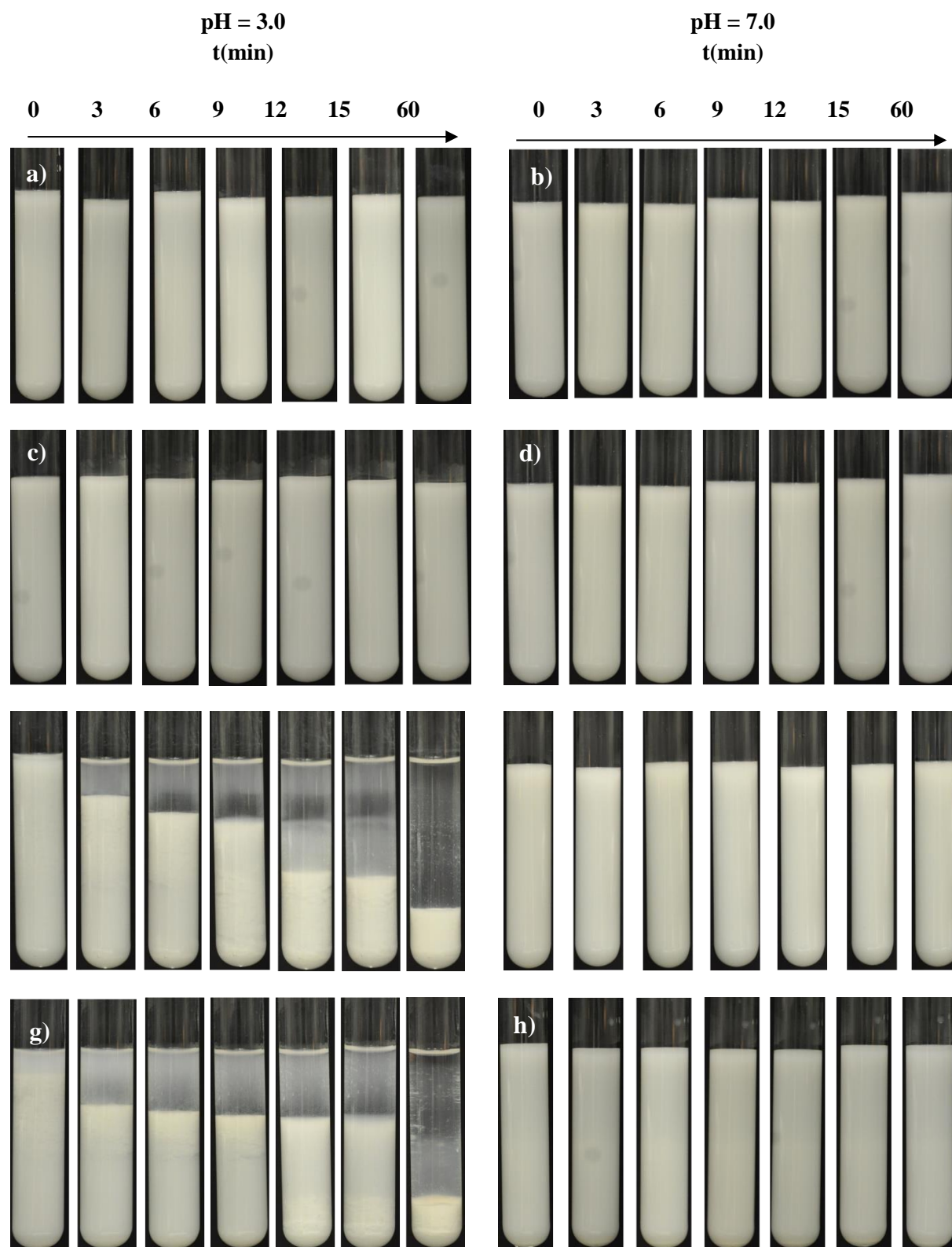


**Figure 4.11** Pictures of the sedimentation process (height of test tube = 15.3 cm) for SP-B (a, b), SP-C (c, d), SP-B-2(e, f) and SP-C-2(g, h) particles over 60 min at pHs 3.0 and 7.0 respectively.



## CHAPTER 5      ARTICLE 2: TUNING PARTICLE-PARTICLE INTERACTIONS TO CONTROL PICKERING EMULSIONS CONSTITUENTS SEPARATION

Faezeh Sabri, Kevin Berthomier, Chang-Sheng Wang, Louis Fradette, Jason R. Tavares and Nick Virgilio

<sup>a</sup> Center for Applied Research on Polymers and Composites (CREPEC), Department of Chemical Engineering, Polytechnique Montréal, Montréal, Québec, H3C 3A7, Canada

This work was published in *Green Chemistry* on February 11, 2019

DOI: [10.1039/c8gc03007c](https://doi.org/10.1039/c8gc03007c)

### 5.1 Abstract

We demonstrate that the separation and recovery of solid-stabilized (Pickering) emulsions constituents is significantly improved via a simple filtration approach – without any additional chemical agent – by initially grafting sodium alginate (SA), a natural polysaccharide, onto silane-modified sub-micrometer silica particles. The combination of surface-grafted trimethoxy(propyl)silane (TMPS) and (3-aminopropyl)trimethoxysilane (APTMS) controls particle wettability, verified via zeta potential and contact angle measurements. Rheometry and filtration experiments reveal that further grafting of SA via APTMS enhances particle-particle and droplet-droplet interactions. This work provides an approach towards the design of environmental-friendly Pickering emulsions based chemical engineering processes with easy-to-separate and reusable particles, allowing waste reduction and reduced toxicity advantages

### 5.2 Introduction

Solid-stabilized (or Pickering) emulsions are multiphase systems composed of liquid droplets dispersed in a second immiscible liquid. They are stabilized by sub-micrometer or nanometer-sized particles adsorbed at the liquid/liquid interface (Leal-Calderon & Schmitt, 2008). This surfactant-

free composition, combined with an exceptional stability, has generated interests in fields such as food formulations (Xiao, Li, & Huang, 2016), cosmetics (Y. Zhou et al., 2018), drug delivery (Laredj-Bourezg, Bolzinger, Pelletier, & Chevalier, 2017), oil recovery (Kumar, Gaur, & Mandal, 2017), nanocatalysis (Crossely, 2010; B. Y. Yang, Leclercq, Clacens, & Nardello-Rataj, 2017) and waste water treatment (H. Z. Zhang et al., 2008) to name a few. However, their stability is also a concern when it comes to designing processes in which these emulsions must be broken, and the components separated, for material recovery. As a result, the separation of Pickering emulsions constituents has become an important research topic over the years. For example, one of the major issues in the petroleum industry is the breakdown of undesirable Pickering emulsions formed during the different stages of oil recovery processing (Umar, Saaïd, Sulaimon, & Pilus, 2018). At the moment, synthetic and/or toxic chemicals and polymers are often used (Olajire, 2014; Raffa, Broekhuis, & Picchioni, 2016). In pharmaceutical and food applications (Furtado, Picone, Cuellar, & Cunha, 2015; Laredj-Bourezg et al., 2017) the possibility of triggering the release of encapsulated compounds is likewise of significant interest. As a result, emulsions that can be destabilized on demand by modifying the surface activity of the particles in response to an external trigger such as changes in pH (J. Kim et al., 2010; H. Liu, Wang, Zou, Wei, & Tong, 2012; Morse et al., 2013; Qi, Luo, & Lu, 2018; Tang et al., 2015), CO<sub>2</sub> concentration (Qian et al., 2014), light sensitivity (Jiang, Ma, Cui, & Binks, 2016), temperature (Tsuji & Kawaguchi, 2004), magnetic field (Cho et al., 2018; Peng et al., 2012), or combinations thereof, have recently been developed. The main approaches currently explored to separate Pickering emulsion constituents can be classified as chemical (Dyab, 2012), mechanical (Kruglyakov et al., 2004), magnetic (Kaiser, Liu, Richtering, & Schmidt, 2009) and electrically-based (Hwang et al., 2010). Chemical techniques are the most common and popular; however, they often involve large quantities of additives such as surfactants or polymers (Hernandez et al., 2016; Mirvakili, Rahimpour, & Jahanmiri, 2012) leading to water contamination and environmental pollution (Dyab, 2012). Mechanical destabilization methods such as centrifugal separation require high initial capital investment and maintenance (Howe A. M, 1990). In the case of magnetic and electrical approaches, the former is effective only under certain circumstances such as breaking droplets stabilized by magnetic particles, while the latter is feasible only for charged particles (Cho et al., 2018). As a result, there is still a demand for simple, ecofriendly and low-cost techniques for the separation of solid-stabilized emulsions constituents.

In our previous work, we demonstrated that surface-modified particles grafted with sodium alginate (SA), a natural pH sensitive gelling polysaccharide composed of two randomly distributed guluronic and mannuronic acid units on its chain, displayed enhanced aggregation/disaggregation properties. This behavior in aqueous solution is due to the reversible hydrogen bond formed between neighboring particles – these “sticky” particles form significantly larger flocs as compared to unmodified particles, resulting in easier and faster sedimentation (F. Sabri et al., 2018). Chen et al. have also synthesized pH-responsive SA grafted silica nanoparticles in applications related to drug delivery, exploiting the formation of a three-dimensional network of grafted SA chains to create high-stability systems (K. Chen et al., 2017).

In the present work, we hypothesize that these “sticky” particles could not only enhance interparticle interactions in solution, but also droplet-droplet interactions when adsorbed at the oil/water interface in Pickering emulsions. Therefore, the main objective of this work is to design and prepare solid-stabilized emulsions using SA-modified silica particles, and to assess if these particles can facilitate the separation and recovery of the emulsion’s constituents by a simple filtration approach.

## 5.3 Experimental section

### 5.3.1 Materials

Sub-micrometer silica particles (SP) were provided by Nippon Shokubai Trading Co. (average diameter  $d \approx 290 \pm 13$  nm validated by SEM, specific surface area  $S = 42 \pm 2$  m<sup>2</sup>·g<sup>-1</sup>, measured by BET with a Micromeritics ASAP 2020 instrument). (3-Aminopropyl)trimethoxysilane (APTMS, 97%), alginic acid sodium salt from brown algae (CAS 9005-38-3, low viscosity, molecular weight  $\approx 60$  kDa, pKa = 3.5), (T. Harnsilawat, Pongsawatmanit, & McClements, 2006) *N*-(3-dimethylaminopropyl)-*N*′-ethylcarbodiimide hydrochloride (EDC, > 98%), trimethoxy(propyl)silane (TMPS, 97%), *N*-hydroxysuccinimide (NHS, 98%), sodium azide (> 99%), Na<sub>2</sub>CO<sub>3</sub>-NaHCO<sub>3</sub> buffer solution (pH 10.01) and 5-(4,6-dichlorotriazinyl) aminofluorescein (DTAF) (D0531) were all purchased from Sigma-Aldrich and used without further purification. Ethanol (99.8%) was obtained from Thermo Fisher Scientific. HCl 1 N and NaOH 12 N solutions were of analytical grade and prepared without further purification with Milli-Q water (DI water,

18.2 M $\Omega$ -m, Synergy 185 system by Fischer Scientific). Low viscosity white mineral oil (Puretol™ 7, density of 0.846 kg/l and viscosity of 12.2 cSt at 40 °C) was provided by Petro-Canada.

### 5.3.2 Particles Surface Modification

#### 5.3.2.1 Silane Grafting

In order to graft SA onto silica particles and to control particle wettability, two types of silane agents were surface-grafted simultaneously. In a typical batch, 10 g of SP particles were dispersed in a hydrophobized Erlenmeyer flask containing 100 ml of a 95% v/v ethanol solution and DI water, while stirring at 600-700 rpm with a magnetic stirrer.(Arkles, 2006) The pH was then adjusted to 4.5 - 5.5 using HCl 1 N. APTMS and TMPS were added dropwise while stirring at room temperature, targeting a surface coverage of 10 molecules·nm<sup>-2</sup> (1:1 APTMS:TMPS relative composition) (**Scheme 5.1**) (F. Sabri et al., 2018). Typically, to modify 10 g of particles,  $6.10 \times 10^{-1}$  ml of APTMS and  $6.15 \times 10^{-1}$  ml of TMPS were added to the medium and the reaction was carried for 12 h at room temperature. The particles were collected by centrifugation (Sorvall RC 6+, Thermo Fisher Scientific) at 8000 rpm for 15 min and cleaned by washing twice with ethanol in order to rinse off any remaining unreacted silane. The particles were finally dried in a vacuum oven at 70 °C for 2 h.

#### 5.3.2.2 Sodium alginate grafting

A fraction of the silane-modified particles (SP-Sil) were further modified by grafting SA on their surface. In a typical experiment, 0.4 g of SA was first dissolved in 40 ml of DI water (1% w/v).  $1.4 \times 10^{-2}$  g of EDC and  $0.9 \times 10^{-2}$  g of NHS (1:1 EDC:NHS molar ratio) were then added to the solution (EDC/-COOH molar ratio = 0.1, relative to the -COOH groups of alginate)(Gabriele Giani, Serena Fedi, & Rolando Barbucci, 2012). Then, 4 g of SP-Sil particles were added to the reaction medium and the pH was adjusted to 4.5 with HCl 1 N (**Scheme 5.1**). The reaction proceeded for 15 h at room temperature and the mixture was subsequently centrifuged at 8000 rpm to collect the modified particles, which were washed with DI water 3 times. Finally, the particles modified with alginate (SP-SA) were dried in a vacuum oven at 70 °C for 10 h.

### 5.3.3 Particle surface characterization

#### 5.3.3.1 Zeta potential measurements

The zeta potential ( $\zeta$ ) of particles was measured with a Zetasizer Nano ZSP instrument (Malvern Instruments Ltd., Worcestershire, UK). Particles were first dispersed in DI water at pH 3.0, pH 7.0 or pH 10 (adjusted by adding HCl 1 N and NaOH 12 N) at a  $0.001 \text{ g}\cdot\text{ml}^{-1}$  concentration. The measurements were performed at  $25^\circ\text{C}$ , using at least three different samples for each particle type, by microelectrophoresis. Disposable zeta potential folded capillary cells (DTS1070) were used. The instrument determined the electrophoretic mobility, and the Smoluchowski model was then applied by the software for the calculation of  $\zeta$  (Lattuada & Hatton, 2007).

#### 5.3.3.2 Contact angle measurements

Since the silica particles locate at the oil/water interface (the contact angles are formed between the silica, water and oil phases), contact angles were measured by depositing a droplet of water on a disk of compressed particles, immersed in oil. Contact angles were measured using an OCA20 optical tensiometer (DataPhysics Instruments GmbH) at  $25^\circ\text{C}$ . First, disks composed of compressed particles (SP, SP-Sil or SP-SA) were prepared with a laboratory press (Model C 3100-212, Carver laboratory Press, USA). For each disk (12 mm diameter, 0.5 mm thick), 0.1 g of dried particles were compressed at 70.2 MPa for 2 min. For a typical contact angle measurement experiment, a disk was immersed in a quartz cuvette containing 5 ml of mineral oil. Then, a  $4 \mu\text{L}$  droplet of deionized water was carefully deposited on the disk's surface with a syringe (0.52 mm internal needle diameter, Hamilton model 1750TLL 500  $\mu\text{L}$ ). Images of the sessile water droplet were automatically acquired at 10 frames per second, until the water droplet completely penetrated into the pellet. The image illustrating the first contact between the water droplet and the pellet was considered as corresponding to the contact angle,  $\theta_{o/w}$ . Four compressed disks were prepared for each type of particles, and one measurement was realized on each.

#### 5.3.3.3 Emulsions preparation and characterization

Emulsions were prepared in screw cap glass vials (internal diameter = 1.2 cm, height = 4.6 cm) using a Cole-Parmer LabGEN 125 Homogenizer with a homogenization element of inner diameter 0.5 cm, at 18,000 rpm for 4 min. All emulsions contained 4% (w/v) particles (0.6 g) dispersed in

15 ml of liquid, at pH 3.0 or 7.0 (adjusted with HCl 1N or NaOH 12N), with the oil volume fraction  $\phi_o$  ranging from 0.1 to 0.9. Particles were added in the vial and dispersed in water by homogenization, followed by the dropwise addition of the required volume of oil, while homogenizing. Pictures of emulsions in glass vials and other photographs were taken with a Nikon DX AF-S Nikkor 18-55mm f:3.5-5.6 G VR II objective camera. Homogenizer processing did not alter or break silica particles, as the SEM of **Figure 5.9** illustrate.

#### **5.3.3.4 Droplet observation and diameter measurement**

Dispersed phase droplets were observed by dark field optical microscopy (Olympus BX51 by Cytoviva, objectives = 10x UPL Fluorite Oil, and 100x UPL Fluorite Oil Camera Q imaging, Retigna 2000R fast 1394, cooled color 12 bit). A drop of emulsion was first diluted in water at pH 3.0 or 7.0 before observation using glass slides (Fisher Scientific). Images were analyzed using the ImageJ software to determine drop size and to calculate the number-average diameter  $d$  of the observed droplets. Droplet size was also measured by laser diffraction using a MasterSizer 3000 instrument (Malvern Instruments, Canada).

#### **5.3.3.5 Rheological behavior**

The rheological properties of freshly prepared emulsions with SP or SP-SA particles were measured with an Anton Paar MCR502 stress-controlled rheometer instrument. Disposable measuring plates D-PP25/AL/S07 (diameter: 25 mm) and dish EMS/CTD 600 (diameter: 56 mm) geometries from Anton Paar, covered with extra fine (320) sand paper, were used to avoid emulsion slipping. To prevent water evaporation during experiments, the geometry was covered with a solvent trap. All experiments were performed at 21°C.

After emulsion preparation, prior to the rheological tests, the samples were first stored under vacuum for 15 min to remove any trapped air bubbles. Then, the samples were carefully loaded into the rheometer and the top plate geometry was lowered to a 1 mm gap. Samples were pre-sheared at  $0.1 \text{ s}^{-1}$  for 2 min. After determining the linear viscoelastic (LVE) regime, the storage and loss moduli ( $G'$  and  $G''$ , respectively) were measured during dynamic time sweeps ( $\omega = 1 \text{ rad}\cdot\text{s}^{-1}$ ,  $\gamma_0 = 1\%$ ) for 2 h.

### 5.3.3.6 Confocal microscopy (CLSM)

Emulsions were observed using an Olympus IX 71 inverted confocal microscope (Olympus Canada Inc., Richmond Hill, ON, Canada). SA was covalently labeled with 5-(4,6-dichlorotriazinyl) aminofluorescein (DTAF) (D0531, Sigma). This fluorescent dye directly reacts with hydroxyl groups to form stable, covalent links between the dye and substrate at room temperature in an aqueous solution at pH 9. (M.S., 2010) Briefly, 10 mg of DTAF was first dissolved into a 50 mL  $\text{Na}_2\text{CO}_3$ - $\text{NaHCO}_3$  buffer solution (0.1 M, pH = 10). 2.0 g of SA was then solubilized into the prepared DTAF solution. The mixture was allowed to react overnight at room temperature at a stirring speed of 600-700 rpm. The pH was adjusted to 7.0 to stop the reaction, as well as to ensure a quick diffusion rate for counterions during the following dialysis step. The mixture was dialyzed against Milli-Q water for 48 h to remove unreacted DTAF and the counterions. Sodium azide (0.02% (w/v)) was added to inhibit bacteria growth, and the Milli-Q water was changed every 2 h during dialysis. Suspensions were next cooled at  $-20^\circ\text{C}$ . After freeze-drying, a yellow powder was obtained. Observation of fluorescent SP-SA particles was made by excitation of DTAF at 488 nm (emission recorded between 510 and 550 nm). Micrographs were taken after approximately 24 h using 40x and 60x objective lenses at a  $2048 \times 2048$  pixels resolution (1 pixel =  $0.9 \times 0.9 \mu\text{m}^2$ ).

### 5.3.3.7 Separation tests and particles recovery

Emulsions composed of 4% (w/v) particles (SP or SP-SA) and various oil contents  $\phi_o$  were prepared and stored for about 4 weeks at room temperature. The emulsions were then filtered using stainless steel strainers (2 mm mesh size). The filtered oil droplets were weighted to calculate the mass fraction of retained oil droplets and solid particles.

The filtered oil droplets were then collected and transferred into vials containing 10 ml of mineral oil, which were next stirred with a magnetic stirrer at 600 rpm for 5 min. The mixtures were then centrifuged at 10 000 rpm for 10 min. The separated top oil phase was removed, and 30 ml of ethanol were added to the particles remaining in the container. They were hand-shook and re-centrifuged at 1000 rpm for 10 min. This step was repeated twice to ensure there was no oil remaining. Finally, particles were dried in a vacuum oven at  $60^\circ\text{C}$  for 2 h. The particles were weighted to calculate the recovery yield.

## 5.4 Results

### 5.4.1 Zeta potential and contact angle measurements confirm sodium alginate grafting

The zeta potentials ( $\zeta$ ) and contact angles ( $\theta_{o/w}$ ) were measured as a function of pH for bare silica particles (SP), silanized particles (SP-Sil) and particles modified with SA (SP-SA) (Table 5.1). SP particles display a slightly positive  $\zeta$  at pH 3.0 that decreases to negative values as the pH increased to 7.0 and 10.0. This behavior is expected due to the deprotonation of hydroxyl groups on the surface. This behavior is expected due to the deprotonation of hydroxyl groups on the surface ( $pK_a \sim 4.5$ ) (Knoblich & Gerber, 2001; Leung, Nielsen, & Criscenti, 2009).

**Table 5.1 Zeta potential  $\zeta$  and contact angle  $\theta_{o/w}$  of silica particles: pristine (SP), silanized (SP-Sil), and grafted with sodium alginate (SP-SA), as a function of pH (3.0, 7.0 and 10.0).**

	pH = 3.0		pH = 7.0		pH = 10.0	
Particle type	$\zeta$ (mV)	$\theta_{o/w}$ (°)	$\zeta$ (mV)	$\theta_{o/w}$ (°)	$\zeta$ (mV)	$\theta_{o/w}$ (°)
SP	$7.4 \pm 1.8$	$103 \pm 2$	$-52.2 \pm 1.5$	$98 \pm 4$	$-52.1 \pm 1.7$	$93 \pm 2$
SP-Sil	$77.4 \pm 3.2$	$157 \pm 9$	$45.1 \pm 2.1$	$151 \pm 2$	$36.9 \pm 0.16$	$159 \pm 6$
SP-SA	$7.6 \pm 2.1$	$98 \pm 8$	$-47.7 \pm 2.9$	$100 \pm 3$	$-47.2 \pm 2.6$	$97 \pm 10$

SP-Sil show a positive  $\zeta$  value of +77.4 mV at pH 3.0 due to the substantial protonation of  $-\text{NH}_2$  groups of APTMS. Increasing the pH to 7.0 and 10.0 resulted in a decreasing but still positive  $\zeta$  of +45.1 and +36.9 mV, respectively. This is explained by the deprotonation of surface bound



hydroxyl groups and the gradual deprotonation of APTMS  $\text{-NH}_3^+$  groups to neutral  $\text{-NH}_2$  groups. At pH 3.0, SP-SA particles present a similar behavior as compared to unmodified SP particles ( $\zeta = +7.6$  mV) because of the protonation of the SA carboxylate groups ( $\text{pK}_a = 3.5$ ), (T. Harnsilawat et al., 2006) confirming the subsequent grafting of SA with surface-bound APTMS. At pH 7.0 and 10.0,  $\zeta$  drops to  $-47.7$  mV and  $-47.2$  mV, respectively, since we are above the  $\text{pK}_a$  of SA and the  $\text{-COOH}$  groups on the surface are deprotonated, like a number of other polysaccharides (e.g. xanthan gum). The wetting properties of bare SP, and modified SP-Sil and SP-SA were evaluated via the contact angles ( $\theta_{o/w}$ ) of water droplets deposited on compressed disks of particles, immersed in a white mineral oil bath, at pH 3.0, 7.0 and 10.0 (**Table 5.1**). On bare SP,  $\theta_{o/w}$  slightly decreases from  $103^\circ$  to  $93^\circ$  as the pH increases from 3.0 to 10.0. After modification with APTMS and TMPS (SP-Sil),  $\theta_{o/w}$  increased above  $150^\circ$ , the particles becoming more hydrophobic due to the aliphatic carbon chains grafted on their surfaces. Further modification with SA resulted in a decrease of  $\theta_{o/w}$  to values nearly identical to unmodified SP particles, due to the hydrophilic nature of SA that compensates the hydrophobic character of the grafted silanes. Both  $\zeta$  and  $\theta_{o/w}$  confirmed surface grafting of APTMS and TMPS silanes onto bare silica particles, followed by the covalent reaction of SA with APTMS, yielding pH-sensitive sodium alginate grafted sub- $\mu\text{m}$  particles (F. Sabri et al., 2018). XPS and FTIR characterization of the particles before and after surface modification was completed previously (F. Sabri et al., 2018). These experiments confirmed the sequential grafting of the silane coupling agent (APTMS) and sodium alginate onto SP particles. The presence of grafted APTMS was confirmed by two different components related to N-H bonds observable in the spectra (extracted from the N1s peak in high resolution XPS) and one component linked to C-N bonds. Grafting of APTMS was also confirmed independently by FTIR analysis with a band associated to N-H bond asymmetrical deformation vibration at  $1450\text{ cm}^{-1}$ .

#### 5.4.2 Sodium alginate modified particles stabilize oil-in-water emulsions

We next assessed the amphiphilic properties of SP and SP-SA particles via their propensity to stabilize emulsions comprised of white mineral oil (O) and water (W). Two complementary compositions were prepared ( $\phi_o = 0.3$  or  $0.7$ ), with the addition of 4% (w/v) particles. Two pHs were tested (3.0 and 7.0), and the particles were always dispersed first in the major liquid phase, followed by the gradual addition of the minor liquid phase. **Figure 5.1** shows that, for all tested

conditions, SP and SP-SA particles stabilize oil-in-water emulsions and hence display a more hydrophilic character (Wan & Fradette, 2017). Note that the more hydrophobic SP-Sil were not able to stabilize any emulsion. Also, grafting the two silanes along with alginate was necessary to stabilize emulsions with SP-SA particles (using only APTMS with alginate did not allow emulsion stabilization). Interestingly, emulsions stabilized with SP-SA particles displayed a much thicker/viscous aspect compared to SP particles, at similar particle concentration and oil composition.

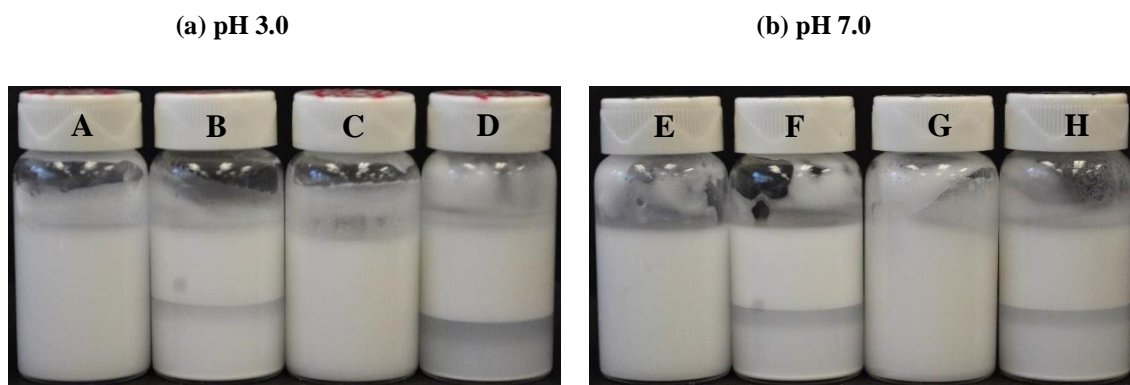


**Figure 5.1** Oil-in-water emulsions all comprising 4% (w/v) particles at pH 3.0 (a) and 7.0 (b). pH 3.0: (A) SP particles,  $\phi_o = 0.7$ ; (B) SP,  $\phi_o = 0.3$ ; (C) SP-SA,  $\phi_o = 0.7$ ; (D) SP-SA,  $\phi_o = 0.3$ . (E) to (H) same as (A) to (D), but at pH 7.0

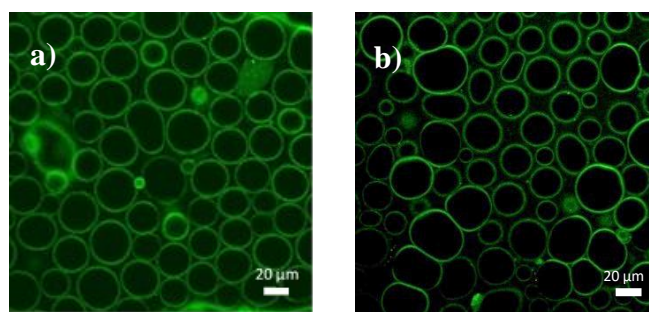


**Figure 5.2** CLSM pictures of Pickering emulsions ( $\phi_o = 0.8$ ) with 4% SP-SA (w/v) particles at pH 3.0 (a) and 7.0 (b).

Interestingly, emulsions stabilized with SP-SA particles display a much thicker/viscous aspect compared to SP particles, at similar particle concentration and oil composition. It does support our initial hypothesis since stronger attractive interactions between neighboring “sticky” particles

should lead intuitively to a higher concentrated emulsion viscosity, or higher viscoelastic properties ( $G'$  and  $G''$ ). Average droplet sizes as a function of composition, and the emulsions' rheological properties results, are presented next to quantify these initial observations. CLSM pictures confirm the interfacial activity of SP-SA particles at pH 3.0 and 7.0 (**Figure 5.2**). The particles were rendered visible by labeling SA with DTAF. We can observe that particles are adsorbed at the oil/water interface and form barriers preventing coalescence, as a number of deformed neighboring droplets illustrate. The oil volume fraction  $\phi_o$  is another important parameter that can have an effect on emulsion type and stability. Keeping the concentration of particles constant at 4% (w/v),  $\phi_o$  was gradually increased from 0.1 to 0.9 (**Figure 5.11**). Both unmodified (SP) and sodium alginate-modified (SP-SA) particles can stabilize oil-in-water emulsions up to  $\phi_o = 0.8$ . (after 4 weeks, the emulsions were still stable, **Figure 5.12**). As mentioned previously, all emulsions prepared with SP-SA particles display a thicker or more viscous texture as compared to emulsions prepared with SP particles (**Figure 5.11e-f**). In agreement with previous findings (F. Sabri et al., 2018), particles modified with SA could experience stronger attractive interparticle interactions due to hydrogen bond formation – especially at pH 3.0, below the pKa of SA –, which might explain the more viscous appearance. Optical microscopy was employed to calculate the average droplet size as a function of  $\phi_o$  and pH. **Figure 5.4** displays the micrographs of emulsions prepared with SP and SP-SA particles, at pH 3.0 and 7.0. As expected, increasing the mineral oil volume fraction up to  $\phi_o = 0.7$  at a constant particle content leads overall to an increasing average droplet size, from 10  $\mu\text{m}$  to 30  $\mu\text{m}$  (**Figures 5.4 and 5.5**). For a given  $\phi_o$ , and for both pHs, droplets are slightly bigger with SP particles (especially at  $\phi_o = 0.3$  and 0.5), compared to SP-SA. A sudden increase in droplet size for SP particles is observed when the oil content increases to  $\phi_o = 0.8$  (**Figure 5.5**). The results from optical microscopy observations are consistent with the results of laser diffraction experiments, as the same trends were obtained (see **Figure 5.12 in Supporting Information**).

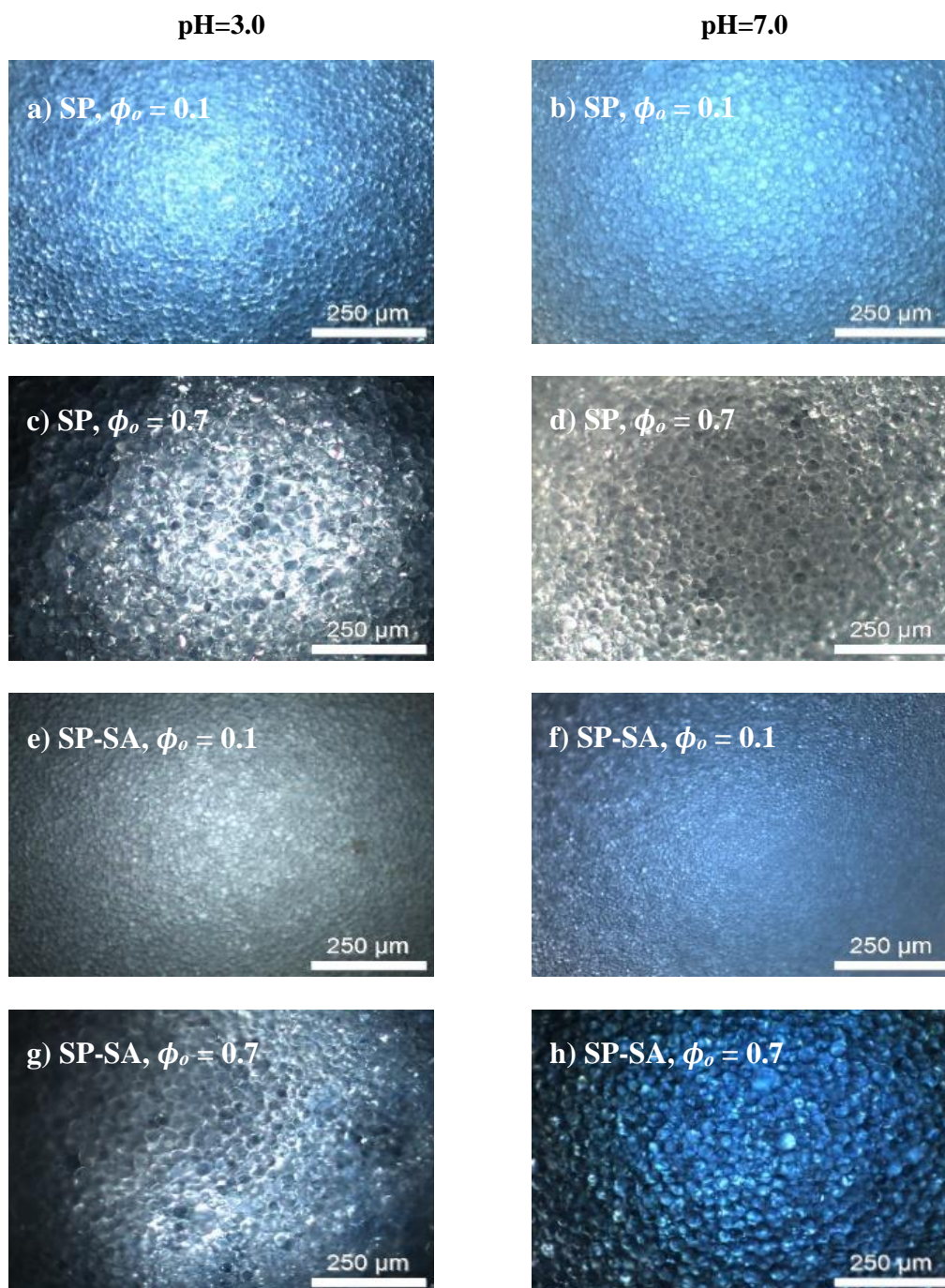


**Figure 5.3** Dark field optical microscopy micrographs showing oil droplets, as a function of oil content  $\phi_o$ , at pH 3.0 (left column) and 7.0 (right column), for SP (a to d), and SP-SA (e to h) particles

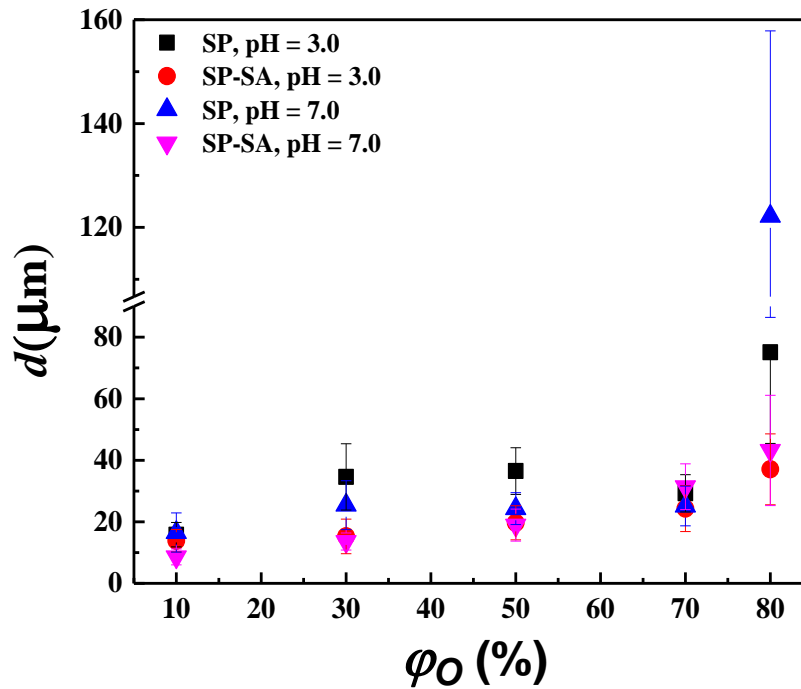


**Figure 5.4** Number average diameter  $d$  of oil droplets as a function of oil volume fraction  $\phi_o$ , for both SP and SP-SA particles, at pH 3.0 and pH 7.0.

#### 5.4.3 Sodium alginate-modified particles enhance the rheological viscoelastic properties of emulsions

**Figure 5.5** shows the evolution of the storage modulus ( $G'$ ) and loss modulus ( $G''$ ) as a function of time, at pH 3.0 and 7.0, for concentrated emulsions at  $\phi_o = 0.8$  with 4% (w/v) particles.  $G'$  and  $G''$  of emulsions prepared with SP-SA particles are about 10 times superior to emulsions prepared with pristine SP particles, in accordance with the qualitative observation in **Figure 5.11e-f**, at both pH 3.0 and 7.0. For a given particle type,  $G'$  is about 5 to 5.5 times higher than  $G''$ , evidence that these concentrated emulsions behave as weak gels.  $G'$  and  $G''$  are also time-dependent and gradually increase, indicating a slow structuration or reorganization process. The enhanced viscoelastic properties and self-holding property of concentrated emulsions prepared with SP-SA particles (**Figures 5.11e-f and 5**) also suggest the possible existence of a yield stress in these systems – i.e. the need to apply a finite mechanical stress to induce flow. To verify this hypothesis, the emulsions

were then molded and subjected to three increasing compressive stresses (193, 290, and 387 Pa) over 275 min (**Figure 5.6**) in order to measure sample compression as a function of time.

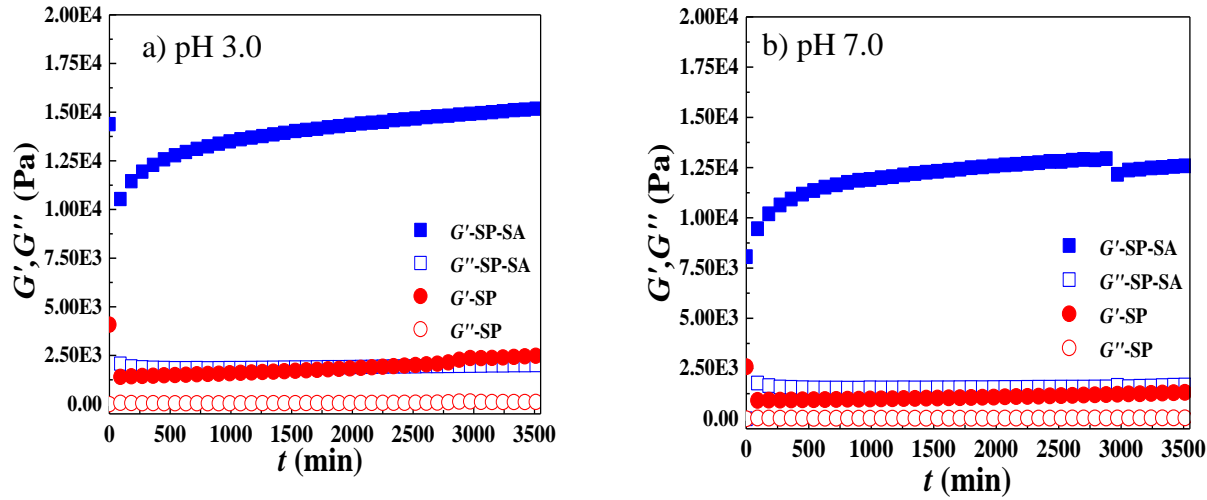


**Figure 5.5** Storage ( $G'$ ) and loss modulus ( $G''$ ) as a function of time ( $t$ ) at 20 °C, for concentrated emulsions ( $\phi_o = 0.8$  and 4% (w/v) particles) at pH 3.0 (a) and 7.0 (b). All tests were performed at  $\omega = 1$  rad/s,  $\gamma_0 = 1\%$ .

At pH 3.0, emulsions prepared with SP-SA particles could withstand all three stresses over the experiment duration, the molded emulsion losing no more than 6% of its initial height (**Figure 5.6a** for version with error bars see **Figure 5.13**). A similar result was obtained at pH 7.0. As **Figure 5.6b-c** illustrate, they are quite solid and can be easily manipulated. In comparison, emulsions prepared with SP particles failed to withstand the lowest applied stress and instantly collapsed, as **Figure 5.6d** illustrates. Finally, as demonstrated in a previous article, SP-SA particles in aqueous suspension strongly interact at pH 3.0 via hydrogen bonding, and a less compact bed is formed after sedimentation (**Figure 5.15**) (F. Sabri et al., 2018).



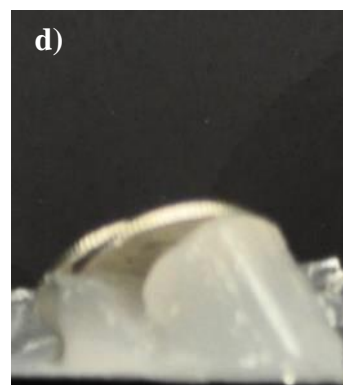
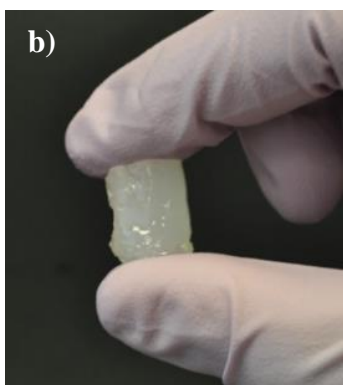
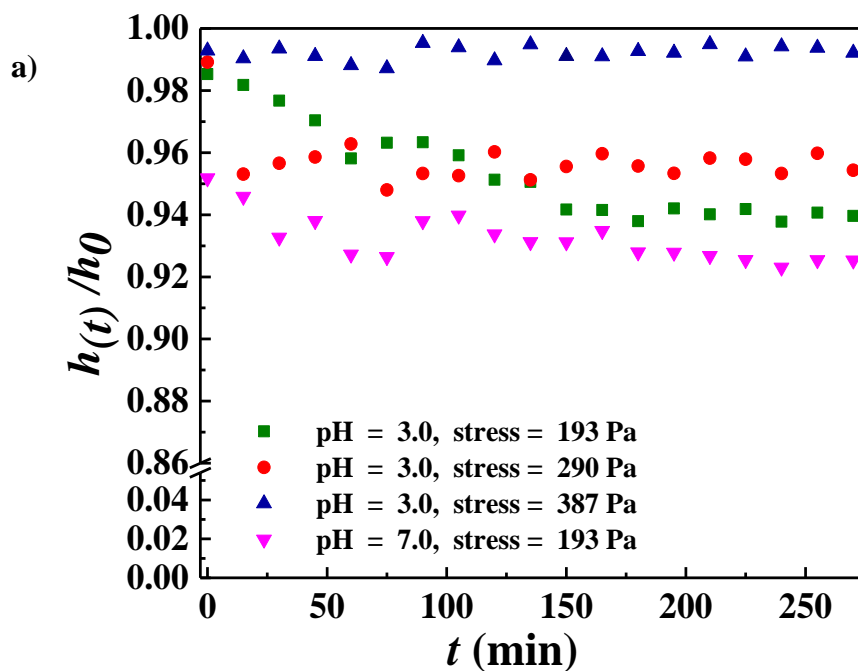


**Figure 5.6** a) Normalized height ( $h(t)/h_0$ ) as a function of time  $t$  and applied stress on molded concentrated emulsions ( $\phi_o = 0.8$ ) comprising 4% SP or SP-SA particles, at pH 3.0 and 7.0; b-c) visual aspect of the solid-like behavior of molded Pickering emulsions comprising 4% SP-SA particles, compared to a concentrated emulsion prepared with pristine SP displaying no yield stress, at pH 3.0;

### 5.4.3 Sodium Alginate-Modified Particles Improve the Separation of Pickering Emulsions Constituents

The enhanced soft (soft solid in the previous section), gel properties, along with the droplet-droplet and particle-particle attractive interactions in emulsions prepared with SP-SA particles, (F. Sabri et al., 2018) led us to hypothesize that the separation of constituents could be realized by filtration – *i.e.* separating the continuous water phase from the oil droplets. **Figure 5.7** illustrates the process for three emulsion compositions ( $\phi_o$  ranging from 0.1 to 0.5) at a constant particle content of 4% (w/v). The initial emulsions are displayed (typically comprising an emulsified oil phase on top (white), an aqueous phase below it (transparent), and unadsorbed particles at the bottom (white), see bottle on the left in Fig. 8a), along with the collected oil droplets and uncollected material. For all three oil compositions, the filtration of emulsions prepared with SP-SA particles at pH 3.0 yielded a significantly higher collected mass fraction of material, as compared to emulsions prepared with SP particles (**Table 5.2**). For example, at  $\phi_o = 0.1$ , there is no oil droplets remaining on top of the aqueous phase after filtration when using SP-SA particles (**Figure 5.7d**), as compared to SP particles (**Figure 5.7a**). Furthermore, the collected fraction for the SP-SA system even reaches 176% (calculated by dividing the initial emulsion content, by the mass of collected material), meaning that water is also retained with the oil droplets. As the oil fraction increases, the collected mass fraction gradually decreases for both SP-SA and SP emulsions due to the collected fraction's own weight. However, in all cases, the collected mass for SP-SA emulsions is nearly twice as much compared to SP systems. As a result, the amount of recovered dried particles (calculated based on the amount of emulsified particles) is always significantly superior for SP-SA particles, as compared to SP particle, at a given oil content  $\phi_o$ , as the last column of **Table 5.2** illustrates. Finally, the recovered oil and SP-SA particles (for the emulsion composed of 10% oil) were next re-used, with additional fresh SP-SA particles to reach 4% w/v), to form an emulsion again (at  $\phi_o = 0.7$ ), as **Figure 5.8** illustrates, demonstrating the potential of reusing particles. This opens up interesting perspectives for cleaner separation processes.



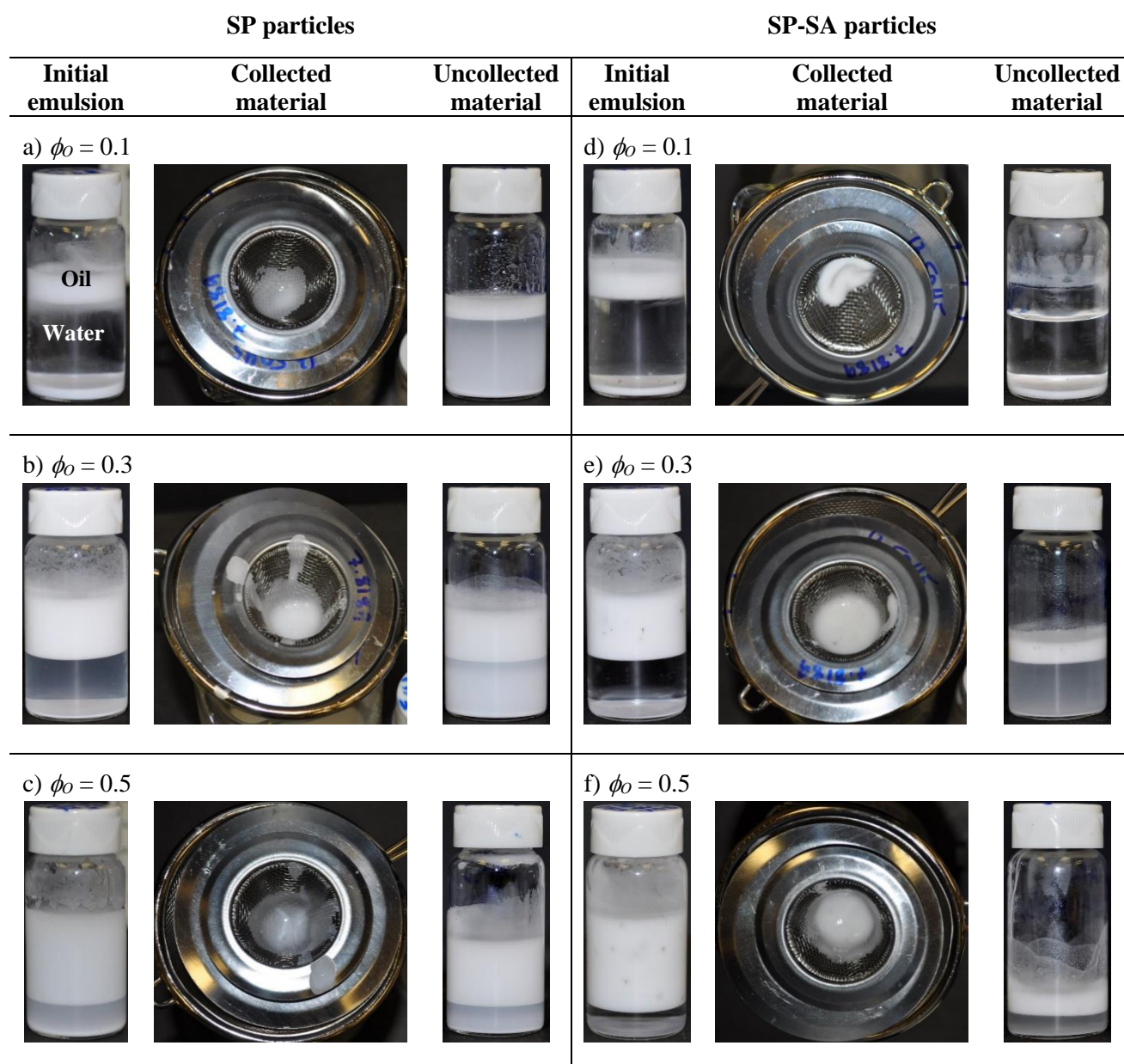


**Figure 5.7** Filtration of Pickering emulsions prepared at pH 3.0 with 4% particles: a-c) emulsions prepared with pristine SP particles with oil content  $\phi_o = 0.1$ , 0.3 and 0.5, respectively; d-f) same as (a-c), but with sodium alginate modified particles (SP-SA).

**Table 5.2 Gravimetric analysis of collected material after filtration experiments**

Emulsion Composition (Particle type / $\phi_o$ )	Emulsion (oil + particles) initial content <sup>1</sup> (g)	Collected Material <sup>2</sup> (g) / (%)	Recovered Particles in Collected Material <sup>3</sup> (%)
SP / 0.1	1.39	$0.96 \pm 0.08$ (69%)	2
SP / 0.3	4.22	$1.51 \pm 0.71$ (36%)	9
SP / 0.5	6.79	$1.77 \pm 0.24$ (26%)	29
SP-SA / 0.1	1.41	$2.48 \pm 0.57$ (176%)	47
SP-SA / 0.3	4.37	$2.81 \pm 0.59$ (64%)	23
SP-SA / 0.5	6.95	$3.27 \pm 1.03$ (47%)	34

<sup>1</sup>: obtained by subtracting the mass of un-adsorbed particles,  $m_{\text{un-adsorbed}}$ , obtained by image analysis; <sup>2</sup>: % is calculated by dividing the mass of collected material, by the initial emulsion content in column 2; <sup>3</sup>: compared to weight of emulsified particles ( $0.6 \text{ g} - m_{\text{un-adsorbed}}$ ).

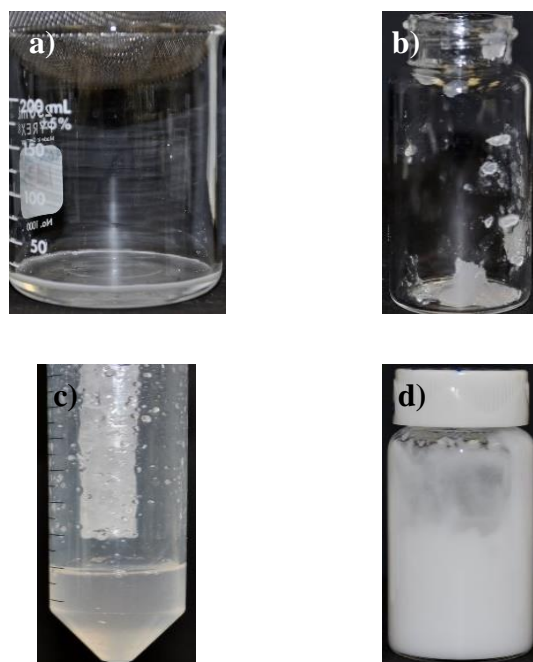


**Figure 5.8** a) Remaining aqueous phase after the filtration of oil droplets, b) collected oil droplets and particles, c) re-dispersion of collected material (oil + particles) in oil phase and d) stabilization of emulsion using recovered particles.

## 5.5 Discussion

By modifying the surface properties of silica particles with a natural polysaccharide, in this case sodium alginate, we have improved the separation process of Pickering emulsions constituents via a simple filtration process, avoiding the use of potentially toxic chemicals. The collected mass fraction after filtration does not reach 100% (**Figure 5.7** and **Table 5.2**), even for emulsions prepared with SP-SA particles, mainly for two reasons: (1) a fraction of the oil droplets passes through the mesh, as the uncollected fraction illustrates for  $\phi_o = 0.3$  and 0.5. This could be improved by increasing interparticle and droplet-droplet interactions via careful tuning of particle surface chemistry. Increasing the SA molecular weight, changing the SA guluronic/mannuronic block ratio, and testing other gelling polysaccharides such as xanthan gum, would be pertinent to look at. From a more fundamental perspective, controlling how grafting occurs – i.e. controlling the conformation of grafted molecules on the surface – also needs to be investigated. The combined result would be a significant improvement of particle recovery and overall components separation. Surface modification in this work serves two purposes. One is to adjust the wettability properties of particles in order to form Pickering emulsions (**Table 5.1**), a strategy that has been employed by various groups in past publications (G. Giani et al., 2012; Mirvakili et al., 2012; Olajire, 2014). In our case, we first use two complementary silanes. The first one, TMPS, increases the hydrophobic character of silica particles. The second, APTMS, is a linker allowing sodium alginate grafting, which is more hydrophilic. The second purpose of surface modification is to tune interparticle interactions, in order to increase particle-particle attraction – in the case of SA, via hydrogen bond formation as we demonstrated in a previous article (F. Sabri et al., 2018). Interparticle interactions can occur between particles adsorbed on the same droplet – which should increase the mechanical resistance of the particle layer, a hypothesis that remains to be verified –, or between particles in contact adsorbed on neighboring droplets – increasing at the same time droplet-droplet interactions. In that case, we should expect, for concentrated emulsions, increases for  $G'$  and/or  $G''$  values, which we did observe (**Figure 5.5**). Similar results were obtained by Chen et al. in Pickering emulsions comprised of paraffin oil, water and sodium alginate modified particles (K. Chen et al., 2017). Enhanced attractive interactions are also supported by the existence of a yield stress for concentrated emulsions prepared with SP-SA particles (**Figure 5.6**), which is not observed for emulsions prepared with pristine SP particles. Finally, stronger attractions help to retain oil droplets

in the collected materials after emulsion filtration. In a previous article (F. Sabri et al., 2018), we demonstrated that interparticle attractive interactions between sodium alginate modified particles are maximized at low pH. SA in solution forms a gel at low pH due to the protonation of its carboxylic acid groups (the molecule is nearly neutral), which promotes the formation of intermolecular hydrogen bonds. While we observed significant increases for both  $G'$  and  $G''$  at pH 3.0 for concentrated emulsions prepared with SP-SA particles, as compared to SP particles, unexpected increases were also observed at pH 7.0, which might be due to the confinement of the particles both at the oil/water interface, and close contact between neighboring droplets. This remains to be elucidated.

## 5.6 Conclusion

This article demonstrates that grafting a natural polysaccharide, sodium alginate, on the surface of silica particles stabilizing oil-in-water Pickering emulsions, can significantly improve the subsequent separation and recovery of the initial constituents via a simple filtration approach – leading to significant waste and toxicity reductions by avoiding the use of toxic chemicals to alter the chemical state of the emulsion (pH, ionic strength). Particle surface modification, herein realized with two silane agents and sodium alginate, plays two distinct and complementary roles. The first is to tune particle wettability in order to stabilize the emulsions – this is achieved with the choice of silane reagents. The second is to enhance particle-particle and droplet-droplet attractive interactions, in order to facilitate their filtration and the separation of constituents – achieved with sodium alginate via intermolecular hydrogen bonding. As a result, two opposite features – stabilization vs separation – are independently controlled with a single type of particles. The wide choices of silane agents and natural polysaccharides/proteins should next allow a finer tuning and optimization of this approach, which is of interest for the development of greener chemical engineering processes involving particulates dispersed in fluids with reduced environmental impact.

## 5.7 Acknowledgements

We acknowledge the financial support of Imperial Oil through a University Research Award grant, Total (Industrial Research Chair), the National Sciences and Engineering Research Council

(Discovery Grant), CREPEC (Projets Structurants), Polytechnique Montreal (UPIR undergraduate research grants) and the Canada Foundation for Innovation (John R. Evans Leaders Fund). We would like to thank Mr. Wendell Raphael for optical microscopy observations, and Dr. Ebrahim Jalali Dil and Mr. Matthieu Gauthier for SEM observation and rheological measurement, Dr. Gilles L'enfant, and Dr. Olivier Drevelle for fruitful discussions and technical support.

## 5.8 Supporting Information Article 2 : Tuning particle–particle interactions to control Pickering emulsions constituents separation

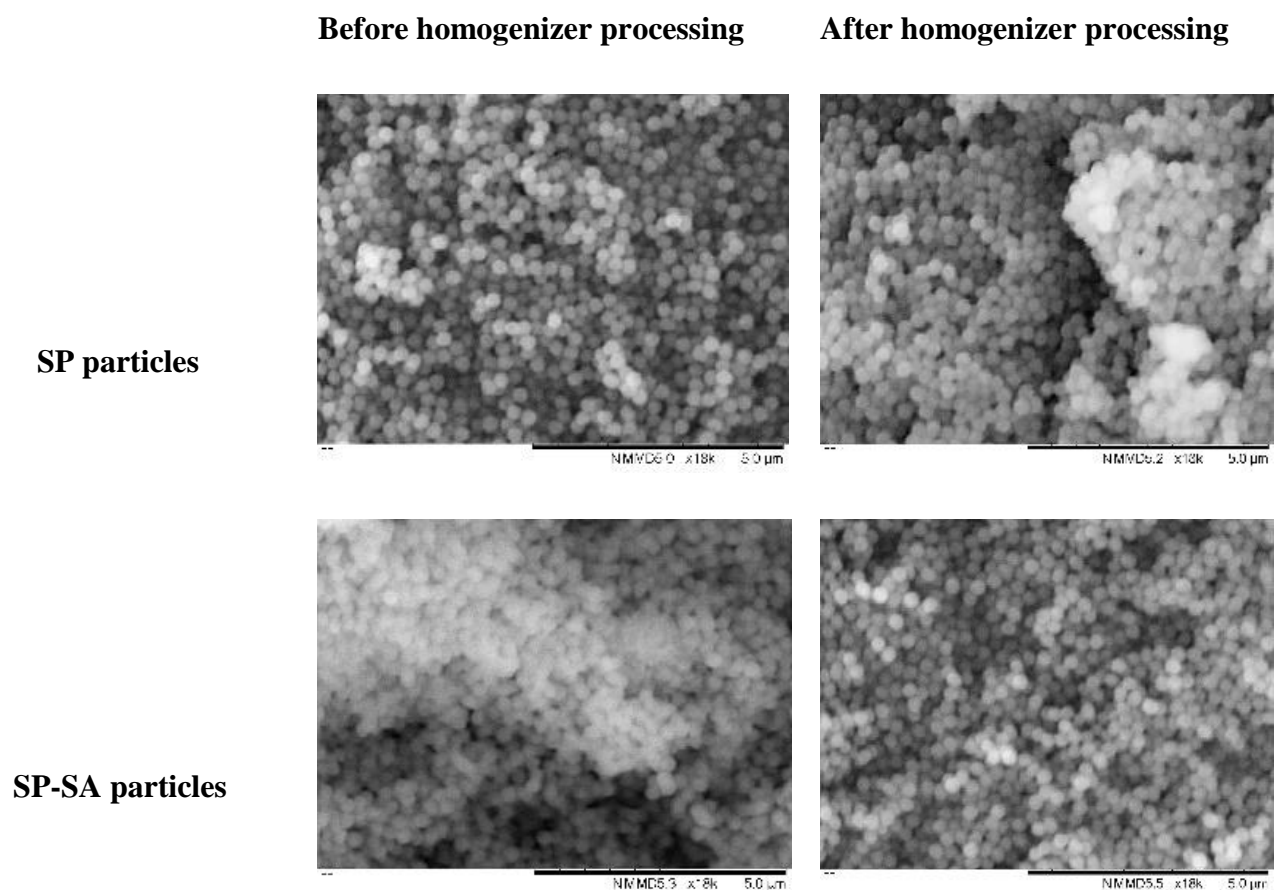


**Figure 5.9** SEM micrographs of SP and SP-SA particles before and after homogenizer processing.

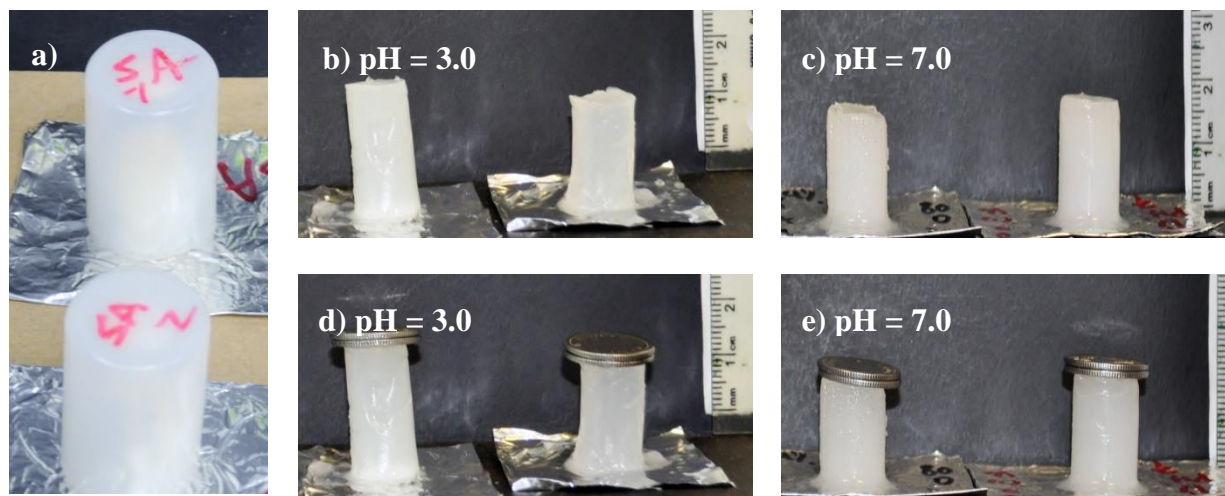


**Figure 5.10** Pictures of concentrated oil-in-water Pickering emulsions comprising 4% SP-SA particles ( $\phi_o = 0.8$ ) when contained into the plastic molds (a), removed from plastic molds (b, c), and under compressive stress (d, e).

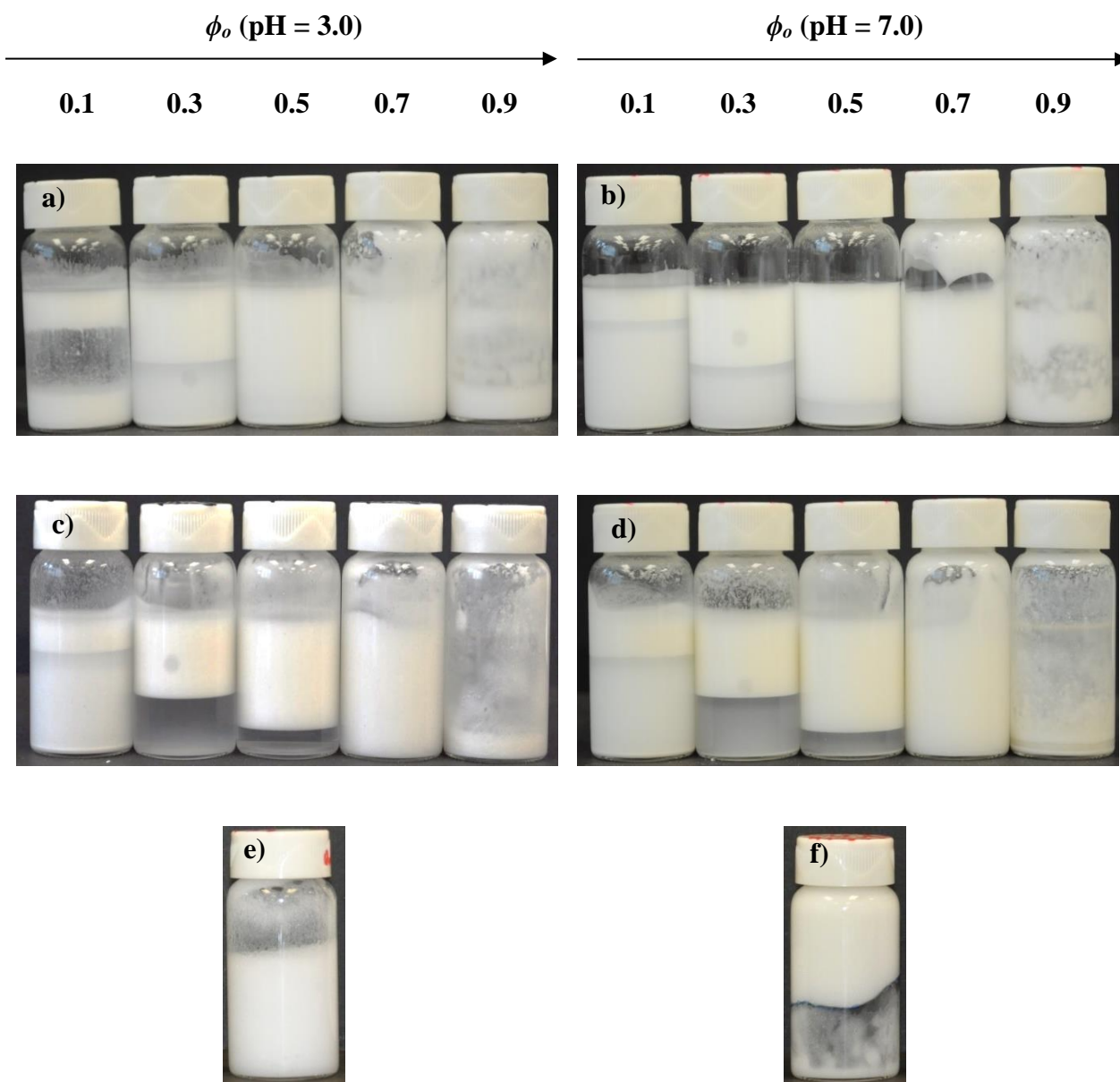


**Figure 5.11** Effect of oil volume fraction  $\phi_o$  on emulsion aspect, with 4% (w/v) particles: a) and b), emulsions prepared with unmodified silica particles (SP) at pHs 3.0 and 7.0, respectively; c) and d), emulsions prepared with sodium alginate-modified particles (SP-SA), at pHs 3.0 and 7.0; e) emulsion composed of SP particles (4% w/v) at  $\phi_o = 0.8$ , compared to f) emulsion composed of SP-SA particles (4% w/v) at  $\phi_o = 0.8$ .



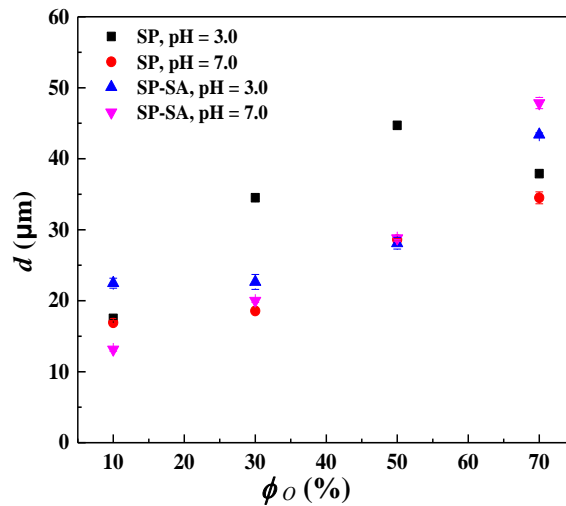


**Figure 5.12** Number average diameter  $d$  of oil droplets as a function of oil volume fraction  $\phi_o$ , for both SP and SP-SA particles, at pH 3.0 and 7.0, as obtained by laser diffraction (Mastersizer).

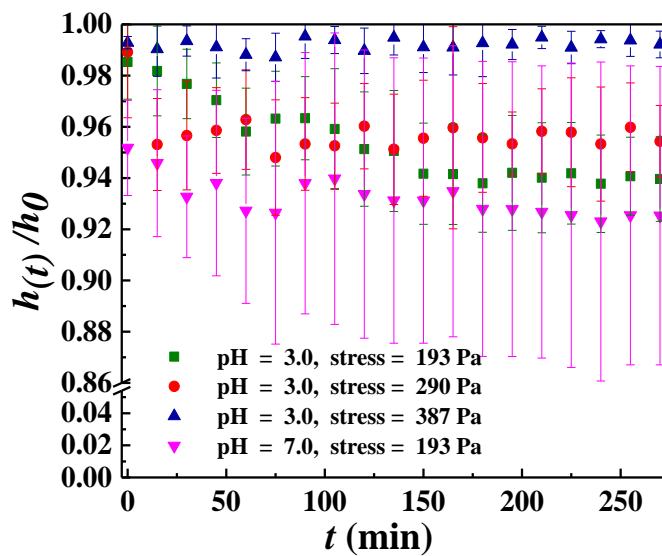


**Figure 5.13** Normalized height ( $h(t)/h_0$ ) with the error bars as a function of time  $t$  and applied stress on molded concentrated emulsions ( $\phi_o = 0.8$ ) comprising 4% SP or SP-SA particles, at pH 3.0 and 7.0.



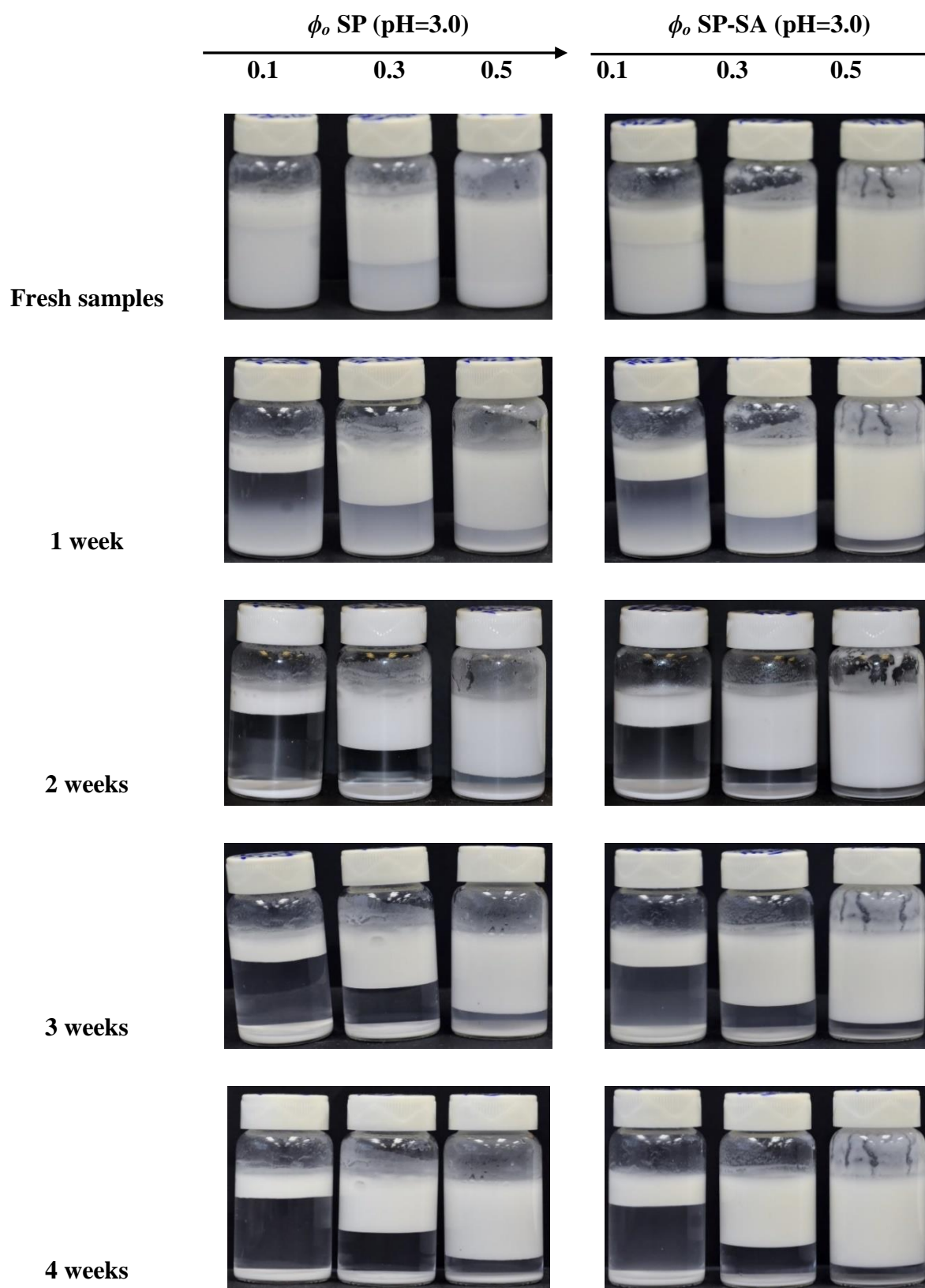


**Figure 5.14** Emulsion stability in time with 3 different oil volume fraction  $\phi_o$ , and constant 4% (w/v) particles.

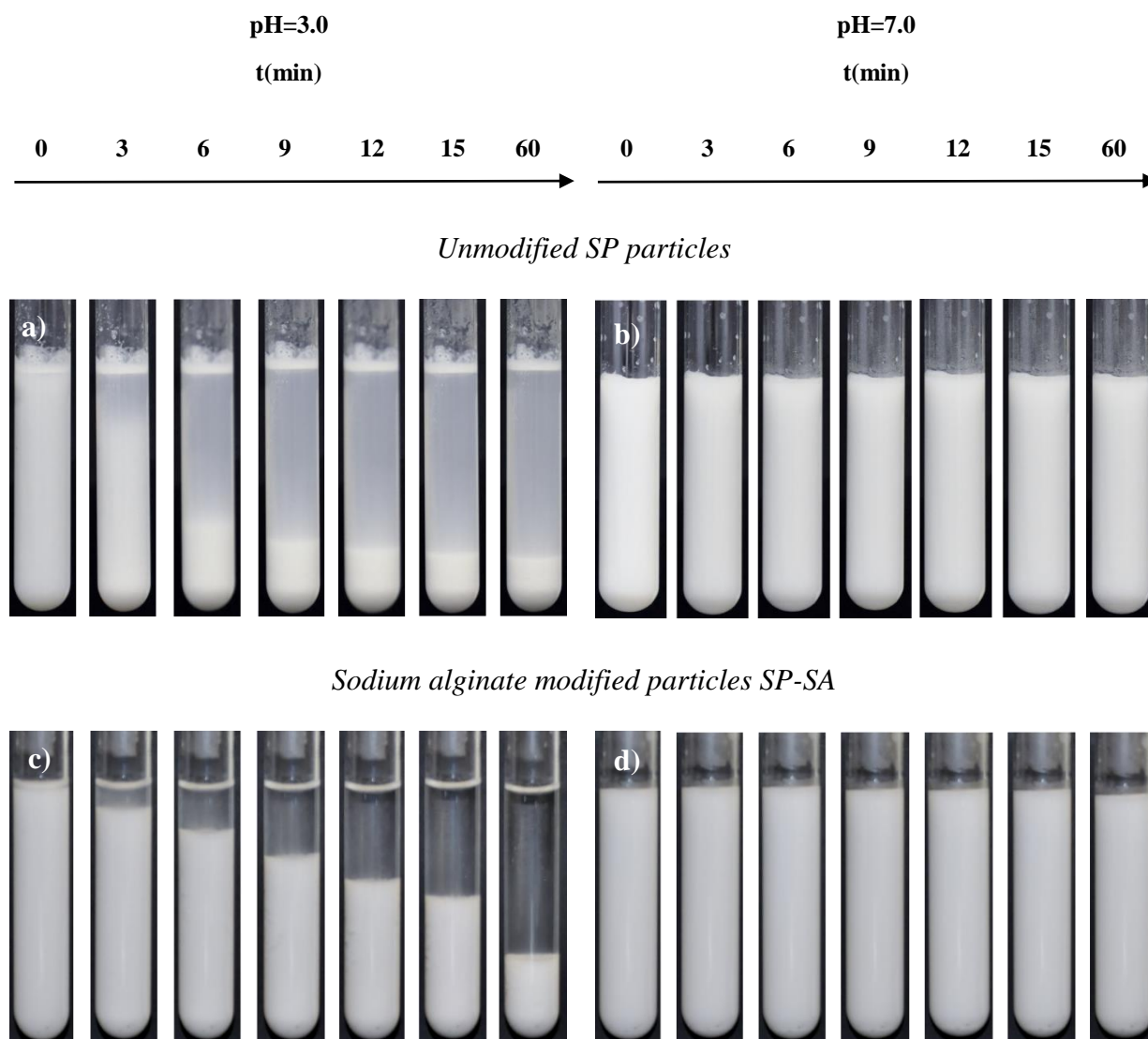
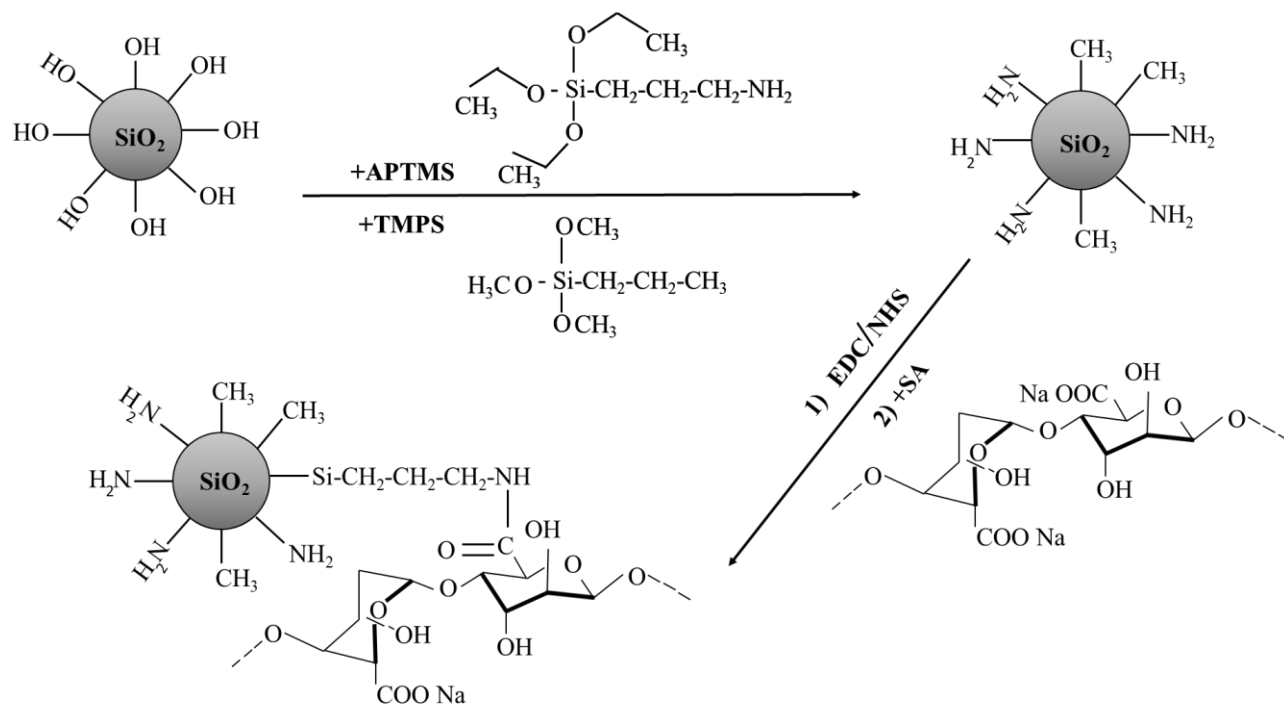


**Figure 5.15** Pictures of the particle's behaviour (height of test tube = 15.3 cm) for SP (a, b), SP-A (c, d), over 60 min at pHs 3.0 and 7.0 without oil droplets.



**Scheme 5.1** Reaction Schemes to modify SP particles with APTMS, TMPS and SA molecules respectively

## CHAPTER 6      ARTICLE 3: ONE-STEP PROCESSING OF HIGHLY VISCOUS MULTIPLE PICKERING EMULSIONS

Faezeh Sabri, Wendell Raphael, Kevin Berthomier, Louis Fradette, Jason R. Tavares and Nick Virgilio\*

Center for Applied Research on Polymers and Composites (CREPEC), Department of Chemical Engineering, Polytechnique Montréal, Montréal, Québec, H3C 3A7, Canada

This work has been submitted to *Journal of Colloids and Interface Science*.

### 6.1 Abstract

The processing of double emulsions typically requires two types of surface-active particulates/surfactants, and two processing steps. In this work, we demonstrate that double water-in-oil-in-water (W/O/W) solid-stabilized (Pickering) emulsions are obtained in a single processing step when using high viscosity silicone oil and a single type of sub- $\mu\text{m}$  silica particles modified with two grafted silanes and sodium alginate. The formation of water sub-inclusions proceeds via a phase-inversion mechanism. These sub-inclusions are subsequently stabilized and retained in the oil phase due to its viscosity, limiting sub-inclusions mobility, and the presence of adsorbed particles forming dense layers at oil-water interfaces, acting as barriers. The process we present is simple, requires a minimum number of components, and allows the preparation of multiple emulsions which could then be used to protect and/or transport a variety of sensitive encapsulated compounds.

### 6.2 Introduction

Multiple emulsions are multiphase fluids displaying a droplets-within-droplets type of dispersed phase. The simplest ones are “double emulsions”, which are either water-in-oil-in-water (W/O/W) or oil-in-water-in-oil (O/W/O) systems (B. P. Binks & Lumsdon, 1999; Garti, 1997). Multiple emulsions have a wide range of potential applications in fields such as the pharmaceuticals (Lindenstruth & Muller, 2004) and cosmetics (Gallarate, Carlotti, Trotta, & Bovo, 1999; Miyazawa, Yajima, Kaneda, & Yanaki, 2000) industries, and food systems (Aserin, 2007). They

can be used as carriers for the triggered release of encapsulated drugs, active compounds or sensitive molecules (L. Liu, Wang, Ju, Xie, & Chu, 2010; Vaziri & Warburton, 1994), or as potential substitutes for red blood cells (Zheng, Zheng, Beissinger, Wasan, & McCormick, 1993), to name a few.

Surfactants are typically employed to stabilize multiple emulsions: hydrophilic surfactants for the oil-in-water droplets, and hydrophobic surfactants for water-in-oil drops (Hong, Sun, Cai, & Ngai, 2012). However, surfactants can desorb from interfaces if exposed to temperatures above 70°C, which can be undesirable, and can pose toxicity problems (Dion et al., 2014; Wen & Ding, 2004). Furthermore, when using surfactants, multiple emulsions are typically thermodynamically and kinetically unstable (Zhu, Sun, Yi, Wei, & Liu, 2016). The kinetic barrier is caused by surfactant adsorption at the interface or the viscosity increase of the continuous phase between the droplets, while the thermodynamic barrier results from the considerable energy input required to disperse the surfactants (Sacanna, Kegel, & Philipse, 2007). Solid-stabilized emulsions, also known as ‘Pickering’ emulsions, can overcome these limitations (Thompson et al., 2015). Pickering emulsions involve solid particulates strongly adsorbing at fluid/fluid interfaces, stabilizing the droplets of a fluid dispersed in a second immiscible one, with the added benefit of avoiding the use of potentially harmful organic surfactants (Frelichowska et al., 2009).

Multiple Pickering emulsions are most often produced via a two-step process and require two different and complementary interfacial stabilizers (Y. Sela) – one hydrophilic, and one hydrophobic. During the first step of emulsification, a primary emulsion is produced with the first interfacial stabilizer. Then, during the second emulsification step, this primary emulsion is in turn emulsified with the second stabilizer, resulting in a droplets-in-droplets dispersion. Microfluidic approaches (Shum, Zhao, Kim, & Weitz, 2011; Utada et al., 2005) using various flow-focusing (D. Lee & Weitz, 2008; Nie, Xu, Seo, Lewis, & Kumacheva, 2005) techniques have also been developed to produce multiple emulsions via one step processes. However, these techniques typically display low production yields, limiting their industrial applications (S. Kim et al., 2018).

In order to obtain double Pickering emulsions, solid particles need to stabilize two different interfaces with different/complementary curvatures. Janus particles (B. P. Binks, Fletcher, Holt, Beaussoubre, & Wong, 2010; B. P. Binks & Whitby, 2004; Hong et al., 2012; Nonomura, Kobayashi, & Nakagawa, 2011; Tu & Lee, 2014a; White et al., 2011), block copolymers (Hong et

al., 2012; Y. Zhou et al., 2018) and colloidal particles such as fumed silica particles (B. P. Binks & Rodrigues, 2003; B. P. Binks & Whitby, 2004; White et al., 2011) and bowl-like silicone resins (Nonomura et al., 2011) have been used to form multiple Pickering emulsions. Nanofibrillated cellulose and cellulose nanocrystals have also been used to produce Pickering double emulsions. Two types of nanocelluloses, pristine and surface-modified, have been used to form O/W/O emulsions (Cunha et al., 2014). In addition, the combination of surfactants with solid particles (Frasch-Melnik, Spyropoulos, & Norton, 2010), amphiphilic copolymers (Hong et al., 2012) and various polymers such as poly(ethylene imine) (Williams, Warren, et al., 2014), a commercial water-soluble polymer, grafted onto silica particles have been used to prepare multiple Pickering emulsions with low viscosity oils and solvents (B. P. Binks et al., 2005; Cunha et al., 2014; Frasch-Melnik et al., 2010; S. Kim et al., 2018; Morais, Rocha-Filho, & Burgess, 2009).

Regarding the effect of viscosity ( $\mu$ ), previous studies (Fournier et al., 2009; Y. H. Liu, Carter, Gordon, Feng, & Friberg, 2012; Tsabet & Fradette, 2015b, 2015c, 2016) have demonstrated that the oil phase viscosity has an effect on the formation of Pickering emulsions, in particular on droplet size (Y. H. Liu et al., 2012; Tsabet & Fradette, 2015a, 2015b, 2015c). Increasing the viscosity of the dispersed oil phase typically results in the formation of larger droplets. However, the effect of viscosity remains only partially understood when it comes to the processing and formation of Pickering emulsions – especially for fluids with  $\mu > 5,000$  cSt – and has not been investigated when it comes to the formation of multiple Pickering emulsions. The main objective of this work is to assess the impact of high viscosity oils on the processing and microstructure of solid-stabilized emulsions. Quite surprisingly, by using a single type of sub- $\mu\text{m}$  silica particles modified with surface-grafted sodium alginate (SA), a natural polysaccharide (Faezeh Sabri et al., 2019), we demonstrate that multiple emulsions are formed when the oil viscosity reaches a value of 10,000 cSt.

## 6.3 Experimental section

### 6.3.1 Materials

Sub- $\mu\text{m}$  silica particles (SP) were supplied by Nippon Shokubai Trading Co. (average diameter  $d \approx 100$  nm, specific surface area  $S = 72 \pm 3 \text{ m}^2 \cdot \text{g}^{-1}$ , measured by BET with an ASAP 2020 instrument

from Micromeritics Instrument Corporation). (3-aminopropyl)trimethoxysilane (APTMS, 97%), alginic acid sodium salt (SA) from brown algae (CAS. 9005-38-3, low viscosity, molecular weight  $\approx 60$  kDa,  $pK_a = 3.5$ )(T. Harnsilawat et al., 2006), *N*-(3-dimethylaminopropyl)-*N'*-ethylcarbodiimide hydrochloride (EDC, > 98%), trimethoxy(propyl)silane (TMPS, 97%), *N*-hydroxysuccinimide (NHS, 98%), sodium azide (> 99%),  $\text{Na}_2\text{CO}_3$ - $\text{NaHCO}_3$  buffer solution (pH 10.01) and 5-(4,6-dichlorotriazinyl)aminofluorescein (DTAF) (D0531) were all purchased from Sigma-Aldrich and used without further purification. Ethanol (99.8%) was obtained from Thermo Fisher Scientific. HCl 1 N and NaOH 12 N solutions were of analytical grade and prepared without further purification with Milli-Q (DI) water (18.2  $\Omega$ , Synergy 185 system by Fischer Scientific). Silicone oils with a broad viscosity range (linear polydimethylsiloxane fluids 10, 1,000, 5,000, 10,000 and 30,000 cSt) were purchased from Clearco Products Co., Inc.

## 6.3.2 Particle Surface Modification

### 6.3.2.1 Silanes Surface Grafting

In order to alter surface wettability and graft SA on silica particles, two different silanes were grafted simultaneously on the surface of silica particles. In a typical batch, as previously reported (F. Sabri et al., 2018) , 10 g of SP particles were added in a hydrophobized erlenmeyer flask containing 100 ml of a 95% v/v solution of ethanol and DI water, while stirring at 600-700 rpm with a magnetic stirrer (Arkles, 2006) . The pH was then adjusted to 4.5 - 5.5 using HCl 1 N. 1.04 ml of APTMS (allowing the subsequent grafting of alginate) and 1.05 ml of TMPS (allowing control of particle surface wettability) were added simultaneously dropwise while stirring at room temperature, following a targeted surface concentration of 10 molecules. $\text{nm}^{-2}$  (5 molecules. $\text{nm}^{-2}$  of APTMS, and 5 molecules. $\text{nm}^{-2}$  of TMPS) (K. L. Pickering et al., 2015). The reaction was carried for 12 h at room temperature. The particles were collected by centrifugation (Sorvall RC 6+, Thermo Fisher Scientific) at 12,000 rpm for 20 min and cleaned by washing twice with ethanol in order to rinse off any remaining unreacted silane. The silane grafted particles, identified as SP-Sil, were finally dried in a vacuum oven at 70 °C for 2 hrs.

### 6.3.2.2 Sodium Alginate Grafting

A fraction of the SP-Sil particles were further modified by grafting SA using a 1% w/v aqueous solution. In a typical experiment, 0.4 g of SA was first dissolved in 40 ml of DI water (1% w/v). 0.29 g of EDC and 0.17 g of NHS (EDC/NHS molar ratio = 1) were then added to the solution (EDC/-COOH molar ratio = 0.1, relative to the -COOH groups of alginate) (Gabriele Giani et al., 2012). Then, 4 g of SP-Sil particles were added to the mixture and the pH was adjusted to 4.5 with HCl 1 N. The reaction proceeded for 15 hrs at room temperature and the mixture was subsequently centrifuged at 12,000 rpm for 20 min to collect the sodium alginate modified particles, designated from this point as SP-SA particles. They were washed with DI water 3 times and were next dried in a vacuum oven at 70 °C for 10 hrs.

## 6.3.3 Particle Surface Characterization

### 6.3.3.1 Zeta Potential Measurements

The zeta potential ( $\zeta$ ) was measured with a Zetasizer Nano ZSP instrument (Malvern Instruments Ltd., Worcestershire, UK) for SP, SP-Sil and SP-SA particles. Particles were first dispersed in DI water adjusted at pH 2.0 to 10.0 (by adding HCl 1 N or NaOH 12 N), and the measurements were performed at 25 °C on at least three different samples, at a particle concentration of 0.01 g·ml<sup>-1</sup>. Disposable zeta potential folded capillary cells (DTS1070) were used and all samples tested were freshly prepared. The instrument determined the electrophoretic mobility, and the Smoluchowski model was then applied by the software for the calculation of  $\zeta$  (Lattuada & Hatton, 2007).

### 6.3.3.2 Contact Angle Measurements

Water/particles contact angles  $\theta$  were measured using an OCA20 tensiometer (DataPhysics Instruments GmbH) at 25°C. The contact angles were directly measured on the surface of compressed pellets (0.1 g, 12 mm diameter and 0.5 mm thickness) made from SP or SP-SA particles, using a laboratory press (Model C 3100-212, Carver, laboratory Press, USA) applying a pressure of 70.2 MPa, which was maintained for 2 min once reached. Each pellet was then placed on the instrument and a ~4  $\mu$ L droplet of DI water at the desired pH (2.0 to 10.0, adjusted using HCl 1 N or NaOH 12 N) was carefully placed on the surface of the compressed pellet using a syringe with an internal needle diameter of 0.52 mm (Hamilton, model 1750TLL, 500  $\mu$ L). Images



of the sessile water droplets on the pellets were automatically recorded every 0.1 s, until the drops completely penetrated into the pellets. The first images were used as values of the contact angles. For both SP and SP-SA particles, three compressed pellets were prepared for each tested pH.

### 6.3.4 Emulsions Preparation and Characterization

Oil/water emulsions were prepared in screw cap glass vials (i.d. 1.2 cm, h. 4.6 cm), with the oil volume fraction  $\phi_o$  ranging from 0.1 to 0.8, and particle concentration varying from 2% to 12% ( $\text{g} \cdot 100 \text{ ml}^{-1}$ ), at pH 7.0 for a total volume of 15 ml. Unless explicitly mentioned, the emulsions were all prepared by weighing the required mass of particles (0.6 g) in the glass vials, followed by the addition of the required volume of water. The oil phase was next added dropwise over 4 min and dispersed using a Cole-Parmer LabGEN 125 homogenizer with a 0.5 cm (inner diameter) element, at 24,000 rpm. Once the oil was completely added, mixing was continued for another 2 min.

#### 6.3.4.1 Optical Characterization of Emulsions

The emulsions were observed by dark field optical microscopy (Olympus BX51 by Cytoviva, Objectives = 10x and 50x Plan Fluorite, and 60x UPL Fluorite Oil, and 100x UPL Fluorite Oil Camera Q imaging, Retigna 2000R fast 1394, cooled color 12 bit). A drop of each emulsion was diluted with a drop of water at pH 7.0. The diluted emulsion was then spread on a dimple glass slide (Fisher Scientific). Photographs of glass vials containing the emulsions were taken with a Nikon DX AF-S Nikkor 18-55mm 1:3.5-5.6 G camera.

#### 6.3.4.2 Confocal Laser Scanning Microscopy (CLSM) Analysis

CLSM observations were realized with an Olympus IX 71 inverted confocal microscope (Olympus Canada Inc., Richmond Hill, ON, Canada) using 40x and 60x objective lenses at a  $2048 \times 2048$  pixels resolution. 5-(4,6-dichlorotriazinyl)aminofluorescein (DTAF - D0531, Sigma), a fluorescent dye, was covalently linked with SA. This dye was specifically chosen since it reacts directly with hydroxyl, amino, thiol or amide groups to form stable, covalent links with the substrate at room temperature in an aqueous solution at pH 9.0 (M.S., 2010). 10 mg of DTAF were first added into a 50 mL  $\text{Na}_2\text{CO}_3$ - $\text{NaHCO}_3$  buffer solution (0.1 M, pH = 10.0), followed by the dissolution of 2.0 g of SA into the DTAF solution. The mixture was then left overnight to react at room temperature

with stirring at 600-700 rpm. Finally, the reaction was stopped the following morning by adjusting the pH to 7.0. This value also ensured a quick diffusion rate for counterions in the next dialysis step in which the solution is dialyzed against Milli-Q water for 48 hrs to remove counterions and unreacted DTAF. Bacteria growth was inhibited with sodium azide (0.02 wt%) and the Milli-Q water was changed every 2 hrs. After dialysis and freeze-drying, a yellow powder was recovered (DTAF-labelled SA). The observation of fluorescent SP-SA particles was realized by recording the emission between 510 nm and 550 nm, by exciting DTAF at 488 nm.

## 6.4 Results

### 6.4.1 Zeta potential and contact angle measurements

Zeta potentials ( $\zeta$ ) and contact angles ( $\theta$ ) were measured as a function of pH for pristine silica particles (SP), silanized particles (SP-Sil, only for  $\zeta$ ) and particles modified with SA (SP-SA) (Figure 6.1).

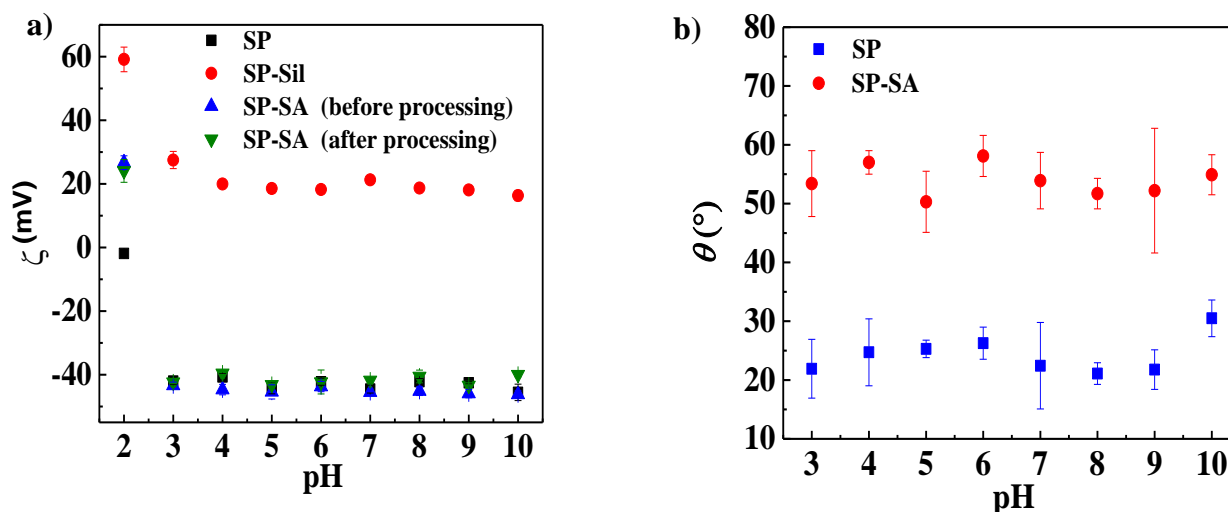


**Figure 6.1** Zeta potential  $\zeta$  (a) and contact angle  $\theta$  (b) of silica particles: pristine (SP), silanized (SP-Sil), and grafted with sodium alginate (SP-SA), as a function of pH (2.0 to 10.0).

SP particles display a slightly negative  $\zeta$  value at pH 2.0 that decreases to a nearly constant negative values (-40 mV) as the pH increases from 3.0 to 10.0 (Figure 6.1a). This behavior is expected due to the deprotonation of hydroxyl groups ( $pK_a = 3.5$  (Leung et al., 2009)) on the surface as the pH

increases (Knoblich & Gerber, 2001). SP-Sil particles show a positive  $\zeta$  value of +58.0 mV at pH 2.0 due to the substantial protonation of APTMS amino ( $-\text{NH}_2$ ) groups at low pH. When the pH ranges from 3.0 to 10.0, an inferior and nearly constant positive  $\zeta$  value of +25.0 mV is obtained. This is explained by the deprotonation of the surface bound hydroxyl groups and the gradual deprotonation of positively charged APTMS ( $-\text{NH}_3^+$ ) groups to neutral  $-\text{NH}_2$  groups. Finally, at pH 2.0, SP-SA particles present a different behavior as compared to unmodified SP particles and  $\zeta$  increases to +22.5 mV because of the protonation of both ( $-\text{COOH}$ ) groups and remaining surface amino ( $-\text{NH}_2$ ) groups. As the pH increases, the gradual deprotonation of both amino groups and SA carboxylate groups ( $\text{pK}_a = 3.5$ ) results in a nearly constant  $\zeta$  value of -40 mV. Furthermore, the homogenization processing of SP-SA particles did not alter the surface chemistry, since the  $\zeta$  patterns of particles before and after processing are similar. These results confirm the grafting of both silane reagents, and subsequent grafting of SA with the surface-bound APTMS. Similar results were obtained in a previous publication (Faezeh Sabri et al., 2019).

The wetting properties of SP and SP-SA particles were evaluated via the contact angle ( $\theta$ ) of water droplets deposited on compressed disks of particles, over a pH range of 2.0 to 10.0 (**Figure 6.1b**). On bare SP,  $\theta$  slightly increases from  $22^\circ$  to  $30.5^\circ$  as the pH increases from 2.0 to 10.0. After modification with SA,  $\theta$  increases above  $50^\circ$  and the particles become more hydrophobic compared to pristine particles (but more hydrophilic compared to SP-Sil particles, see (Faezeh Sabri et al., 2019), which is due to a balance effect between the hydrophobic silanes and hydrophilic SA. Both  $\zeta$  and  $\theta$  measurements confirm the surface grafting of APTMS and TMPS silanes onto pristine silica particles, followed by the covalent linking of SA with APTMS. (F. Sabri et al., 2018)

#### 6.4.2 Emulsion stabilization with pristine and modified silica particles

We first assessed the capacity of SP, SP-Sil and SP-SA particles to stabilize emulsions comprised of low and high viscosity silicone oils (SO, 10 and 10,000 cSt) and water (W) (**Figure 6.2**). Both SP and SP-SA particles stabilize oil-in-water emulsions with 10 cSt oil (**Figure 6.2a-b**). However, only SP-SA particles stabilize 10,000 cSt oil droplets (**Figure 6.2c-d**) – this is one of the highest tested oil viscosity reported in the literature for the preparation of Pickering emulsions. SP-Sil particles do not stabilize emulsions.

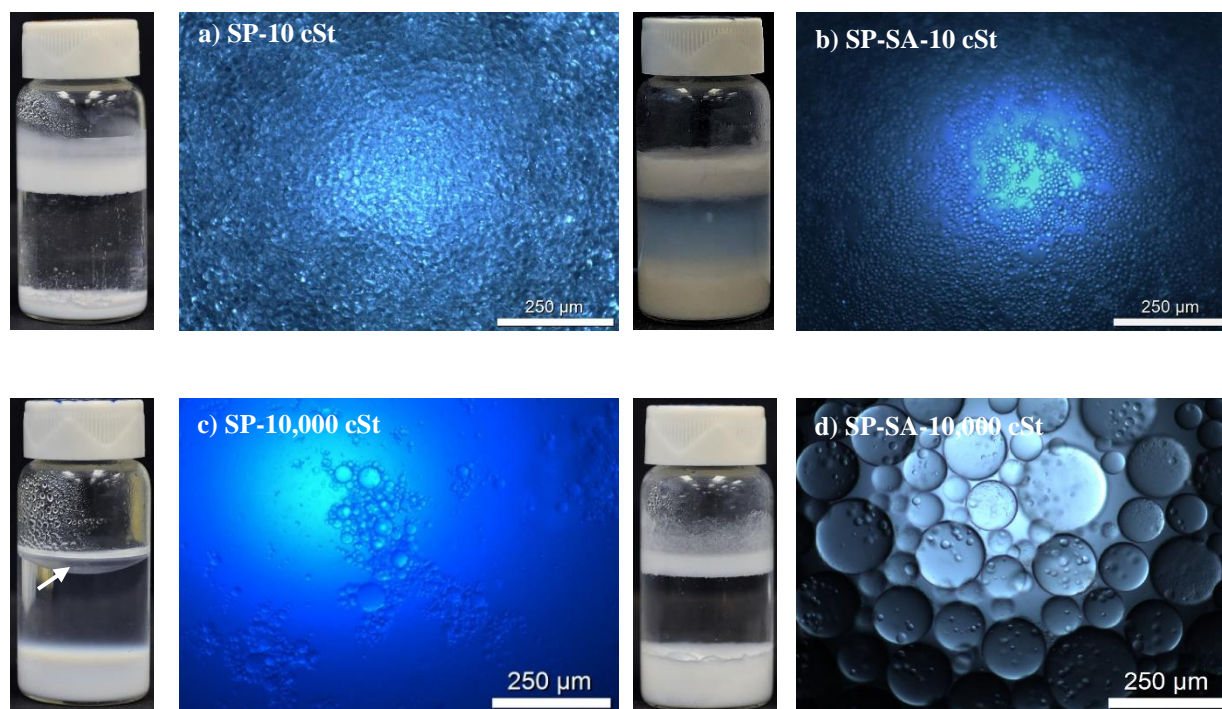


**Figure 6.2** Macroscopic aspect and optical microscopy pictures of Pickering emulsions prepared with 4% particles (w/v) at  $\phi_o = 0.1$  : a) SP particles with 10 cSt oil; b) SP-SA particles with 10 cSt oil; c) SP particles with 10,000 cSt oil (un-emulsified oil indicated with white arrow; d) SP-SA particles with 10,000 cSt oil.

Looking at the microstructure, oil droplets obtained with the SP-SA particles and the 10,000 cSt oil show a significant amount of sub-inclusions within the droplets (see also **Supporting Information video file** [“Emulsion - 10 000 cSt oil.avi”](#) showing flowing droplets with sub-inclusions). Such a feature is not observed in the 10 cSt oil droplets. This was an unexpected result, since multiple emulsions prepared with only one type of particles (herein SP-SA particles) have not been reported so far – especially at such a high oil viscosity. In the next section, oils of increasing viscosities are used to detect the onset of formation of these composite droplets using SP-SA particles.

#### 6.4.3 Effect of oil viscosity on the formation of multiple emulsions

Following the results displayed in **Figure 6.2**, the effect of oil viscosity was investigated next. **Figure 6.3** illustrates the effect of oil viscosity on droplet microstructure, for constant contents of

SP-SA particles and oil volume fraction ( $\phi_o$ ) of 4% and 0.1, respectively. The oil viscosity increases from 1,000 to 30,000 cSt. Interestingly, stabilized oil droplets are observed even at such high oil viscosities. At 1,000 cSt and 5,000 cSt (**Figure 6.3a-b**), a few water droplets sub-inclusions can be observed (although not obvious, see white arrows in **Figure 6.3a and b**) in certain oil drops. The number and size of water droplets sub-inclusions significantly increases when the oil viscosity reaches 10,000 and 30,000 cSt (**Figure 6.3c-d**). At 10,000 cSt (**Figure 6.3c**), nearly all of the observed oil droplets contain sub-inclusions.

Viscosity is clearly a key-factor driving the formation of these multiple emulsions. In the next section, confocal laser scanning microscopy is employed to see if SP-SA particles are present at the surface of both oil droplets and water sub-inclusions.

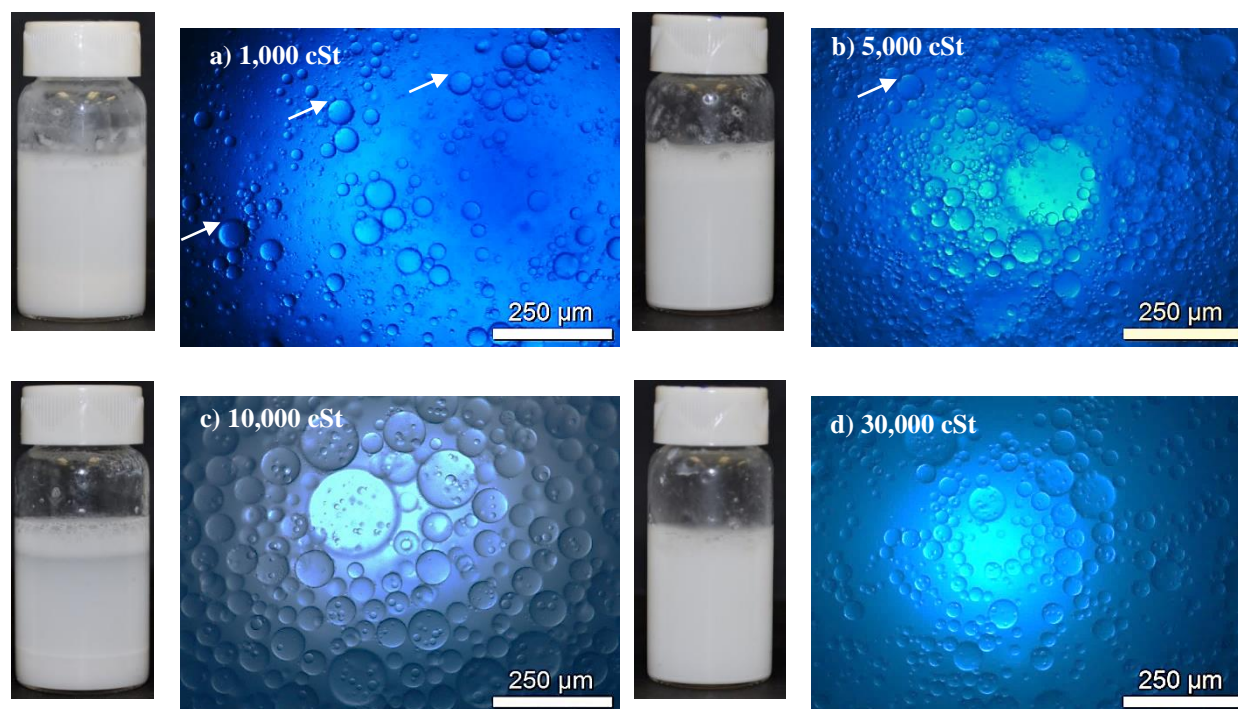


**Figure 6.3** Macroscopic aspect and optical microscopy pictures of Pickering emulsions prepared with 4% particles (w/v) at  $\phi_o = 0.1$  : a) SP particles with 10 cSt oil; b) SP-SA particles with 10 cSt oil; c) SP particles with 10,000 cSt oil (un-emulsified oil indicated with white arrow; d) SP-SA particles with 10,000 cSt oil.



#### 6.4.4 Internal drop microstructure investigated by confocal microscopy

In order to visualize the SP-SA particles by CLSM, the particles were tagged with DTAF. **Figure 6.4** shows the particle distribution in an emulsion with 4% SP-SA particles, at an oil content  $\phi_o = 0.1$  (10,000 cSt). The images clearly indicate that the particles are surface-active and form dense layers, both on the surface of the oil droplets, and at the surface of sub-inclusions – indicating that the sub-inclusions are comprised of water. This means that these SP-SA particles can indeed stabilize both O/W and W/O emulsions, even though a previous article (Faezeh Sabri et al., 2019) shows that they prefer the former conformation.

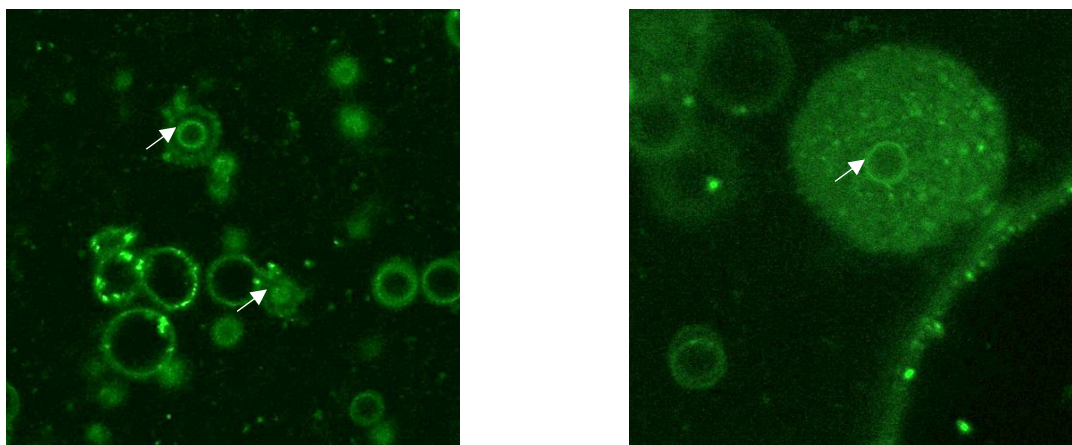


**Figure 6.4** CLSM pictures of Pickering emulsions ( $\phi_o = 0.1$ , 10,000 cSt) with 4% (wt/vol) SP-SA particles tagged with DTAF, showing the interfacial adsorption of particles both at the oil surface and water sub-inclusions (indicated with white arrows in the latter case).

#### 6.4.5 Effects oil and particle concentrations

To investigate the effect of oil and water contents on the formation of these double emulsions, four different oil volume fractions were compared (for the 10,000 cSt silicone oil), namely  $\phi_o = 0.05$ , 0.1, 0.2 and 0.3, at a constant particle content of 4% (w/v). The results are shown in **Figure 6.5**. At  $\phi_o = 0.05$  (**Figure 6.5a**), most of the oil phase was emulsified, and multiple droplets were obtained. Increasing the silicone oil fraction to  $\phi_o = 0.1$  also resulted in the formation of multiple droplets, further increase in silicone oil fraction at  $\phi_o = 0.2$  and 0.3 led to an apparent wider size distribution,

but again to the formation of sub-inclusions. It's interesting to note that the amount of oil seems to have no significant effect on the amount or size of sub-inclusions.

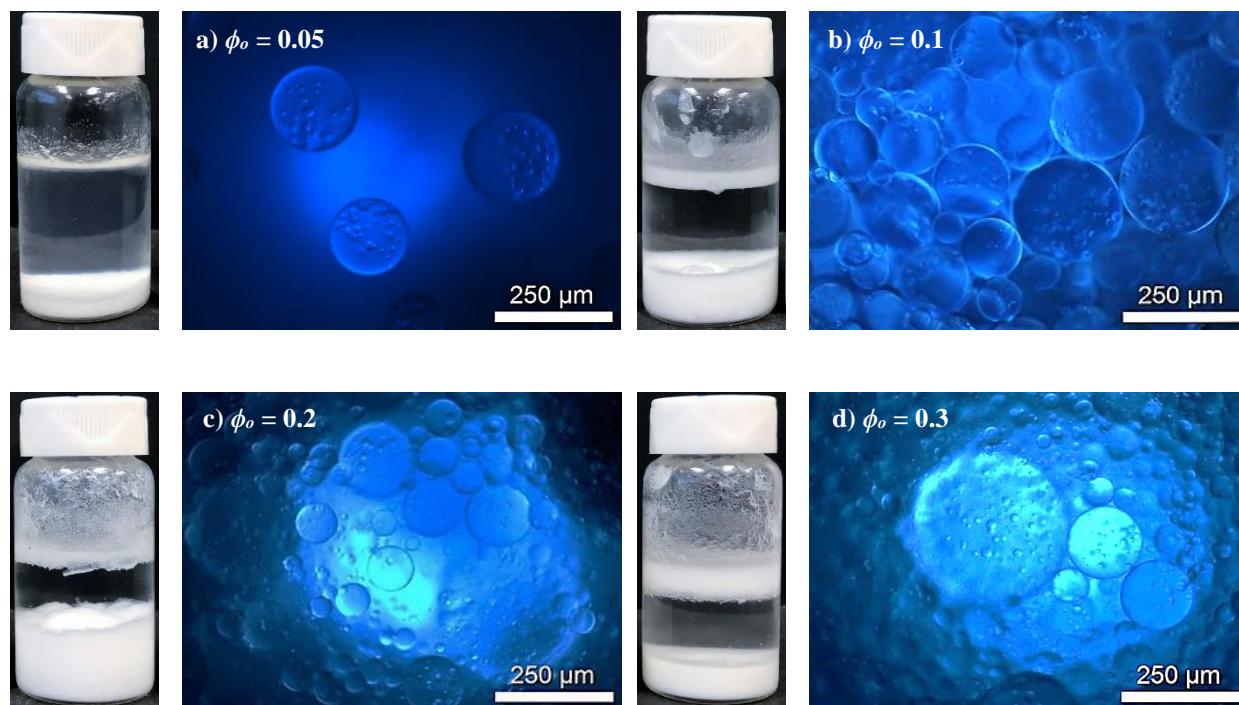


**Figure 6.5** Effect of oil fraction  $\phi_o$  on the formation of multiple emulsions comprised of 4% (w/v) SP-SA particles and 10,000 cSt silicone oil, at pH = 7.0: a)  $\phi_o = 0.05$ ; b)  $\phi_o = 0.1$ ; c)  $\phi_o = 0.2$  and d)  $\phi_o = 0.3$  (d). Vials display emulsion stability after 10 months.

A similar conclusion is reached when the particle content is varied, at a constant oil content. **Figure 6.6** illustrates the internal structure of oil droplets (10,000 cSt silicone oil,  $\phi_o = 0.1$ ) when the particle concentration increases from 2% to 12% (w/v). Again, we can see that increasing the particle content does not have a significant impact on the number and size of water sub-inclusions in the oil droplets (except at 12% content, where we can see more smaller droplets without sub-inclusions), even though it has an impact on the macroscopic appearance of the emulsions. We then next investigated the effects of three processing parameters: (1) the duration of oil addition, (2) the processing time and (3) the components mixing sequence.

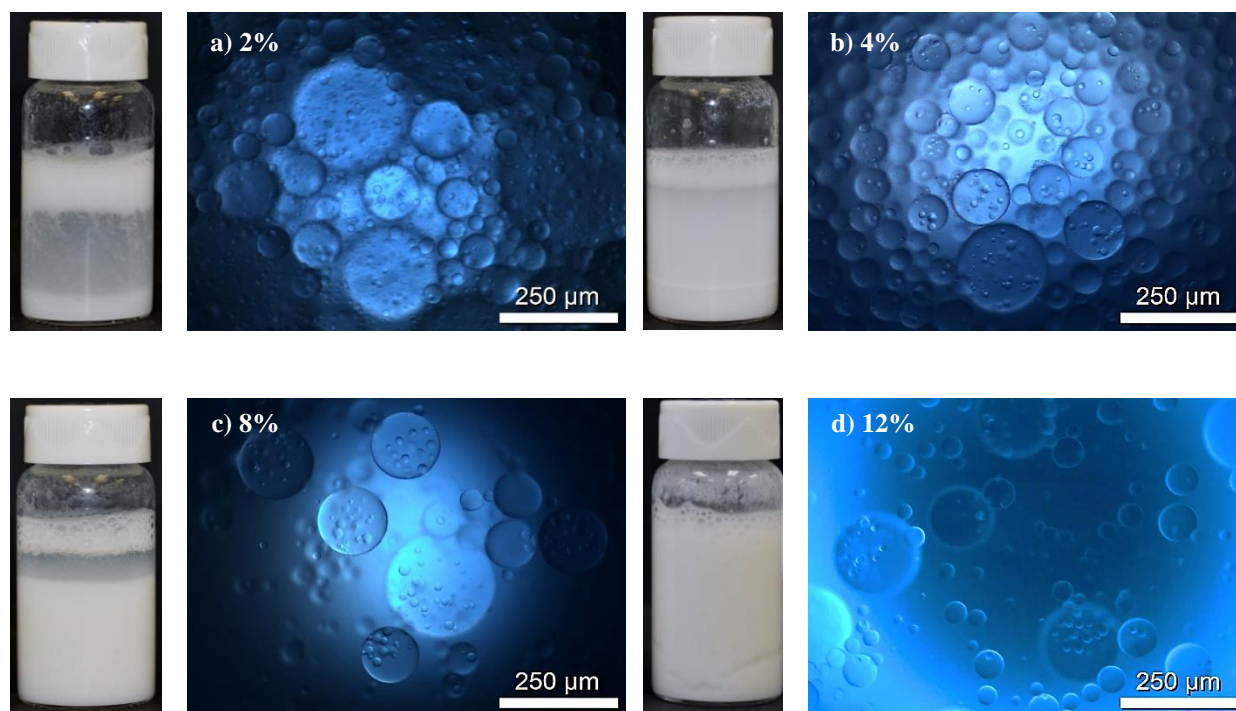


**Figure 6.6** Effect of particle concentration on the oil droplets internal structure in emulsions prepared with SP-SA particles (w/v) with 10,000 cSt silicone oil ( $\phi_o = 0.1$ ) at pH=7.0: a) 2% particles (w/v); b) 4%; c) 6% and d) 12%.

#### 6.4.6 Effects of processing variables: duration of oil addition, processing time, and sequence of mixing

The effect of silicone oil addition duration is illustrated in **Figure 6.9**, for emulsions comprised of 4% particles and 10,000 cSt oil ( $\phi_o = 0.1$ ). Adding the oil in 1 min (+ 5 minutes of additional processing time) or 6 min (with no additional processing time) does not significantly alter the internal oil droplet structure in terms of water sub-inclusion number and size. If the duration of oil addition instead is kept constant at 4 min, while the additional processing time is varied – 2 min vs 8 min –, again no clear difference is observed, as **Figure 6.10** shows.

This led us to look at the sequence of components addition (**Figure 6.7**). Until now, the particles were first added to water, and the oil phase was gradually added to form an oil-in-water emulsion. In **Figure 6.7a-b**, the particles were first mixed with water, and the resulting suspension was gradually added to the minor oil phase while homogenizing (final composition:  $\phi_o = 0.2$ ). In the



second row, **Figure 6.7c-d**, the particles were dispersed first in the oil phase, and water was gradually added subsequently (final composition:  $\phi_o = 0.2$ ). In **Figure 6.7a and c**, mixing was stopped right after phase inversion (right after the formation of an oil-in-water emulsion), when water becomes the continuous phase, while in **Figure 6.7b and d**, mixing is continued for 2 min after the complete addition of the aqueous particle suspension (b) or water (d). In all cases, we observe that the oil droplets contain a large number of very small water droplets sub-inclusions (**Figure 6.7b and c** are particularly striking), contrasting sharply with the previous results, which showed less but larger sub-inclusions. This indicates that phase inversion probably plays an important role during the formation of these multiple emulsions, while further processing after phase inversion does not affect significantly the sub-inclusions (at least for a short additional processing time).

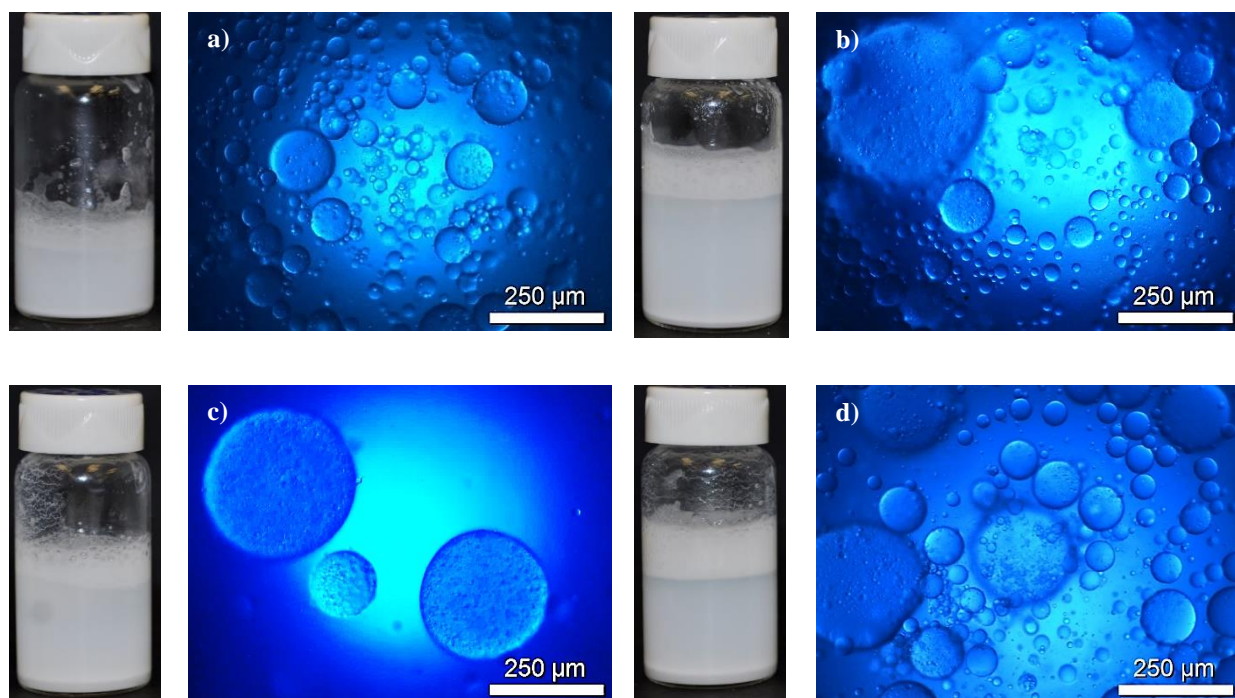


**Figure 6.7** Effect of mixing sequence on Pickering emulsions appearance and microstructure, prepared with 4% (w/v) SP-SA particles and 10,000 cSt oil at pH = 7.0. In (a, b), particles are first dispersed in water, then the aqueous suspension is gradually added in oil while homogenizing: a) processing stopped when phase inversion occurs (oil-in-water emulsion is formed); b) homogenizing is prolonged 2 min after the complete addition of particle suspension ( $\phi_o = 0.2$ ). In (c, d), particles are first dispersed in the oil phase, then water is gradually added in

the (oil + particle) suspension while homogenizing: c) process stopped after phase inversion occurs; d) homogenizing is prolonged 2 min after complete addition of water ( $\phi_o = 0.2$ ).

## 6.5 Proposed mechanism for the formation of multiple Pickering emulsions

By modifying the surface chemistry of silica particles with a natural polysaccharide, in this case sodium alginate, and by using highly viscous silicone oils, we have promoted the formation of multiple (W/O/W) Pickering emulsions via a one step process – this contrasts sharply with the more traditional approach using two types of particles/surfactants, and two successive mixing steps. Viscosity clearly plays an important role, since multiple emulsions are only significantly formed for 10,000 and 30,000 cSt oils (**Figure 6.3**). CLSM observations also reveal that SP-SA particles cover both interfaces – the outer oil-water interface of the primary emulsion, and the water-oil interface associated to water sub-inclusions (**Figure 6.4**). This can be explained by the SP-SA particulates “intermediate” wettability – less hydrophilic than the pristine SP particles, but more hydrophilic compared to the silane grafted particles (SP-Sil) (**Figure 6.1**).

It is pertinent to note that the oil volume fraction and particle content do not have a significant impact on the sub-inclusions size and number when the oil is added dropwise to the major water phase containing particles (**Figures 6.5 and 6.6**). However, when water (with or without particles) is added dropwise to the minor oil phase until phase inversion occurs, the internal structure of the oil droplets reveals a high number of smaller water droplets sub-inclusions, that remain trapped in the oil phase as processing continues (at least for a few minutes, **Figure 6.7**). Clearly, phase inversion plays an important role. When emulsions are prepared by adding dropwise the aqueous phase (**Figure 6.7**), water droplets are dispersed in the oil phase and are stabilized by SP-SA particles, forming the first emulsion. When phase inversion occurs, the oil-in-water emulsion is formed, and the initial water droplets in the oil phase remain trapped in the oil droplets. We believe that this phenomenon is due to (1) the reduced mobility of droplets in a very viscous liquid, and (2) to the shell of particles formed at the surface of the oil droplets – explaining the persistence of sub-inclusions when processing is prolonged.

In the case when the oil phase is added dropwise (with oil being the minor (and ultimately) dispersed phase, **Figures 6.3, 6.5 and 6.6**), water sub-inclusions are rapidly formed in the highly viscous and initially large oil droplets, before they significantly reduce in size (due to the high viscosity, oil droplets are larger and more difficult to form), which would explain why fewer sub-inclusions are observed for these processing conditions. Schematic illustrations explaining the formation of multiple emulsions via gradual water addition and phase inversion, or by gradual oil addition, are presented in **Figure 6-8**.

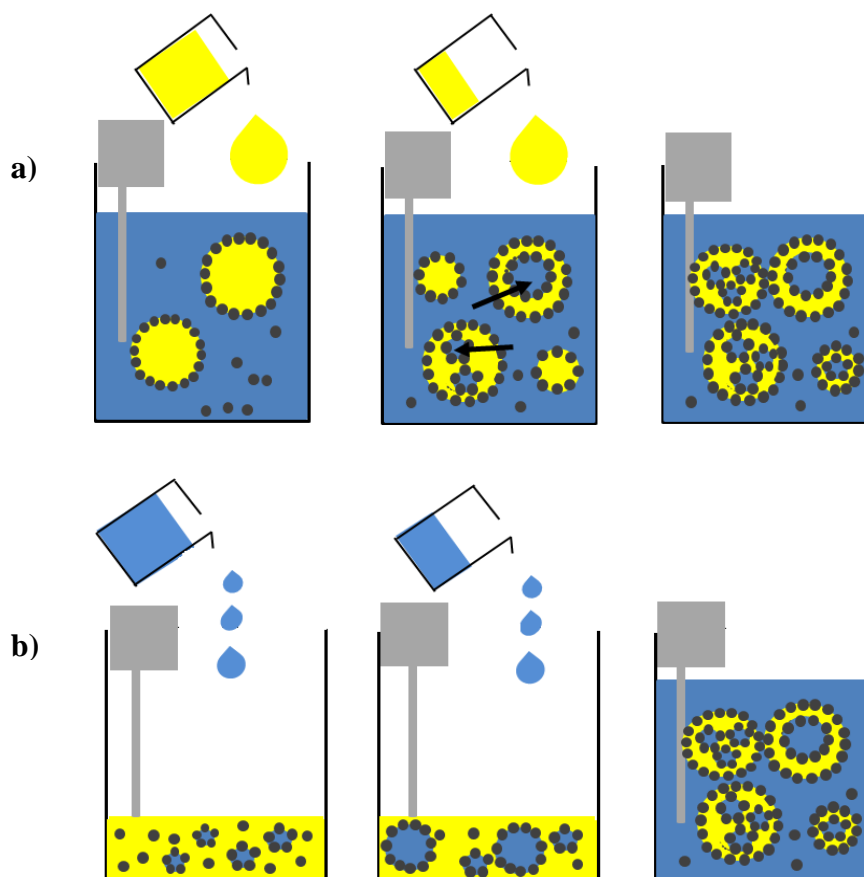


**Figure 6.8** Schematic illustrations of the formation of multiple emulsions by gradual oil addition, first big droplets of oil formed and due to intense mixing the water droplets were formed and migrated into those big oil droplets (a) and water gradual addition resulting in dispersion of water droplets and as water addition increased, phase inversion happened and oil droplets were dispersed (b) (It should be noted because of high viscosity of oil, big droplets were formed)

The formation of sub-inclusions via phase inversion in highly viscous systems has been reported in binary melt-processed polymer blends of polypropylene/polycarbonate and polyethylene copolymer/polyamide by Favis et al. (B. D. Favis, and D. Therrien, 1990; B. D. Favis, and J. P. Chalifoux, 1988; B. D. Favis, Lavallee, & Derdouri, 1992). They found that increasing the viscosity of the dispersed phase (polypropylene) caused an increase in the concentration of sub-inclusion droplets because of the lower sub-inclusion droplets mobility – also resulting in a higher retention of sub-inclusions in the dispersed phase. Interestingly, they were also able to increase significantly the number of sub-inclusions in polyamide droplets via a phase inversion process during the processing of polyethylene copolymer/polyamide blends, like we demonstrate in Figure 7. By prolonging the mixing time, they demonstrated that the sub-inclusions gradually migrated to the matrix phase – unlike our system, the polymer droplets were not covered with particulates shells preventing the transfer of sub-inclusions. This approach represents an interesting and simple strategy to prepare multiple emulsions with a minimum number of components.

## 6.6 Conclusion

We have prepared multiple (O/W/O) Pickering emulsions using highly viscous silicone oils and a single type of sub- $\mu\text{m}$  silica particles surface-modified with two silanes, and sodium alginate. The formation of water sub-inclusions is controlled by the oil viscosity, and is enhanced when phase inversion occurs during processing, when water is added dropwise. Furthermore, both the water sub-inclusions/oil droplets, and oil droplets/continuous aqueous phase interfaces, are covered with particles. The high viscosity of the oil phase, combined with the particulate barriers at the interfaces, contribute in stabilizing the water sub-inclusions, and inhibiting their transfer in the continuous aqueous phase during processing.

## 6.7 Acknowledgements

We acknowledge the financial support of Imperial Oil through a University Research Award grant, Total (Industrial Research Chair), the National Sciences and Engineering Research Council (Discovery Grant), CREPEC (Projets Structurants), Polytechnique Montreal (UPIR undergraduate research grants) and the Canada Foundation for Innovation (John R. Evans Leaders Fund). We would like to thank Dr. Chang-Sheng Wang for confocal microscopy observations.

## 6.8 Supporting information Article 3: One-Step Processing of Highly Viscous Multiple Pickering Emulsions

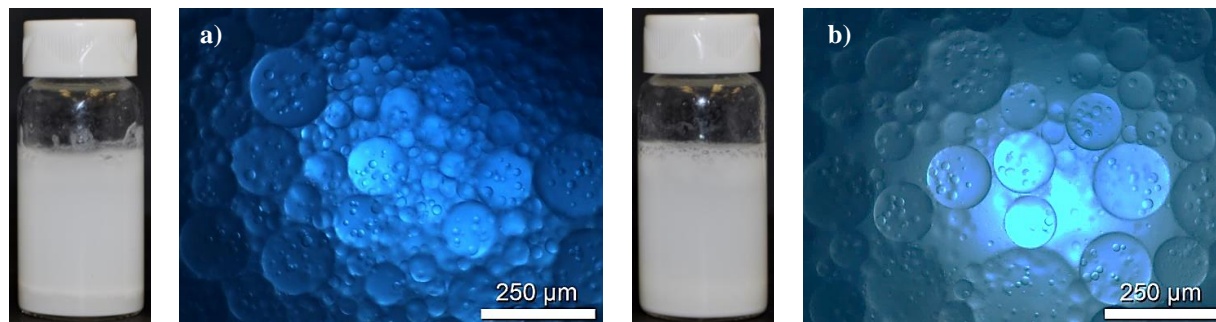


**Figure 6.9** Effect of the duration of oil addition on the macroscopic appearance and internal structure of oil droplets, for Pickering emulsions prepared with 4% SP-SA particles (w/v) with 10,000 cSt silicone oil ( $\phi_o = 0.1$ ): a) oil added in 1 min (+ 5 min of additional processing), b) oil added in 6 min (no additional processing time).

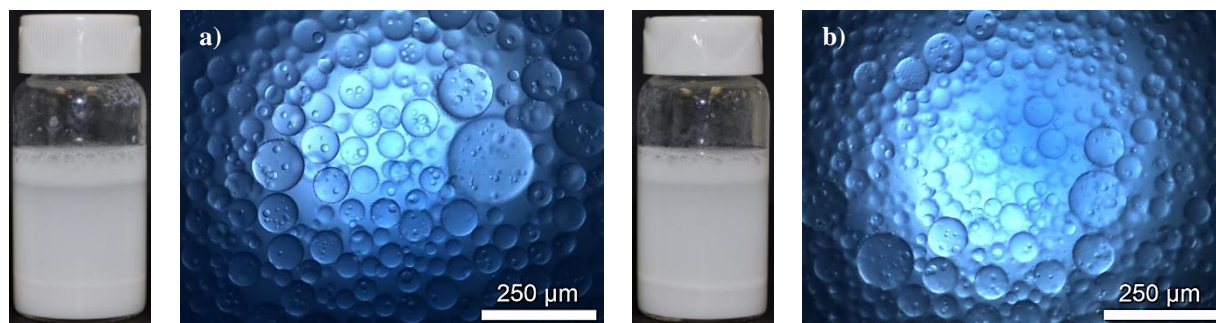


**Figure 6.10** Effect of additional processing time on the macroscopic appearance, and oil drop internal structure, in Pickering emulsions prepared with 4% SP-SA particles (w/v) with 10,000 cSt silicone oil ( $\phi_o = 0.1$ ). Oil added in 4 min + (a) 2 min or (b) 8 min of additional processing.

## CHAPTER 7      GENERAL DISCUSSION

Solid-stabilized (Pickering) emulsions are composed of two immiscible liquids in which the droplets of one liquid are dispersed in the other one. The dispersed droplets are stabilized by the adsorption of solid particles at the interface between the two liquids. The stabilization of these Pickering emulsions has been widely studied - however, techniques to ease the separation of the constituents have not been as much investigated nor developed.

Initially, we considered “*Click*” chemistry reactions - diels-alder and boronic acid-diol chemistries, forming reversible covalent bonds sensitive to temperature - to bind particles together reversibly in order to separate the emulsion constituents. We designed and prepared the required surface-modified magnetic iron oxide ( $\text{Fe}_3\text{O}_4$ ), glass beads and silica particles with complementary chemical groups. The ability of surface-modified particles to bind together reversibly (aggregate/disaggregate) by changing the temperature was tested at various temperatures and densities of grafted functional groups. NMR spectroscopy characterization revealed that Diels-Alder reactions took place between particles but failed to promote reversible aggregation/disaggregation. We hypothesized that the bonds formed via this “click” reaction were not strong or numerous enough to promote the formation of aggregates. Next, we tried a reversible complexation reaction between boronic acids and diols. This approach also proved unsuccessful.

Here is the schematic demonstration of the Diels-Alder click chemistry used initially in this work to promote the reversible aggregation/disaggregation of solid particles via the temperature change. **Figure 7.1(a,b)** summarizes the surface modification of glass beads/silica and  $\text{Fe}_3\text{O}_4$  with amino-maleimide and amino furan compounds respectively. **Figure 7.1c** presents the Diels-alder reaction between those surface modified particles via the temperature change to induce the reversible aggregation of solid particles.

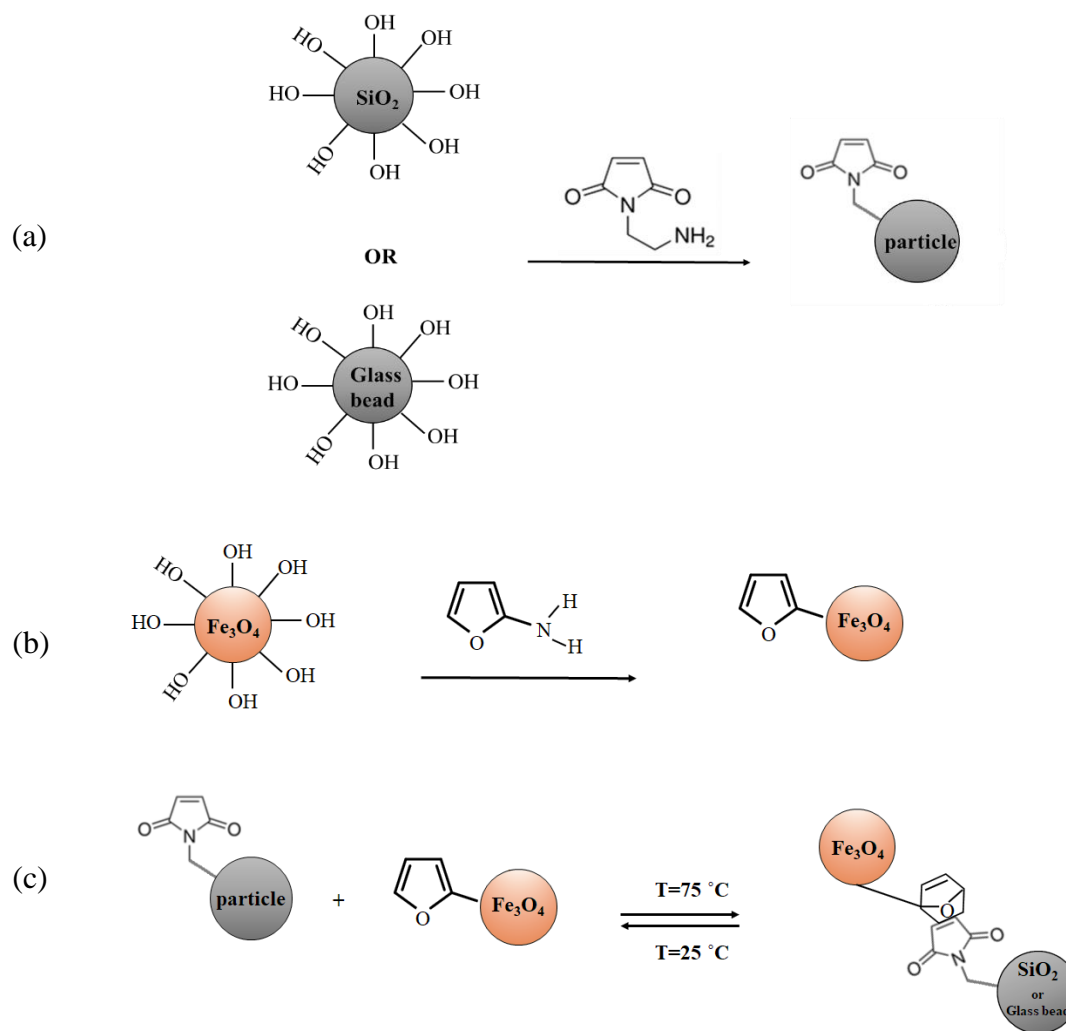


**Figure 7.1** Surface grafting of functional groups on silica/glass bead (a) and  $\text{Fe}_3\text{O}_4$  (b)

Diels Alder reaction between amino-maleimide functional groups on silica/glass beads and magnetic  $\text{Fe}_3\text{O}_4$  (c).

**Figure 7.2** demonstrates the surface modification of silica particles with 3-glycidypropyltrimethoxysilane and 3-Aminophenylboronic acid respectively. Scheme 5 reveals the reaction between those grafted diol groups and boric functional groups to promote the aggregation reversibly via a pH change. These surface modified particles did not present any macroscopic aggregation in aqueous media, therefore we decided to increase the length of carbon chain on diol-functional molecule to increase the chance of aggregation between solid particles.

Here was the step where we decided to use bio-macromolecules such as sodium alginate and xanthan gum to target pH-responsive properties.

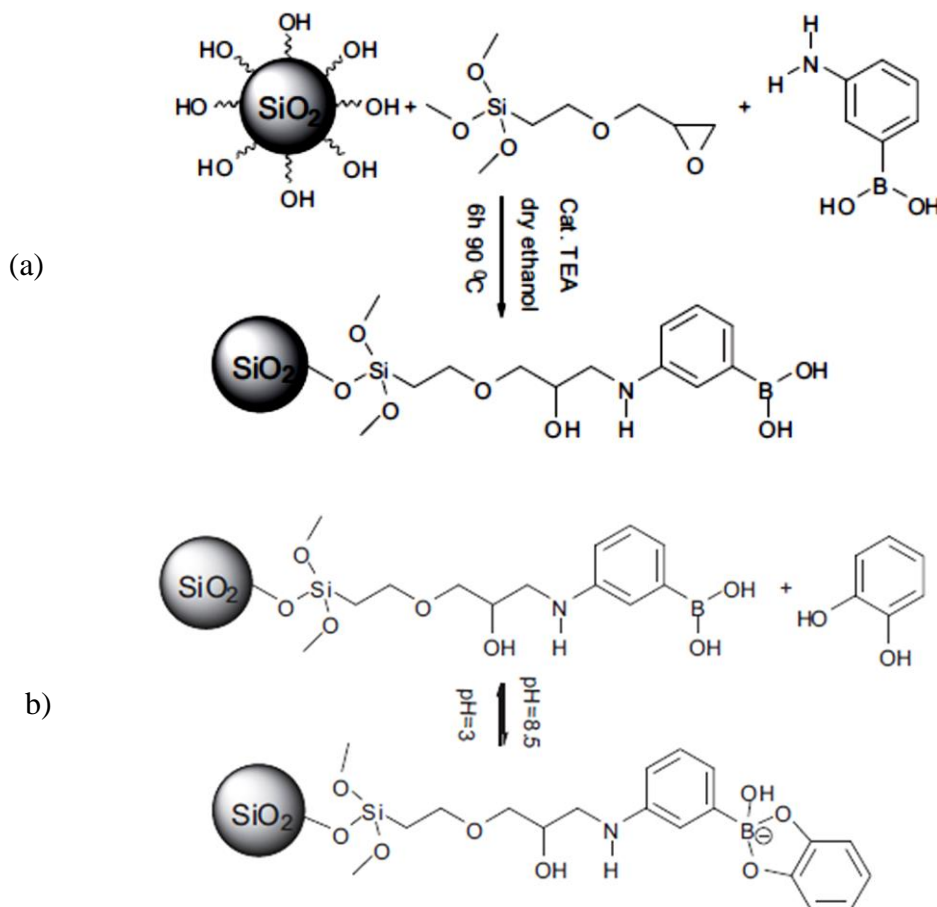


**Figure 7.2** Surface grafting of boronic acid and diol functional groups on silica particles and adsorption and desorption processes between these surface modified particles (Y. Wang et al., 2015).

Clearly, finding the right surface chemistry to promote and enhance the reversible aggregation/disaggregation of particles has constituted the most challenging and time-consuming aspect of this thesis, until we tested gelling polysaccharides such as sodium alginate and xanthan gum. Hence, it was difficult to predict in advance the stability or the efficiency of novel surface treatment or chemistry for the separation of Pickering emulsions constituents until to test it practically in the lab.



The first objective of this work was to design and prepare surface-modified particles grafted with a gelling natural polysaccharide, presenting reversible gelling properties in aqueous solution by changing the pH (article 1, chapter 4). Thus, in the first part of this research, we have designed and prepared 300 nm surface-grafted sodium alginate silica particles with enhanced reversible aggregation/disaggregation properties in aqueous solution. By analyzing and comparing the results of zeta potential, XPS and FTIR before and after modification, we have confirmed that the surface chemistry of these silica particles had been modified covalently by a silane coupling agent (APTMS), and sodium alginate (SA). Furthermore, the experimental results obtained from optical microscopy, sedimentation tests and UV-Vis spectroscopy illustrated how surface grafting of SA onto silica particles enhanced the size of particle aggregates up to 10 times at low pH, compared to unmodified particles. The aggregates formed by SA-modified particles were reversible and could be broken and dispersed again when the pH was increased back to 7.0. We have explained these enhanced and reversible aggregation properties by the intermolecular hydrogen bonds between neighboring SA-modified particles at pH 3.0 - an hypothesis confirmed by using urea as a hydrogen bond disruptor.

In second part, (article 2, chapter 5), we further developed our methodology to use these SA-modified particles first to stabilize, and then destabilize and separate the constituents of oil-in-water Pickering emulsions. We demonstrated that using SA-modified particles allowed simple separation of the components via filtration - with the advantage of reusing the particles after each filtration assay. To control the surface wettability of particles, two silane agents with complementary roles and molecular chemistries were mixed and used for the first step of surface modification. The first one, TMPS, increased the hydrophobic property of the surface due to its alkyl groups. The second silane agent, APTMS, was a linker (coupling agent) that allowed SA grafting via amide bonds. Compared to emulsions prepared with unmodified particles, the rheological ( $G'$  and  $G''$ ) and mechanical properties of concentrated emulsions prepared with these SA-surface modified particles were significantly superior due to particle-particle and droplet-droplet interactions – i.e. “sticking”. We then demonstrated that these “sticky” droplets could be separated more easily via filtration, and the particles could be collected and reused several times for the preparation of emulsions, while respecting the principles of green chemistry techniques.

Finally, in the last part (article3, chapter 6) we considered using these SA-surface modified particles for highly viscous Pickering emulsion systems which are involved in various industrial applications and processes. Hence, we used the same methodology to modify and control the surface wettability of smaller particles (herein 100 nm silica) simultaneously with the two different silanes (APTMS and TPMS), followed by grafting sodium alginate. The ability of these SA-surface modified particles to stabilize highly viscous oil droplets was analyzed and compared with unmodified silica particles. When studying the effect of viscosity, we unexpectedly observed the formation of multiple W/O/W emulsions - only obtained with SA-modified particles and high viscosity oils. Therefore, we changed the direction of our investigation to study and understand the mechanism responsible for the formation of these multiple W/O/W emulsions. Different parameters such as oil viscosity (from 1,000 to 30,000 cSt), particle concentration, oil fraction, as well as processing parameters and duration of mixing were investigated. The ability of using only one type of solid particles, herein surface modified-SA particles, with a one-step process is a significant step towards the development of a simple process for the production of multiple Pickering emulsions.

Therefore, the ability of using these surface modified particles as a green and simple alternative for the separation of Pickering emulsions constituents paves the way for different industrial processes. For instance, it can contribute to the separation of oil from tar sands where the sands and fine solid particles stabilized the tiny water droplets. These particles can be used to clean the oil spills from water by sticking the oil droplets together simply via a pH change. These surface modified particles can be also applied in the micro-encapsulation system where temporary stability is desired to release the entrapped component.

## CHAPTER 8 CONCLUSION AND RECOMMENDATIONS

### 8.1 Conclusion

Pickering emulsions usually display significant stability in time once formed, with limited coalescence and coarsening. As a result, the subsequent separation of their constituents can represent a challenge from a processing point of view and represents an interesting opportunity for both fundamental and applied research fields.

The first part of this thesis was devoted to design and prepare surface modified particles with SA, to obtain enhanced and reversible aggregation-disaggregation properties in aqueous media – in our case by changing the pH. The results we obtained clearly illustrated how stimuli-sensitive surface modified particles can be used as a potential approach to facilitate the aggregation of particles, and to ease separation processes.

The second part of this research project focused on how the preparation of solid-stabilized emulsions using surface-modified particles with natural gelling polysaccharides, demonstrated herein with SA, also significantly eased and enhanced the separation and recovery of Pickering emulsions constituents by simple filtration, without the addition of chemicals. The key results of this part revealed that surface modification of particles with sodium alginate strongly enhance interparticle and “interdroplets” interactions. This is explained by strong intermolecular hydrogen bonding between alginate molecules covalently grafted on neighboring particles in the emulsions. As a result, emulsion droplets bind more strongly together, allowing constituents separation. This filtration approach could lead to significant reductions in waste generation, elimination of nasty surfactants to environment and toxic chemicals usage. These surface modified particles can prove both economically and environmentally attractive for various industrial applications due to their reusable property and the resulting reduced dependence on potentially harmful organics and surfactants.

This PhD work contributes to scientific knowledge by:

1. Designing and preparing surface modified particles that can undergo reversible aggregation/disaggregation cycles;

2. Applying those surface modified particles grafted with sodium-alginate can stabilize Pickering emulsions, as well as improving the separation and recovery of Pickering emulsions constituents via their “sticky” properties
3. Providing a simple and one step process for the preparation of multiple Pickering emulsions, using only one type of solid particle and stabilizing highly viscous oils.

This work provides guidelines to design and prepare surface modified solid particles with natural polysaccharides which can tune the interactions between neighboring particles via a pH change. The reversible aggregation/disaggregation properties of these SA-surface modified particles have promoted a fundamental and original path towards the separation and recovery of Pickering emulsions’ constituents via a simple filtration. Finally, current study has addressed a simple pathway to emulsify highly viscous oils as well as the formation of multiple Pickering emulsions via one step and using one type of solid particle.

## 8.2 Recommendations

The following aspects are recommended for more exploration in future works:

- To investigate the effect of adding these tailored particles (SA-surface modified) to the existing Pickering emulsions system;
- The quantification of  $-NH_2$  groups and grafted APTMS before and after grafting SA, since it can finely tune and optimize particle-particle interactions;
- Investigate the effect of SA molecular weight and architecture (guluronic/mannuronic ratio), and other gelling polysaccharides, on the aggregation properties of surface modified particles;
- Study the low acidification methods as they can promote the aggregation of surface modified particles with polysaccharides to obtain better solid-like phase for separation of constituents applied in Pickering emulsions
- It would be necessary to improve the filtration test results and the separation of constituents by changing, for example, the ratio of EDC to  $-COOH$ , when grafting sodium alginate, or by using other polysaccharides;

- Test SA modified particles for the separation of the constituents of highly viscous Pickering emulsions
- To use these multiple Pickering emulsions for the encapsulation of specific molecules for either drug delivery or food application;
- Investigate further the proposed mechanism leading to the formation of multiple emulsions, since such a system is of great interest for drug delivery applications;

## BIBLIOGRAPHY

- Abreu, C. M., Paula, H. C., Seabra, V., Feitosa, J. P., Sarmento, B., & de Paula, R. C. (2016). Synthesis and characterization of non-toxic and thermo-sensitive poly(N-isopropylacrylamide)-grafted cashew gum nanoparticles as a potential epirubicin delivery matrix. *Carbohydrate Polymers*, 154, 77-85. doi:10.1016/j.carbpol.2016.08.031
- Arkles, B. (2006). Silane Coupling Agents: Connecting Across Boundaries. In.
- Aserin, A. (2007). *Multiple Emulsion: Technology and Applications* (1st ed ed.): Wiley-Interscience.
- Bakhteeva, I. A., Medvedeva, I. V., Uimin, M. A., Byzov, I. V., Zhakov, S. V., Yermakov, A. E., & Shchegoleva, N. N. (2016). Magnetic sedimentation and aggregation of Fe<sub>3</sub>O<sub>4</sub>@SiO<sub>2</sub> nanoparticles in water medium. *Separation and Purification Technology*, 159, 35-42. doi:10.1016/j.seppur.2015.12.043
- Bakumov, V., & Kroke, E. (2008). Polysilazane-induced aggregation of hydrophobic silver colloids. *Langmuir*, 24(19), 10709-10716. doi:10.1021/la801104b
- Ballauff, M., & Lu, Y. (2007). "Smart" nanoparticles: Preparation, characterization and applications. *Polymer*, 48(7), 1815-1823. doi:10.1016/j.polymer.2007.02.004
- Binks, B. P. (2002). Particles as surfactants-similarities and differences. *Current Opinion in Colloid & Interface Science*, 7, 21-41.
- Binks, B. P., Fletcher, P. D., Holt, B. L., Beaussoubre, P., & Wong, K. (2010). Phase inversion of particle-stabilised perfume oil-water emulsions: experiment and theory. *Physical Chemistry Chemical Physics*, 12(38), 11954-11966. doi:10.1039/c0cp00558d
- Binks, B. P., Isa, L., & Tyowua, A. T. (2013). Direct measurement of contact angles of silica particles in relation to double inversion of pickering emulsions. *Langmuir*, 29(16), 4923-4927. doi:10.1021/la4006899
- Binks, B. P., & Lumsdon, S. O. (1999). Stability of oil-in-water emulsions stabilised by silica particles. *Physical Chemistry Chemical Physics*, 1(12), 3007-3016. doi:DOI 10.1039/a902209k
- Binks, B. P., & Lumsdon, S. O. (2000). Catastrophic phase inversion of water-in-oil emulsions stabilized by hydrophobic silica. *Langmuir*, 16(6), 2539-2547. doi:DOI 10.1021/la991081j
- Binks, B. P., & Lumsdon, S. O. (2001). Pickering emulsions stabilized by monodisperse latex particles: Effects of particle size. *Langmuir*, 17(15), 4540-4547. doi:DOI 10.1021/la0103822
- Binks, B. P., Murakami, R., Armes, S. P., & Fujii, S. (2005). Temperature-induced inversion of nanoparticle-stabilized emulsions. *Angewandte Chemie, International Edition in English*, 44(30), 4795-4798. doi:10.1002/anie.200501073
- Binks, B. P., & Olusanya, S. O. (2017). Pickering emulsions stabilized by coloured organic pigment particles. *Chem Sci*, 8(1), 708-723. doi:10.1039/c6sc03085h
- Binks, B. P., & Rocher, A. (2009). Effects of temperature on water-in-oil emulsions stabilised solely by wax microparticles. *Journal of Colloid and Interface Science*, 335(1), 94-104. doi:10.1016/j.jcis.2009.03.089
- Binks, B. P., & Rodrigues, J. A. (2003). Types of phase inversion of silica particle stabilized emulsions containing triglyceride oil. *Langmuir*, 19(12), 4905-4912. doi:10.1021/la020960u
- Binks, B. P., & Rodrigues, J. A. (2007). Enhanced stabilization of emulsions due to surfactant-induced nanoparticle flocculation. *Langmuir*, 23(14), 7436-7439. doi:10.1021/la700597k

- Binks, B. P., & Whitby, C. P. (2004). Silica particle-stabilized emulsions of silicone oil and water: aspects of emulsification. *Langmuir*, 20(4), 1130-1137. doi:10.1021/la0303557
- Binks, B. P., & Yin, D. (2016). Pickering emulsions stabilized by hydrophilic nanoparticles: in situ surface modification by oil. *Soft Matter*, 12(32), 6858-6867. doi:10.1039/c6sm01214k
- Binks, B. P. I., L., Tyowua, A. T. (2013). Direct measurement of contact angles of silica particles in relation to double inversion of pickering emulsions. *Langmuir*, 29(16), 4923-4927. doi:10.1021/la4006899
- Bjorkegren, S., Nordstierna, L., Torncrona, A., & Palmqvist, A. (2017). Hydrophilic and hydrophobic modifications of colloidal silica particles for Pickering emulsions. *Journal of Colloid and Interface Science*, 487, 250-257. doi:10.1016/j.jcis.2016.10.031
- Borkovec, M., & Papastavrou, G. (2008). Interactions between solid surfaces with adsorbed polyelectrolytes of opposite charge. *Current Opinion in Colloid & Interface Science*, 13(6), 429-437. doi:10.1016/j.cocis.2008.02.006
- Céline Durand-Gasselin, N. S., and Nicolas Lequeux. (2011). Reversible Controlled Assembly of Thermosensitive Polymer-Coated Gold Nanoparticles. *Langmuir*, 27(20), 12329-12335.
- Cervantes Martinez, A., Rio, E., Delon, G., Saint-Jalmes, A., Langevin, D., & Binks, B. P. (2008). On the origin of the remarkable stability of aqueous foams stabilised by nanoparticles: link with microscopic surface properties. *Soft Matter*, 4(7). doi:10.1039/b804177f
- Chai, L. Y., Yan, X., Li, Q. Z., Yang, B. T., Wang, X., & Wang, Q. W. (2015). Enhancement of ZnO particles aggregation and sedimentation using polysaccharide and amino acid: Importance in abiological granular sludge (ABGS) formation. *Separation and Purification Technology*, 151, 66-73. doi:10.1016/j.seppur.2015.07.028
- Chen, K., Yu, G., He, F., Zhou, Q., Xiao, D., Li, J., & Feng, Y. (2017). A pH-responsive emulsion stabilized by alginate-grafted anisotropic silica and its application in the controlled release of lambda-cyhalothrin. *Carbohydrate Polymers*, 176, 203-213. doi:10.1016/j.carbpol.2017.07.046
- Chen, W., Liu, X., Liu, Y., Bang, Y., & Kim, H.-I. (2011). Preparation of O/W Pickering emulsion with oxygen plasma treated carbon nanotubes as surfactants. *Journal of Industrial and Engineering Chemistry*, 17(3), 455-460. doi:10.1016/j.jiec.2010.10.027
- Ching-Ju Chin, S. Y., and Costas Tsouris. (2001). Probing DLVO Forces Using Interparticle Magnetic Forces: Transition from Secondary-Minimum to Primary-Minimum Aggregation. *Langmuir*, 17, 6065-6071.
- Cho, J., Cho, J., Kim, H., Lim, M., Jo, H., Kim, H., . . . Kim, J. W. (2018). Janus colloid surfactant catalysts for in situ organic reactions in Pickering emulsion microreactors. *Green Chemistry*, 20(12), 2840-2844. doi:10.1039/c8gc00282g
- Crossely, S., J. Faria, M. Shen, D. E. Resasco. (2010). Solid Nanoparticles that Catalyze Biofuel Upgrade Reactions at the Water/Oil Interface. *Science*, 327(5961), 68-72.
- Cui, Z. G., Cui, C. F., Zhu, Y., & Binks, B. P. (2012). Multiple phase inversion of emulsions stabilized by in situ surface activation of CaCO<sub>3</sub> nanoparticles via adsorption of fatty acids. *Langmuir*, 28(1), 314-320. doi:10.1021/la204021v
- Cunha, A. G., Mougél, J. B., Cathala, B., Berglund, L. A., & Capron, I. (2014). Preparation of double Pickering emulsions stabilized by chemically tailored nanocelluloses. *Langmuir*, 30(31), 9327-9335. doi:10.1021/la5017577
- Dai, S., Ravi, P., & Tam, K. C. (2008). pH-Responsive polymers: synthesis, properties and applications. *Soft Matter*, 4(3), 435-449. doi:10.1039/b714741d

- Destribats, M., Eyharts, M., Lapeyre, V., Sellier, E., Varga, I., Ravaine, V., & Schmitt, V. (2014). Impact of pNIPAM microgel size on its ability to stabilize Pickering emulsions. *Langmuir*, 30(7), 1768-1777. doi:10.1021/la4044396
- Destribats, M., Lapeyre, V., Sellier, E., Leal-Calderon, F., Ravaine, V., & Schmitt, V. (2012). Origin and control of adhesion between emulsion drops stabilized by thermally sensitive soft colloidal particles. *Langmuir*, 28(8), 3744-3755. doi:10.1021/la2043763
- Dion, C. A. D., Raphael, W., Tong, E., & Tavares, J. R. (2014). Photo-initiated chemical vapor deposition of thin films using syngas for the functionalization of surfaces at room temperature and near-atmospheric pressure. *Surface & Coatings Technology*, 244, 98-108. doi:10.1016/j.surfcoat.2014.01.043
- Doshi, B., Repo, E., Heiskanen, J. P., Sirvio, J. A., & Sillanpaa, M. (2017). Effectiveness of N,O-carboxymethyl chitosan on destabilization of Marine Diesel, Diesel and Marine-2T oil for oil spill treatment. *Carbohydrate Polymers*, 167, 326-336. doi:10.1016/j.carbpol.2017.03.064
- Dyab, A. K. F. (2012). Destabilisation of Pickering emulsions using pH. *Colloids Surf., A* 402, 2-12. doi:10.1016/j.colsurfa.2012.02.041
- E. S. Read, S. F., J. I. Amalvy, D. P. Randall, and S. P. Armes. (2004). Effect of Varying the Oil Phase on the Behavior of pH-Responsive Latex-Based Emulsifiers: Demulsification versus Transitional Phase Inversion. *Langmuir*, 20, 7422-7429.
- Fan, Y., Simon, S., & Sjoblom, J. (2010). Influence of nonionic surfactants on the surface and interfacial film properties of asphaltenes investigated by Langmuir balance and Brewster angle microscopy. *Langmuir*, 26(13), 10497-10505. doi:10.1021/la100258h
- Favis, B. D., and D. Therrien. (1990). Factors influencing structure formation and phase size in an immiscible polymer blend of polycarbonate and polypropylene prepared by twin-screw extrusion. *Polymer*, 32(8), 1474-1481.
- Favis, B. D., and J. P. Chalifoux. (1988). Influence of composition on the morphology of polypropylene/polycarbonate blends. *Polymer*, 29, 1761-1767.
- Favis, B. D., Lavallee, C., & Derdouri, A. (1992). Preparation of Composite Dispersed Phase Morphologies in Incompatible and Compatible Blends during Melt Processing. *Journal of Materials science*, 27(15), 4211-4218. doi:10.1007/Bf01105129
- Feifel, S. C., & Lisdar, F. (2011). Silica nanoparticles for the layer-by-layer assembly of fully electro-active cytochrome c multilayers. *J Nanobiotechnology*, 9(59), 59. doi:10.1186/1477-3155-9-59
- Feng, X., Mussone, P., Gao, S., Wang, S., Wu, S. Y., Masliyah, J. H., & Xu, Z. (2010). Mechanistic study on demulsification of water-in-diluted bitumen emulsions by ethylcellulose. *Langmuir*, 26(5), 3050-3057. doi:10.1021/la9029563
- Fournier, C. O., Fradette, L., & Tanguy, P. A. (2009). Effect of dispersed phase viscosity on solid-stabilized emulsions. *Chemical Engineering Research & Design*, 87(4a), 499-506. doi:10.1016/j.cherd.2008.11.008
- Frasch-Melnik, S., Spyropoulos, F., & Norton, I. T. (2010). W1/O/W2 double emulsions stabilised by fat crystals--formulation, stability and salt release. *Journal of Colloid and Interface Science*, 350(1), 178-185. doi:10.1016/j.jcis.2010.06.039
- Fredrick, E., Walstra, P., & Dewettinck, K. (2010). Factors governing partial coalescence in oil-in-water emulsions. *Advances in Colloid and Interface Science*, 153(1-2), 30-42. doi:10.1016/j.cis.2009.10.003



- Frelichowska, J., Bolzinger, M. A., Valour, J. P., Mouaziz, H., Pelletier, J., & Chevalier, Y. (2009). Pickering w/o emulsions: drug release and topical delivery. *International Journal of Pharmaceutics*, 368(1-2), 7-15. doi:10.1016/j.ijpharm.2008.09.057
- Fuma, T., & Kawaguchi, M. (2015). Rheological responses of Pickering emulsions prepared using colloidal hydrophilic silica particles in the presence of NaCl. *Colloids and Surfaces A: Physicochemical and Engineering Aspects*, 465, 168-174. doi:10.1016/j.colsurfa.2014.10.050
- Furtado, G. F., Picone, C. S. F., Cuellar, M. C., & Cunha, R. L. (2015). Breaking oil-in-water emulsions stabilized by yeast. *Colloids Surf B Biointerfaces*, 128, 568-576. doi:10.1016/j.colsurfb.2015.03.010
- Gallarate, M., Carlotti, M. E., Trotta, M., & Bovo, S. (1999). On the stability of ascorbic acid in emulsified systems for topical and cosmetic use. *International Journal of Pharmaceutics*, 188(2), 233-241. doi:10.1016/S0378-5173(99)00228-8
- Garti, N. (1997). Double emulsions - Scope, limitations and new achievements. *Colloids and Surfaces a-Physicochemical and Engineering Aspects*, 123, 233-246. doi:10.1016/S0927-7757(96)03809-5
- Ge, S., Xiong, L., Li, M., Liu, J., Yang, J., Chang, R., . . . Sun, Q. (2017). Characterizations of Pickering emulsions stabilized by starch nanoparticles: Influence of starch variety and particle size. *Food Chemistry*, 234, 339-347. doi:10.1016/j.foodchem.2017.04.150
- George, M., & Abraham, T. E. (2006). Polyionic hydrocolloids for the intestinal delivery of protein drugs: alginate and chitosan--a review. *J Control Release*, 114(1), 1-14. doi:10.1016/j.jconrel.2006.04.017
- Giani, G., Fedi, S., & Barbucci, R. (2012). Hybrid Magnetic Hydrogel: A Potential System for Controlled Drug Delivery by Means of Alternating Magnetic Fields. *Polymers*, 4(4), 1157-1169. doi:10.3390/polym4021157
- Giani, G., Fedi, S., & Barbucci, R. (2012). Hybrid Magnetic Hydrogel: A Potential System for Controlled Drug Delivery by Means of Alternating Magnetic Fields. *Polymers*, 4(2), 1157-1169. doi:10.3390/polym4021157
- Glasing, J., Bouchard, J., Jessop, P. G., Champagne, P., & Cunningham, M. F. (2017). Grafting well-defined CO<sub>2</sub>-responsive polymers to cellulose nanocrystals via nitroxide-mediated polymerisation: effect of graft density and molecular weight on dispersion behaviour. *Polymer Chemistry*, 8(38), 6000-6012. doi:10.1039/c7py01258f
- Guillot, S., Bergaya, F., de Azevedo, C., Warmont, F., & Tranchant, J. F. (2009). Internally structured pickering emulsions stabilized by clay mineral particles. *Journal of Colloid and Interface Science*, 333(2), 563-569. doi:10.1016/j.jcis.2009.01.026
- Haase, M. F., Grigoriev, D., Moehwald, H., Tiersch, B., & Shchukin, D. G. (2010). Encapsulation of Amphoteric Substances in a pH-Sensitive Pickering Emulsion. *The Journal of Physical Chemistry C*, 114(41), 17304-17310. doi:10.1021/jp104052s
- Harnsilawat, T., Pongsawatmanit, R., & McClements, D. (2006). Characterization of  $\beta$ -lactoglobulin-sodium alginate interactions in aqueous solutions: A calorimetry, light scattering, electrophoretic mobility and solubility study. *Food Hydrocolloids*, 20(5), 577-585. doi:10.1016/j.foodhyd.2005.05.005
- Harnsilawat, T., Pongsawatmanit, R., McClements, D.J. (2006). Characterization of  $\beta$ -lactoglobulin-sodium alginate interactions in aqueous solutions: A calorimetry, light scattering, electrophoretic mobility and solubility study. *Food Hydrocolloids*, 20(50), 577-585.

- Hemraz, U. D., Lu, A., Sunasee, R., & Boluk, Y. (2014). Structure of poly(N-isopropylacrylamide) brushes and steric stability of their grafted cellulose nanocrystal dispersions. *Journal of Colloid and Interface Science*, 430, 157-165. doi:10.1016/j.jcis.2014.05.011
- Hernandez, E. I., Castro-Sotelo, L. V., Avendano-Gomez, J. R., Flores, C. A., Alvarez-Ramirez, F., & Vazquez, F. (2016). Synthesis, Characterization, and Evaluation of Petroleum Demulsifiers of Multibranched Block Copolymers. *Energy & Fuels*, 30(7), 5363-5378. doi:10.1021/acs.energyfuels.6b00419
- Hong, L., Sun, G., Cai, J., & Ngai, T. (2012). One-step formation of w/o/w multiple emulsions stabilized by single amphiphilic block copolymers. *Langmuir*, 28(5), 2332-2336. doi:10.1021/la205108w
- Hosseini, A., Zare, E., Ayatollahi, S., Vargas, F. M., Chapman, W. G., Kostarelos, K., & Taghikhani, V. (2016). Electrokinetic behavior of asphaltene particles. *Fuel*, 178, 234-242. doi:10.1016/j.fuel.2016.03.051
- Howe A. M, R. M. M. (1990). Determination of gravitational separation in dispersions from concentration profiles. *Colloids and Surfaces*, 43(1), 83-94.
- Hu, Y. T., Ting, Y., Hu, J. Y., & Hsieh, S. C. (2017). Techniques and methods to study functional characteristics of emulsion systems. *J Food Drug Anal*, 25(1), 16-26. doi:10.1016/j.jfda.2016.10.021
- Hu, Z., Ballinger, S., Pelton, R., & Cranston, E. D. (2015). Surfactant-enhanced cellulose nanocrystal Pickering emulsions. *Journal of Colloid and Interface Science*, 439, 139-148. doi:10.1016/j.jcis.2014.10.034
- Hwang, K., Singh, P., & Aubry, N. (2010). Destabilization of Pickering emulsions using external electric fields. *Electrophoresis*, 31(5), 850-859. doi:10.1002/elps.200900574
- Jakša, G., Štefane, B., & Kovač, J. (2013). XPS and AFM characterization of aminosilanes with different numbers of bonding sites on a silicon wafer. *Surface and Interface Analysis*, 45(11-12), 1709-1713. doi:10.1002/sia.5311
- Jia, X., Zhao, X., Tian, K., Zhou, T. T., Li, J. G., Zhang, R. N., & Liu, P. (2016). Novel fluorescent pH/reduction dual stimuli-responsive polymeric nanoparticles for intracellular triggered anticancer drug release. *Chemical Engineering Journal*, 295, 468-476. doi:10.1016/j.cej.2016.03.065
- Jiang, J., Ma, Y., Cui, Z., & Binks, B. P. (2016). Pickering Emulsions Responsive to CO<sub>2</sub>/N<sub>2</sub> and Light Dual Stimuli at Ambient Temperature. *Langmuir*, 32(34), 8668-8675. doi:10.1021/acs.langmuir.6b01475
- Jiang, J., Zhu, Y., Cui, Z., & Binks, B. P. (2013). Switchable pickering emulsions stabilized by silica nanoparticles hydrophobized in situ with a switchable surfactant. *Angewandte Chemie, International Edition in English*, 52(47), 12373-12376. doi:10.1002/anie.201305947
- Juarez, J. A., & Whitby, C. P. (2012). Oil-in-water Pickering emulsion destabilisation at low particle concentrations. *J Colloid Interface Sci*, 368(1), 319-325. doi:10.1016/j.jcis.2011.11.029
- Kaiser, A., Liu, T., Richtering, W., & Schmidt, A. M. (2009). Magnetic capsules and pickering emulsions stabilized by core-shell particles. *Langmuir*, 25(13), 7335-7341. doi:10.1021/la900401f
- Kawaguchi, S. T. a. H. (2008). Thermosensitive Pickering Emulsion Stabilized by Poly(N-isopropylacrylamide)-Carrying Particles. *Langmuir*, 24, 3300-3305.

- Kim, J., Cote, L. J., Kim, F., Yuan, W., Shull, K. R., & Huang, J. X. (2010). Graphene Oxide Sheets at Interfaces. *Journal of the American Chemical Society*, 132(23), 8180-8186. doi:10.1021/ja102777p
- Kim, S., Kim, K., & Choi, S. Q. (2018). Controllable one-step double emulsion formation via phase inversion. *Soft Matter*, 14(7), 1094-1099. doi:10.1039/c7sm02134h
- Knoblich, B., & Gerber, T. (2001). Aggregation in SiO<sub>2</sub> sols from sodium silicate solutions. *Journal of Non-Crystalline Solids*, 283(1-3), 109-113. doi:10.1016/S0022-3093(01)00356-8
- Kruglyakov, P. M., Nushtayeva, A. V., & Vilkova, N. G. (2004). Experimental investigation of capillary pressure influence on breaking of emulsions stabilized by solid particles. *J. Colloid Interface. Sci.*, 276(2), 465-474. doi:10.1016/j.jcis.2004.03.059
- Kumar, N., Gaur, T., & Mandal, A. (2017). Characterization of SPN Pickering emulsions for application in enhanced oil recovery. *Ind. Eng. Chem.*, 54, 304-315. doi:10.1016/j.jiec.2017.06.005
- Kupczak, A., Bratasz, L., Krysiak-Czerwenka, J., & Kozłowski, R. (2018). Moisture sorption and diffusion in historical cellulose-based materials. *Cellulose*, 25(5), 2873-2884. doi:10.1007/s10570-018-1772-9
- Lan, Q., Liu, C., Yang, F., Liu, S., Xu, J., & Sun, D. (2007). Synthesis of bilayer oleic acid-coated Fe<sub>3</sub>O<sub>4</sub> nanoparticles and their application in pH-responsive Pickering emulsions. *Journal of Colloid and Interface Science*, 310(1), 260-269. doi:10.1016/j.jcis.2007.01.081
- Laredj-Bourezg, F., Bolzinger, M. A., Pelletier, J., & Chevalier, Y. (2017). Pickering emulsions stabilized by biodegradable block copolymer micelles for controlled topical drug delivery. *International Journal of Pharmaceutics*, 531(1), 134-142. doi:10.1016/j.ijpharm.2017.08.065
- Larson-Smith, K., & Pozzo, D. C. (2012). Pickering emulsions stabilized by nanoparticle surfactants. *Langmuir*, 28(32), 11725-11732. doi:10.1021/la301896c
- Lattuada, M., & Hatton, T. A. (2007). Functionalization of monodisperse magnetic nanoparticles. *Langmuir*, 23(4), 2158-2168. doi:10.1021/la062092x
- Leal-Calderon, F., & Schmitt, V. (2008). Solid-stabilized emulsions. *Current Opinion in Colloid & Interface Science*, 13(4), 217-227. doi:10.1016/j.cocis.2007.09.005
- Lee, D., & Weitz, D. A. (2008). Double emulsion-templated nanoparticle colloidosomes with selective permeability. *Advanced Materials*, 20(18), 3498. doi:10.1002/adma.200800918
- Lee, K. Y., & Mooney, D. J. (2012). Alginate: properties and biomedical applications. *Progress in Polymer Science*, 37(1), 106-126. doi:10.1016/j.progpolymsci.2011.06.003
- Leudjo Taka, A., Pillay, K., & Yangkou Mbianda, X. (2017). Nanosponge cyclodextrin polyurethanes and their modification with nanomaterials for the removal of pollutants from waste water: A review. *Carbohydrate Polymers*, 159, 94-107. doi:10.1016/j.carbpol.2016.12.027
- Leung, K., Nielsen, I. M. B., & Criscenti, L. J. (2009). Elucidating the Bimodal Acid-Base Behavior of the Water-Silica Interface from First Principles. *Journal of the American Chemical Society*, 131(51), 18358-18365. doi:10.1021/ja906190t
- Li, C., Liu, Q., Mei, Z., Wang, J., Xu, J., & Sun, D. (2009). Pickering emulsions stabilized by paraffin wax and Laponite clay particles. *Journal of Colloid and Interface Science*, 336(1), 314-321. doi:10.1016/j.jcis.2009.03.080
- Li, Z., Ming, T., Wang, J., & Ngai, T. (2009). High internal phase emulsions stabilized solely by microgel particles. *Angewandte Chemie, International Edition in English*, 48(45), 8490-8493. doi:10.1002/anie.200902103

- Liang, C., Liu, Q., & Xu, Z. (2014). Surfactant-free switchable emulsions using CO<sub>2</sub>-responsive particles. *ACS Appl Mater Interfaces*, 6(9), 6898-6904. doi:10.1021/am5007113
- Liang, F., Shen, K., Qu, X., Zhang, C., Wang, Q., Li, J., . . . Yang, Z. (2011). Inorganic Janus nanosheets. *Angewandte Chemie, International Edition in English*, 50(10), 2379-2382. doi:10.1002/anie.201007519
- Lin, Z., Zhang, Z., Li, Y., & Deng, Y. (2016). Magnetic nano-Fe<sub>3</sub>O<sub>4</sub> stabilized Pickering emulsion liquid membrane for selective extraction and separation. *Chemical Engineering Journal*, 288, 305-311. doi:10.1016/j.cej.2015.11.109
- Lindenstruth, K., & Muller, B. W. (2004). W/O/W multiple emulsions with diclofenac sodium. *Eur J Pharm Biopharm*, 58(3), 621-627. doi:10.1016/j.ejpb.2004.04.003
- Liu, D. W., & He, Y. J. (2011). Separation procedure using the droplets of oil-in-water Pickering emulsions as medium. *Colloids and Surfaces a-Physicochemical and Engineering Aspects*, 380(1-3), 341-344. doi:10.1016/j.colsurfa.2011.03.002
- Liu, H., Wang, C., Zou, S., Wei, Z., & Tong, Z. (2012). Simple, reversible emulsion system switched by pH on the basis of chitosan without any hydrophobic modification. *Langmuir*, 28(30), 11017-11024. doi:10.1021/la3021113
- Liu, K., Jiang, J., Cui, Z., & Binks, B. P. (2017). pH-Responsive Pickering Emulsions Stabilized by Silica Nanoparticles in Combination with a Conventional Zwitterionic Surfactant. *Langmuir*, 33(9), 2296-2305. doi:10.1021/acs.langmuir.6b04459
- Liu, L., Wang, W., Ju, X. J., Xie, R., & Chu, L. Y. (2010). Smart thermo-triggered squirting capsules for nanoparticle delivery. *Soft Matter*, 6(16), 3759-3763. doi:10.1039/c002231d
- Liu, M., Chen, X., Yang, Z., Xu, Z., Hong, L., & Ngai, T. (2016). Tunable Pickering Emulsions with Environmentally Responsive Hairy Silica Nanoparticles. *ACS Appl Mater Interfaces*, 8(47), 32250-32258. doi:10.1021/acsami.6b11931
- Liu, P., Lu, W., Wang, W. J., Li, B. G., & Zhu, S. (2014). Highly CO<sub>2</sub>/N<sub>2</sub>-switchable zwitterionic surfactant for pickering emulsions at ambient temperature. *Langmuir*, 30(34), 10248-10255. doi:10.1021/la502749x
- Liu, Y. H., Carter, E. L., Gordon, G. V., Feng, Q. J., & Friberg, S. E. (2012). An investigation into the relationship between catastrophic inversion and emulsion phase behaviors. *Colloids and Surfaces a-Physicochemical and Engineering Aspects*, 399, 25-34. doi:10.1016/j.colsurfa.2012.02.019
- Luo, Q., Wang, Y., Yoo, E., Wei, P., & Pentzer, E. (2018). Ionic Liquid-Containing Pickering Emulsions Stabilized by Graphene Oxide-Based Surfactants. *Langmuir*, 34(34), 10114-10122. doi:10.1021/acs.langmuir.8b02011
- M.S., G. (2010). *Advanced fluorescence reporters in chemistry and biology I* (D. A.P. Ed. Vol. 8). Berlin Heidelberg: Springer.
- Madivala, B., Vandebril, S., Fransaer, J., & Vermant, J. (2009). Exploiting particle shape in solid stabilized emulsions. *Soft Matter*, 5(8), 1717-1727. doi:10.1039/b816680c
- Martinez-Palou, R., Ceron-Camacho, R., Chavez, B., Vallejo, A. A., Villanueva-Negrete, D., Castellanos, J., . . . Aburto, J. (2013). Demulsification of heavy crude oil-in-water emulsions: A comparative study between microwave and thermal heating. *Fuel*, 113, 407-414. doi:10.1016/j.fuel.2013.05.094
- McClements, D. J. (2012). Crystals and crystallization in oil-in-water emulsions: implications for emulsion-based delivery systems. *Adv Colloid Interface Sci*, 174, 1-30. doi:10.1016/j.cis.2012.03.002

- Mirvakili, A., Rahimpour, M. R., & Jahanmiri, A. (2012). Effect of a Cationic Surfactant as a Chemical Destabilization of Crude Oil Based Emulsions and Asphaltene Stabilized. *Journal of Chemical and Engineering Data*, 57(6), 1689-1699. doi:10.1021/je2013268
- Miyazawa, K., Yajima, I., Kaneda, I., & Yanaki, T. (2000). Preparation of a new soft capsule for cosmetics. *Journal of Cosmetic Science*, 51(4), 239-252.
- Mohammadi, S., Rashidi, F., Mousavi-Dehghani, S. A., & Ghazanfari, M. H. (2016). Modeling of asphaltene aggregation phenomena in live oil systems at high pressure-high temperature. *Fluid Phase Equilibria*, 423, 55-73. doi:10.1016/j.fluid.2016.04.010
- Morais, J. M., Rocha-Filho, P. A., & Burgess, D. J. (2009). Influence of phase inversion on the formation and stability of one-step multiple emulsions. *Langmuir*, 25(14), 7954-7961. doi:10.1021/la9007125
- Morelli, S., Holdich, R. G., & Dragosavac, M. M. (2016). Chitosan and Poly (Vinyl Alcohol) microparticles produced by membrane emulsification for encapsulation and pH controlled release. *Chemical Engineering Journal*, 288, 451-460. doi:10.1016/j.cej.2015.12.024
- Morse, A. J., Armes, S. P., Thompson, K. L., Dupin, D., Fielding, L. A., Mills, P., & Swart, R. (2013). Novel Pickering emulsifiers based on pH-responsive poly(2-(diethylamino)ethyl methacrylate) latexes. *Langmuir*, 29(18), 5466-5475. doi:10.1021/la400786a
- Motornov, M., Sheparovych, R., Lupitskyy, R., MacWilliams, E., Hoy, O., Luzinov, I., & Minko, S. (2007). Stimuli-responsive colloidal systems from mixed brush-coated nanoparticles. *Advanced Functional Materials*, 17(14), 2307-2314. doi:10.1002/adfm.200600934
- Ngai, T., Behrens, S. H., & Auweter, H. (2005). Novel emulsions stabilized by pH and temperature sensitive microgels. *Chem Commun (Camb)*(3), 331-333. doi:10.1039/b412330a
- Nie, Z. H., Xu, S. Q., Seo, M., Lewis, P. C., & Kumacheva, E. (2005). Polymer particles with various shapes and morphologies produced in continuous microfluidic reactors. *Journal of the American Chemical Society*, 127(22), 8058-8063. doi:10.1021/ja042494w
- Nonomura, Y., Kobayashi, N., & Nakagawa, N. (2011). Multiple pickering emulsions stabilized by microbowls. *Langmuir*, 27(8), 4557-4562. doi:10.1021/la2003707
- Olajire, A. A. (2014). Review of ASP EOR (alkaline surfactant polymer enhanced oil recovery) technology in the petroleum industry: Prospects and challenges. *Energy*, 77, 963-982. doi:10.1016/j.energy.2014.09.005
- Pallandre, S., Decker, E. A., & McClements, D. J. (2007). Improvement of stability of oil-in-water emulsions containing caseinate-coated droplets by addition of sodium alginate. *Journal of Food Science*, 72(9), E518-524. doi:10.1111/j.1750-3841.2007.00534.x
- Pan, M., Lyu, F., & Tang, S. K. Y. (2017). Methods to coalesce fluorinated Pickering emulsions. *Analytical Methods*, 9(31), 4622-4629. doi:10.1039/c7ay01289f
- Peng, J. X., Liu, Q. X., Xu, Z. H., & Masliyah, J. (2012). Synthesis of Interfacially Active and Magnetically Responsive Nanoparticles for Multiphase Separation Applications. *Advanced Functional Materials*, 22(8), 1732-1740. doi:10.1002/adfm.201102156
- Pickering, K. L., Khimi, S. R., & Ilanko, S. (2015). The effect of silane coupling agent on iron sand for use in magnetorheological elastomers Part 1: Surface chemical modification and characterization. *Composites Part a-Applied Science and Manufacturing*, 68, 377-386. doi:10.1016/j.compositesa.2014.10.005
- Pickering, S. U. (1907). Emulsions. *Journal of the Chemical society, Transactions*, 91, 2001-2021
- Qi, L., Luo, Z. G., & Lu, X. X. (2018). Facile synthesis of starch-based nanoparticle stabilized Pickering emulsion: its pH-responsive behavior and application for recyclable catalysis. *Green Chemistry*, 20(7), 1538-1550. doi:10.1039/c8gc00143j

- Qian, Y., Zhang, Q., Qiu, X., & Zhu, S. (2014). CO<sub>2</sub>-responsive diethylaminoethyl-modified lignin nanoparticles and their application as surfactants for CO<sub>2</sub>/N<sub>2</sub>-switchable Pickering emulsions. *Green Chemistry*, 16(12), 4963-4968. doi:10.1039/c4gc01242a
- Qiao, P., Niu, Q. S., Wang, Z. B., & Cao, D. P. (2010). Synthesis of thermosensitive micelles based on poly(N-isopropylacrylamide) and poly(L-alanine) for controlled release of adriamycin. *Chemical Engineering Journal*, 159(1-3), 257-263. doi:10.1016/j.cej.2010.02.035
- Raffa, P., Broekhuis, A. A., & Picchioni, F. (2016). Polymeric surfactants for enhanced oil recovery: A review. *Journal of Petroleum Science and Engineering*, 145, 723-733. doi:10.1016/j.petrol.2016.07.007
- Rahelivao, M. P., Andriamanantoanina, H., Heyraud, A., & Rinaudo, M. (2013). Structure and properties of three alginates from Madagascar seacoast algae. *Food Hydrocolloids*, 32(1), 143-146. doi:10.1016/j.foodhyd.2012.12.005
- Rayner, M., Marku, D., Eriksson, M., Sjöö, M., Dejmek, P., & Wahlgren, M. (2014). Biomass-based particles for the formulation of Pickering type emulsions in food and topical applications. *Colloids and Surfaces A: Physicochemical and Engineering Aspects*, 458, 48-62. doi:10.1016/j.colsurfa.2014.03.053
- Rayner, M., Timgren, A., Sjöo, M., & Dejmek, P. (2012). Quinoa starch granules: a candidate for stabilising food-grade Pickering emulsions. *Journal of the Science of Food and Agriculture*, 92(9), 1841-1847. doi:10.1002/jsfa.5610
- Reger, M., Sekine, T., & Hoffmann, H. (2012). Pickering emulsions stabilized by amphiphile covered clays. *Colloids and Surfaces A: Physicochemical and Engineering Aspects*, 413, 25-32. doi:10.1016/j.colsurfa.2011.12.005
- Rodgers, A. N. J., Velicky, M., & Dryfe, R. A. W. (2015). Electrostatic Stabilization of Graphene in Organic Dispersions. *Langmuir*, 31(48), 13068-13076. doi:10.1021/acs.langmuir.5b04219
- Rodrigues, B. P. B. a. J. A. (2007). Synergistic Interaction in Emulsions Stabilized by a Mixture of Silica Nanoparticles and Cationic Surfactant. *Langmuir*, 23, 3626-3636.
- Sabri, F., Berthomier, K., Marion, A., Fradette, L., Tavares, J. R., & Virgilio, N. (2018). Sodium alginate-grafted submicrometer particles display enhanced reversible aggregation/disaggregation properties. *Carbohydrate Polymers*, 194, 61-68. doi:10.1016/j.carbpol.2018.04.012
- Sabri, F., Berthomier, K., Wang, C.-S., Fradette, L., Tavares, J. R., & Virgilio, N. (2019). Tuning particle-particle interactions to control Pickering emulsions constituents separation. *Green Chemistry*, 21(5), 1065-1074. doi:10.1039/c8gc03007c
- Sacanna, S., Kegel, W. K., & Philipse, A. P. (2007). Thermodynamically stable pickering emulsions. *Physical Review Letters*, 98(15), 158301. doi:10.1103/PhysRevLett.98.158301
- Sadeghpour, A., Pirolt, F., & Glatter, O. (2013). Submicrometer-sized Pickering emulsions stabilized by silica nanoparticles with adsorbed oleic acid. *Langmuir*, 29(20), 6004-6012. doi:10.1021/la4008685
- Saigal, T., Dong, H., Matyjaszewski, K., & Tilton, R. D. (2010). Pickering emulsions stabilized by nanoparticles with thermally responsive grafted polymer brushes. *Langmuir*, 26(19), 15200-15209. doi:10.1021/la1027898
- Santini, E., Guzmán, E., Ferrari, M., & Liggieri, L. (2014). Emulsions stabilized by the interaction of silica nanoparticles and palmitic acid at the water-hexane interface. *Colloids and Surfaces A: Physicochemical and Engineering Aspects*, 460, 333-341. doi:10.1016/j.colsurfa.2014.02.054

- Schnepp, Z., Hall, S. R., Hollamby, M. J., & Mann, S. (2011). A flexible one-pot route to metal/metal oxide nanocomposites. *Green Chemistry*, 13(2), 272-275. doi:10.1039/c0gc00338g
- Shan, Y., Yu, C., Yang, J., Dong, Q., Fan, X., & Qiu, J. (2015). Thermodynamically Stable Pickering Emulsion Configured with Carbon-Nanotube-Bridged Nanosheet-Shaped Layered Double Hydroxide for Selective Oxidation of Benzyl Alcohol. *ACS Appl Mater Interfaces*, 7(22), 12203-12209. doi:10.1021/acsami.5b02595
- Shinpei Ohki a, H. O. (1999). Interaction and aggregation of lipid vesicles (DLVO theory versus modified DLVO theory). *Colloids and Surfaces B: Biointerfaces*, 14, 27-45.
- Shum, H. C., Zhao, Y. J., Kim, S. H., & Weitz, D. A. (2011). Multicompartment polymersomes from double emulsions. *Angewandte Chemie, International Edition in English*, 50(7), 1648-1651. doi:10.1002/anie.201006023
- Song, X. Y., Pei, Y. Q., Qiao, M. W., Ma, F. L., Ren, H. T., & Zhao, Q. Z. (2015). Preparation and characterizations of Pickering emulsions stabilized by hydrophobic starch particles. *Food Hydrocolloids*, 45, 256-263. doi:10.1016/j.foodhyd.2014.12.007
- Stular, D., Jerman, I., Naglic, I., Simoncic, B., & Tomsic, B. (2017). Embedment of silver into temperature- and pH-responsive microgel for the development of smart textiles with simultaneous moisture management and controlled antimicrobial activities. *Carbohydrate Polymers*, 159, 161-170. doi:10.1016/j.carbpol.2016.12.030
- Sturzenegger, P. N., Gonzenbach, U. T., Koltzenburg, S., & Gauckler, L. J. (2012). Controlling the formation of particle-stabilized water-in-oil emulsions. *Soft Matter*, 8(28). doi:10.1039/c2sm25176k
- Szekalska, M., Pucilowska, A., Szymanska, E., Ciosek, P., & Winnicka, K. (2016). Alginate: Current Use and Future Perspectives in Pharmaceutical and Biomedical Applications. *International Journal of Polymer Science*, 2016, 1-17. doi:Artn 769703110.1155/2016/7697031
- Tan, K. Y., Gautrot, J. E., & Huck, W. T. (2011). Formation of pickering emulsions using ion-specific responsive colloids. *Langmuir*, 27(4), 1251-1259. doi:10.1021/la102904r
- Tang, J., Quinlan, P. J., & Tam, K. C. (2015). Stimuli-responsive Pickering emulsions: recent advances and potential applications. *Soft Matter*, 11(18), 3512-3529. doi:10.1039/c5sm00247h
- Thakur, S., Sharma, B., Verma, A., Chaudhary, J., Tamulevicius, S., & Thakur, V. K. (2018). Recent progress in sodium alginate based sustainable hydrogels for environmental applications. *Journal of Cleaner Production*, 198, 143-159. doi:10.1016/j.jclepro.2018.06.259
- Thompson, K. L., Mable, C. J., Lane, J. A., Derry, M. J., Fielding, L. A., & Armes, S. P. (2015). Preparation of Pickering double emulsions using block copolymer worms. *Langmuir*, 31(14), 4137-4144. doi:10.1021/acs.langmuir.5b00741
- To Ngai, H. A., and Sven Holger Behrens. (2006). Environmental Responsiveness of Microgel Particles and Particle-Stabilized Emulsions. *Macromolecules*, 39, 8171-8177.
- Tsabet, E., & Fradette, L. (2015a). Effect of Processing Parameters on the Production of Pickering Emulsions. *Industrial & Engineering Chemistry Research*, 54(7), 2227-2236. doi:10.1021/ie504338d
- Tsabet, E., & Fradette, L. (2015b). Effect of the properties of oil, particles, and water on the production of Pickering emulsions. *Chemical Engineering Research and Design*, 97, 9-17.
- Tsabet, E., & Fradette, L. (2015c). Semiempirical Approach for Predicting the Mean Size of Solid-Stabilized Emulsions. *Ind. Eng. Chem. Res*, 54, 11661-11677.

- Tsabet, E., & Fradette, L. (2016). Study of the properties of oil, particles, and water on particle adsorption dynamics at an oil/water interface using the colloidal probe technique. *Chemical Engineering Research & Design*, 109, 307-316. doi:10.1016/j.cherd.2016.02.001
- Tsuji, S., & Kawaguchi, H. (2004). Temperature-sensitive hairy particles prepared by living radical graft polymerization. *Langmuir*, 20(6), 2449-2455. doi:10.1021/la030333k
- Tsuji, S., & Kawaguchi, H. (2008). Thermosensitive pickering emulsion stabilized by poly(N-isopropylacrylamide)-carrying particles. *Langmuir*, 24(7), 3300-3305. doi:10.1021/la701780g
- Tu, F., & Lee, D. (2014a). One-step encapsulation and triggered release based on Janus particle-stabilized multiple emulsions. *Chem Commun (Camb)*, 50(98), 15549-15552. doi:10.1039/c4cc07854c
- Tu, F., & Lee, D. (2014b). Shape-changing and amphiphilicity-reversing Janus particles with pH-responsive surfactant properties. *Journal of the American Chemical Society*, 136(28), 9999-10006. doi:10.1021/ja503189r
- Umar, A. A., Saaïd, I. B., Sulaimon, A. A., & Pilus, R. B. M. (2018). A review of petroleum emulsions and recent progress on water-in-crude oil emulsions stabilized by natural surfactants and solids. *Journal of Petroleum Science and Engineering*, 165, 673-690. doi:10.1016/j.petrol.2018.03.014
- Utada, A. S., Lorenceau, E., Link, D. R., Kaplan, P. D., Stone, H. A., & Weitz, D. A. (2005). Monodisperse double emulsions generated from a microcapillary device. *Science*, 308(5721), 537-541. doi:10.1126/science.1109164
- Vaziri, A., & Warburton, B. (1994). Slow-Release of Chloroquine Phosphate from Multiple Taste-Masked W/O/W Multiple Emulsions. *Journal of Microencapsulation*, 11(6), 641-648. doi:10.3109/02652049409051114
- Verwey, E. J. (1947). Theory of the stability of lyophobic colloids. *J Phys Colloid Chem*, 51(3), 631-636.
- Wan, B., & Fradette, L. (2017). Phase inversion of a solid-stabilized emulsion: Effect of particle concentration. *Can. J. Chem. Eng.*, 95(10), 1925-1933. doi:10.1002/cjce.22892
- Wang, C. S., Natale, G., Virgilio, N., & Heuzey, M. C. (2016). Synergistic gelation of gelatin B with xanthan gum. *Food Hydrocolloids*, 60, 374-383. doi:10.1016/j.foodhyd.2016.03.043
- Wang, S., He, Y. J., & Zou, Y. (2010). Study of Pickering emulsions stabilized by mixed particles of silica and calcite. *Particuology*, 8(4), 390-393. doi:10.1016/j.partic.2010.05.002
- Wang, Y., Zhou, C. P., Sun, L., Yu, B. Q., Cao, M., & Zhong, S. A. (2015). One-step synthesis of boronic acid group modified silica particles by the aid of epoxy silanes. *Applied Surface Science*, 351, 353-357. doi:10.1016/j.apsusc.2015.05.120
- Wen, D. S., & Ding, Y. L. (2004). Effective thermal conductivity of aqueous suspensions of carbon nanotubes (carbon nanotubes nanofluids). *Journal of Thermophysics and Heat Transfer*, 18(4), 481-485. doi:10.2514/1.9934
- Whitby, C. P., Fornasiero, D., & Ralston, J. (2009). Effect of adding anionic surfactant on the stability of Pickering emulsions. *Journal of Colloid and Interface Science*, 329(1), 173-181. doi:10.1016/j.jcis.2008.09.056
- Whitby, C. P., & Wanless, E. J. (2016). Controlling Pickering Emulsion Destabilisation: A Route to Fabricating New Materials by Phase Inversion. *Materials (Basel)*, 9(8). doi:10.3390/ma9080626
- White, K. A., Schofield, A. B., Wormald, P., Tavacoli, J. W., Binks, B. P., & Clegg, P. S. (2011). Inversion of particle-stabilized emulsions of partially miscible liquids by mild drying of



- modified silica particles. *Journal of Colloid and Interface Science*, 359(1), 126-135. doi:10.1016/j.jcis.2011.03.074
- Williams, M., Armes, S. P., Verstraete, P., & Smets, J. (2014). Double emulsions and colloidosomes-in-colloidosomes using silica-based Pickering emulsifiers. *Langmuir*, 30(10), 2703-2711. doi:10.1021/la500219m
- Williams, M., Warren, N. J., Fielding, L. A., Armes, S. P., Verstraete, P., & Smets, J. (2014). Preparation of double emulsions using hybrid polymer/silica particles: new pickering emulsifiers with adjustable surface wettability. *ACS Appl Mater Interfaces*, 6(23), 20919-20927. doi:10.1021/am505581r
- Xiao, J., Li, Y. Q., & Huang, Q. R. (2016). Recent advances on food-grade particles stabilized Pickering emulsions: Fabrication, characterization and research trends. *Trends in Food Science & Technology*, 55, 48-60. doi:10.1016/j.tifs.2016.05.010
- Xu, X. B., Lu, S. Y., Gao, C. M., Wang, X. G., Bai, X., Duan, H. G., . . . Liu, M. Z. (2015). Polymeric micelle-coated mesoporous silica nanoparticle for enhanced fluorescent imaging and pH-responsive drug delivery. *Chemical Engineering Journal*, 279, 851-860. doi:10.1016/j.cej.2015.05.085
- Y. Sela, S. M., N. Garti. Polymeric surfactants based on polysiloxanes—graft-poly (oxyethylene) for stabilization of multiple emulsions. *Colloids and Surfaces A: Physicochemical and Engineering Aspects*, 83(2), 143-150.
- Yan, N. X., Gray, M. R., & Masliyah, J. H. (2001). On water-in-oil emulsions stabilized by fine solids. *Colloids and Surfaces a-Physicochemical and Engineering Aspects*, 193(1-3), 97-107. doi:10.1016/S0927-7757(01)00748-8
- Yang, B. Y., Leclercq, L., Clacens, J. M., & Nardello-Rataj, V. (2017). Acidic/amphiphilic silica nanoparticles: new eco-friendly Pickering interfacial catalysis for biodiesel production. *Green Chemistry*, 19(19), 4552-4562. doi:10.1039/c7gc01910f
- Yang, H., Hou, Q., Wang, S., Guo, D., Hu, G., Xu, Y., . . . Wang, J. (2018). Magnetic-responsive switchable emulsions based on Fe<sub>3</sub>O<sub>4</sub>@SiO<sub>2</sub>-NH<sub>2</sub> nanoparticles. *Chem Commun (Camb)*, 54(76), 10679-10682. doi:10.1039/c8cc04811h
- Yang, H., Zhou, T., & Zhang, W. (2013). A strategy for separating and recycling solid catalysts based on the pH-triggered Pickering-emulsion inversion. *Angewandte Chemie, International Edition in English*, 52(29), 7455-7459. doi:10.1002/anie.201300534
- Yang, X., Wang, Y., Bai, R., Ma, H., Wang, W., Sun, H., . . . Meng, T. (2019). Pickering emulsion-enhanced interfacial biocatalysis: tailored alginate microparticles act as particulate emulsifier and enzyme carrier. *Green Chemistry*. doi:10.1039/c8gc03573c
- Yang, Y., Fang, Z., Chen, X., Zhang, W., Xie, Y., Chen, Y., . . . Yuan, W. (2017). An Overview of Pickering Emulsions: Solid-Particle Materials, Classification, Morphology, and Applications. *Front Pharmacol*, 8, 287. doi:10.3389/fphar.2017.00287
- Yunfeng Yan, D. S., Bingqian Zheng, Ebru Kizilay, Yisheng Xu, and Paul L. Dubin. (2013). pH-Dependent Aggregation and Disaggregation of Native  $\beta$ -Lactoglobulin in Low Salt. *Langmuir*, 29(14), 4584-4593.
- Zhang, H. Z., Fang, S. M., Ye, C. M., Wang, M. H., Cheng, H. J., Wen, H., & Meng, X. L. (2008). Treatment of waste filtrate oil/water emulsion by combined demulsification and reverse osmosis. *Separation and Purification Technology*, 63(2), 264-268. doi:10.1016/j.seppur.2008.05.012
- Zhang, W., Sun, X., Fan, X., Li, M., & He, G. (2017). Pickering emulsions stabilized by hydrophobically modified alginate nanoparticles: Preparation and pH-responsive

- performance in vitro. *Journal of Dispersion Science and Technology*, 39(3), 367-374. doi:10.1080/01932691.2017.1320223
- Zhang, Y., Chen, K., Cao, L., Li, K., Wang, Q., Fu, E., & Guo, X. (2019). Stabilization of Pickering Emulsions by Hairy Nanoparticles Bearing Polyanions. *Polymers (Basel)*, 11(5). doi:10.3390/polym11050816
- Zheng, S. M., Zheng, Y. M., Beissinger, R. L., Wasan, D. T., & McCormick, D. L. (1993). Hemoglobin Multiple Emulsion as an Oxygen Delivery System. *Biochimica et Biophysica Acta*, 1158(1), 65-74. doi:10.1016/0304-4165(93)90098-S
- Zhou, J., Qiao, X., Binks, B. P., Sun, K., Bai, M., Li, Y., & Liu, Y. (2011). Magnetic Pickering emulsions stabilized by Fe<sub>3</sub>O<sub>4</sub> nanoparticles. *Langmuir*, 27(7), 3308-3316. doi:10.1021/la1036844
- Zhou, J., Wang, L., Qiao, X., Binks, B. P., & Sun, K. (2012). Pickering emulsions stabilized by surface-modified Fe<sub>3</sub>O<sub>4</sub> nanoparticles. *Journal of Colloid and Interface Science*, 367(1), 213-224. doi:10.1016/j.jcis.2011.11.001
- Zhou, Y., Sun, S., Bei, W., Zahi, M. R., Yuan, Q., & Liang, H. (2018). Preparation and antimicrobial activity of oregano essential oil Pickering emulsion stabilized by cellulose nanocrystals. *International Journal of Biological Macromolecules*, 112, 7-13. doi:10.1016/j.ijbiomac.2018.01.102
- Zhu, Y., Fu, T., Liu, K., Lin, Q., Pei, X., Jiang, J., . . . Binks, B. P. (2017). Thermoresponsive Pickering Emulsions Stabilized by Silica Nanoparticles in Combination with Alkyl Polyoxyethylene Ether Nonionic Surfactant. *Langmuir*, 33(23), 5724-5733. doi:10.1021/acs.langmuir.7b00273
- Zhu, Y., Jiang, J., Liu, K., Cui, Z., & Binks, B. P. (2015). Switchable Pickering emulsions stabilized by silica nanoparticles hydrophobized in situ with a conventional cationic surfactant. *Langmuir*, 31(11), 3301-3307. doi:10.1021/acs.langmuir.5b00295
- Zhu, Y., Sun, J., Yi, C., Wei, W., & Liu, X. (2016). One-step formation of multiple Pickering emulsions stabilized by self-assembled poly(dodecyl acrylate-co-acrylic acid) nanoparticles. *Soft Matter*, 12(36), 7577-7584. doi:10.1039/c6sm01263a
- Zoppe, J. O., Venditti, R. A., & Rojas, O. J. (2012). Pickering emulsions stabilized by cellulose nanocrystals grafted with thermo-responsive polymer brushes. *Journal of Colloid and Interface Science*, 369(1), 202-209. doi:10.1016/j.jcis.2011.12.011